國立臺灣大學生物資源暨農學院生物科技研究所

博士論文

Institute of Biotechnology
College of Bioresources and Agriculture
National Taiwan University
Doctoral Dissertation

第六型分泌系統在 *Azorhizobium* 與 *Agrobacterium* 之功能與機制研究

Functional and Mechanistic Studies of Type VI Secretion Systems in *Azorhizobium* and *Agrobacterium*

林筱涵

Hsiao-Han Lin

指導教授：劉啓德 博士、賴爾珉 博士

Advisors: Chi-Te Liu, Ph.D., Erh-Min Lai, Ph.D.

中華民國 109 年 1 月

January 2020

doi:10.6342/NTU202000295

國立臺灣大學博士學位論文
口試委員會審定書

第六型分泌系統在 *Azorhizobium* 與 *Agrobacterium* 之功能與機制研究

Functional and mechanistic studies of type VI secretion systems in *Azorhizobium* and *Agrobacterium*

本論文係林筱涵君（學號 D01642010）在國立臺灣大學生物科技研究所完成之博士學位論文，於民國 109 年 1 月 15 日承下列考試委員審查通過及口試及格，特此證明

口試委員：劉啓德（指導教授）

賴喜琪（指導教授）

陳仁治

林乃君　　郭志洲

郭秋萍

所長 劉志雄

謝辭

這本博士論文得以完成，得益於許多人的幫助，筱涵衷心感激。感謝指導教授劉啓德老師與賴爾珉老師，他們對於我博士研究的大力支持與悉心指導，支持我參與國內外各項學術會議，在我實驗不順遂時給予鼓勵與照顧，是本論文得以完成的重要因素。感謝陳仁治老師、林乃君老師、鄭秋萍老師、郭志鴻老師、以及馬麗珊老師對於本論文提出的建議，使得本書各項論點得以更加完善。感謝資格考委員楊建志老師、李昆達老師、以及劉嘉睿老師，對於實驗提出新方向。

感謝 R412 與 A325 的所有成員 、生技所共儀、臺大農學院共儀、中研院植微所共儀、中研院生化所共儀、高雄海科大許德賢老師，對於本研究提供的各項協助。特別感謝研究上的合作夥伴心玫、曉琳、Manda、弈杰、中研院生化所的徐尚德老師以及 Kumar，因為他們的努力，讓本研究的成果更加豐碩。能與各位合作是我的榮幸。感謝我的好戰友凱軍、Nia、輝文、孟淳、承泰、Yoyo 以及 IPMB-PEM 與 IPMB YIA 的所有成員，使我能與你們一同分享做研究的各種酸甜苦辣。感謝小林阿姨以及室貞阿姨的付出，讓我在實驗器具與耗材上無須擔憂。感謝化瑜姐、靜怡、以及植微所所有行政人員，讓我在申辦各項手續都順利。感謝在這一路中所有幫助過我的朋友，你們的幫助永遠在我心中。

最後，謹將此論文獻給我的摯愛家人、榮顥、以及榮顥的家人。我的父母林清富先生與王惠莉女士，對我無私的愛、栽培、教導、與陪伴，以及我的弟弟林家宇先生在童年時的陪伴、以及成年後的支持，成就了今日的我。感謝我的家人、榮顥、以及榮顥的家人在這麼長的歲月中，不求回報的愛與支持、做我最堅強的後盾，讓我自由地追尋自己的理想。若我今日有任何成就與榮耀，都歸功於你們無私的愛與付出。

筱涵謹誌於

中華民國一百零九年一月

doi:10.6342/NTU202000295

中文摘要

第六型細菌分泌系統（Type VI secretion system, T6SS）是一個由 13-14 個核心蛋白質所組成、形狀類似噬菌體尾部、結構橫跨革蘭氏陰性細菌內外雙膜的蛋白質外泌系統，可藉由組裝成長管柱構造穿透真核生物、或原核生物等受體細胞（recipient cells）的細胞膜，將效應蛋白質注入至受體細胞中。綜合許多研究發現，T6SS 的功能除了與致病力有關外，也與細菌間競爭、抗真核生物活性、金屬離子螯合、促進基因水平轉移等息息相關。雖然 T6SS 已知存在四分之一以上的革蘭氏陰性細菌基因體中，其中有許多是植物相關細菌（plant-associated bacteria），包括了病原菌及共生菌，然而 T6SS 在這些細菌中所扮演的生物功能至今仍然存在許多未知。有鑑於此，本研究使用共生莖瘤固氮根瘤菌（*Azorhizobium caulinodans*）與致病根癌農桿菌（*Agrobacterium tumefaciens*）作為材料，闡明 T6SS 在植物共生菌與植物病原菌上所扮演的角色、功能與機制。

A. caulinodans ORS571 基因體上有一套 T6SS 基因簇，本研究依此建構了一系列 T6SS 核心蛋白基因缺失突變株，用以探討 T6SS 分別對於菌株在自由態與共生態上的影響。研究結果發現，雖然有無 T6SS 對於自由態 ORS571 菌株的生長、菌體形態、自由態固氮能力、細菌間競爭、在植物上的定植能力以及共生效益並無顯著影響，當缺失 T6SS 基因的 ORS571 菌株與豆科宿主長喙田菁（*Sesbania rostrata*）建立共生關係時，其共生競爭能力與野生株相較顯著較低。

根癌農桿菌（*A. tumefaciens*）是許多癌腫病的病原菌，其 T6SS 是一種能夠殺死種間和種內細菌的抗菌武器，故本研究使用 *A. tumefaciens* T6SS 來研究細菌間競爭的作用模式。儘管其 T6SS 的分子調控與結構組織已被廣泛研究，但對於受攻擊方的受體細胞（recipient cell）因子所知甚少。因此本研究以 *A. tumefaciens* strain C58 為攻擊者，而缺乏 T6SS 的大腸桿菌為受體細胞，建立了一個高通量細菌競爭篩選平台，以尋找對 T6SS 殺滅力具有抗性的受體菌株。經由篩選得到 16 株對 C58 菌株的 T6SS 殺滅力呈現低敏感表型的突變株，並確認其中四個與增強 C58 菌株的 T6SS 殺滅力有關的大腸桿菌基因（*clpP, gltA,*

doi:10.6342/NTU202000295

ydhS, *ydaE*）。進一步探討 ClpP 蛋白酶與 T6SS 生物功能關連性的試驗結果顯示，當 ClpP 蛋白酶與其銜接蛋白 ClpA 形成 ClpAP 複合物時，大腸桿菌對根癌農桿菌 C58 菌株的 T6SS 攻擊的敏感性便會顯著提昇。

綜合以上結果，本研究指出共生根瘤菌 *A. caulinodans* ORS571 可藉由 T6SS 確保其共生競爭性，進而提昇結瘤佔有率；病原菌 *A. tumefaciens* strain C58 的細菌間競爭則需要多個受體因子的參與，來達到最佳的 T6SS 殺滅力。這些發現不僅擴展了我們對植物相關細菌 T6SS 的理解，且所獲得的知識或可應用於其他具有 T6SS 細菌的相關研究上。

關鍵字：第六型細菌分泌系統、根瘤菌-豆科共生、細菌間競爭、受體細胞、ClpP、莖瘤固氮根瘤菌、根癌農桿菌

doi:10.6342/NTU202000295

Abstract

The type VI secretion system (T6SS) is a protein secretion system composed of 13-14 core proteins, which structurally resembles an inverse phage tail. The T6SS spans the inner and outer membranes of a Gram-negative bacterium and can penetrate the membranes of the eukaryotic or prokaryotic recipient cells. The biological functions of T6SS are versatile, ranging from anti-eukaryotic activity, virulence, interbacterial competition, metal ion sequestering, and facilitating horizontal gene transfer, many of which display in animal-associated bacteria. Despite the existence in more than a quarter of the sequenced Gram-negative bacteria, the biological functions of T6SS in plant-associated bacteria, including mutualistic and pathogenic bacteria, remained mostly unknown. This study used a mutualistic bacterium, *Azorbizobium caulinodans*, and a pathogenic bacterium, *Agrobacterium tumefaciens*, to elucidate the functional and mechanistic aspects of T6SS in rhizobacteria.

With the discovery of a T6SS gene cluster in *A. caulinodans* ORS571, a series of T6SS gene deletion mutants were generated, and their phenotypes were analyzed in free-living and symbiotic states. The results showed that whether the T6SS exists or not, there was no detectable effect on vegetative growth, morphology, free-living nitrogen-fixing ability, interbacterial competition, plant colonization, or symbiotic effectiveness. On the other hand, the strains lacking T6SS showed a reduction in the symbiotic competitiveness when co-infected with a wild-type strain on the stem of the leguminous host plant *Sesbania rostrata*.

A. tumefaciens is a causative agent of crown gall disease in a wide range of plants and harbors T6SS. The T6SS of *A. tumefaciens* strain C58 is an antibacterial weapon

doi:10.6342/NTU202000295

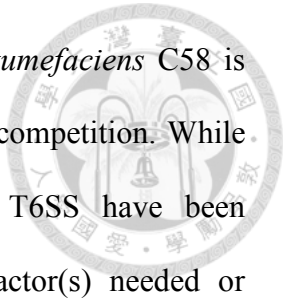

capable of killing both inter- and intra-species bacteria. Thus, *A. tumefaciens* C58 is selected to study the mode of action of T6SS during interbacterial competition. While the molecular mechanisms and structural organization of the T6SS have been extensively studied, little was known about the recipient cell factor(s) needed or subverted for an attack to be successful. Thus, a high-throughput interbacterial competition screening platform was established in search of the recipient strains that were resistant to T6SS killing. *A. tumefaciens* strain C58 served as a model attacker, and the *Escherichia coli* devoid of T6SS served as a recipient cell. From the screening, 16 mutants with less susceptibility to *A. tumefaciens* C58 T6SS-dependent killing were identified. Among them, four genes (*clpP*, *gltA*, *ydhS*, *ydaE*) that participate in enhancing the recipient susceptibility to *A. tumefaciens* T6SS killing were confirmed. Further studies demonstrated that the ClpP protease and its adapter protein ClpA forming the ClpAP complex in the *E. coli* recipient cell act in enhancing the recipient's susceptibility to the *A. tumefaciens* T6SS attack.

In summary, this study discovered that the T6SS of legume symbiont *A. caulinodans* ORS571 functions to ensure the competitiveness of nodule occupancy and that multiple recipient factors are required to maximize T6SS killing efficiency of *A. tumefaciens* C58. The findings expand our understanding of T6SS in plant-associated bacteria, and the knowledge obtained could be applied to other T6SS harboring bacteria.

Keywords: Type VI secretion system, rhizobium-legume symbiosis, antibacterial activity, recipient cells, ClpP, *Azorhizobium caulinodans*, *Agrobacterium tumefaciens*

doi:10.6342/NTU202000295

Table of Contents

doi:10.6342/NTU202000295

doi:10.6342/NTU202000295

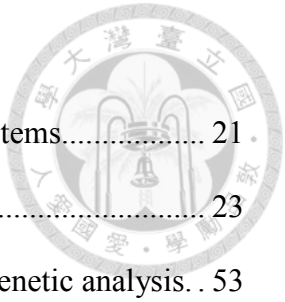

List of Figures

doi:10.6342/NTU202000295

doi:10.6342/NTU202000295

List of Tables

doi:10.6342/NTU202000295

List of Appendix Figures

doi:10.6342/NTU202000295

Chapter 1. Introduction

1.1 Protein secretion systems in Gram-negative bacteria

Bacteria have developed multiple protein secretion systems for robustly translocating proteins into either extracellular milieu or to other organisms. These secreted proteins could play roles in pathogenesis, symbiosis, or increase their fitness when interacting with eukaryotic hosts, or in competing with other bacteria to fight for limited environmental resources. To date, at least nine types (type I-IX) of the secretion systems that transport proteins across the outermost membrane (OM) have been discovered (Figure 1-1) (reviewed in Christie 2019, Filloux and Sagfors 2015). While most of the protein secretion systems are found in Gram-negative bacteria, which harbor two lipid bilayers in their cell membrane, the type VII secretion system (T7SS) is found in Gram-positive bacteria and mycoplasma that harbor one lipid bilayer (Ates, et al. 2016, Bottai, et al. 2017). The type II secretion system (T2SS), type V secretion system (T5SS), type VIII secretion system (T8SS), and type XI secretion system (T9SS) translocate their substrates/effectors across the OM, and requires the secretory (Sec) pathway or twin-arginine translocation (Tat) pathway to export their substrates across the inner membrane (IM). These secretion systems are the two-step systems. As the Sec and Tat pathways do not transfer proteins across the OM, they are not part of the secretion system *per se* (reviewed in De Geyter, et al. 2019). Other secretion systems transfer their substrates from cytoplasm to extracellular milieu or directly into the recipient cells. The following paragraphs introduce the Gram-negative secretion systems that participate in multiple functions. T7SS and T8SS are not covered below as the former is found in the Gram-positive bacteria and the latter only involves in filament assembly (Christie 2019, Filloux and Sagfors 2015).

doi:10.6342/NTU202000295

1.1.1 Type I secretion system (T1SS)

The type I secretion system (T1SS) is also known as the tripartite secretion system as it is composed of three major proteins (Green and Mecsas 2016, Kanonenberg, et al. 2018). The three proteins are the inner membrane component (IMC), the membrane fusion protein (MFP), and the outer membrane protein channel (OMP). The IMP recognizes and translocates its substrate protein from the cytoplasm to the MFP through its ATPase activity. The substrate is further translocated in an unfolded state from MFP to the OMP for secretion into the extracellular space. All T1SS substrate harbors a C-terminal secretion signal that is recognized by the IMC. The T1SS substrate translocates in a C-to-N direction, and the secretion signal is not cleaved during protein translocation.

1.1.2 Type II secretion system (T2SS)

The Type II secretion system (T2SS) spans the IM and OM of a Gram-negative bacteria but translocates protein only from the periplasm to the OM (Costa, et al. 2015). The T2SS substrate passes through the IM via Sec or Tat export systems. T2SS consists of 12-15 components proteins and can be divided into four parts-the cytoplasmic ATPase, the IM complex, the periplasmic pseudopilus, and the OM complex (Costa, et al. 2015, Gu, et al. 2017). After substrates reach periplasm, they are folded and recognized by the periplasmic pseudopilus. The cytoplasmic ATPase fuels the pushing force of the pseudopilus to push substrates through the OM complex to the extracellular milieu.

1.1.3 Type III secretion system (T3SS)

Type III secretion system (T3SS), or the ‘injectisome,’ can transfer proteins across three lipid bilayers-two from a Gram-negative bacterium and one from a eukaryotic host cell

doi:10.6342/NTU202000295

(Galán, et al. 2014). As the T3SS directs protein into a eukaryotic host, it is found in many eukaryotic-interacting bacteria either as pathogens or mutualists and participate in pathogenesis or symbiosis, respectively. The structure of T3SS consists of more than 20 components and can be divided into the cytosolic ATPase complex, the cytoplasmic ring (C-ring), the IM ring, the OM ring, the needle, and the translocation pore (Galán, et al. 2014). The T3SS membrane complex can be assembled either inside-out, in which the IM ring forms before OM ring, or in the opposite order, the outside-in (Deng, et al. 2017). After the assembly of the membrane complex, the needle and the translocation pore form and deliver the protein substrates to the host cell. The signal peptide of the T3SS substrates encompasses the first N-terminal 20-25 amino acids.

1.1.4 Type IV secretion system (T4SS)

The Type IV secretion system (T4SS) is a versatile secretion system that exists in both Gram-positive and Gram-negative bacteria with diverse structures and biological functions, many of which play a pivotal role in pathogenesis (Grohmann, et al. 2018). The known functions of T4SS include transfer DNA into a eukaryotic host, DNA conjugation into another bacteria, DNA release, DNA uptake, effector delivery into other bacteria or eukaryotic hosts (Li, et al. 2019). The T4SS machine consists of 12 components and composed of the substrate receptor, the IM translocase, the transmembrane core complex, and the extracellular pilus. In the case of *Agrobacterium tumefaciens* VirB/VirD4 T4SS, the substrate receptor is the VirD4, the translocase consists of the VirB3-VirB3-VirB6-VirV8, the core complex consists of the VirB7-VirB9-VirB10, and the pilus is composed of the VirB2-VirB5 and perhaps VirB1. *A. tumefaciens* Vir T4SS exports both effector proteins and DNA named as transferred-DNA (T-DNA), which is cleaved at the left border and the right border by the VirD2

doi:10.6342/NTU202000295

endonuclease to form a VirD2-T-DNA substrate (Stachel, et al. 1985). A T4SS substrate is recognized by the VirD4 and translocated through the translocase and the T4SS channel for extracellular/host delivery (Li, et al. 2019). The *A. tumefaciens* VirB/VirD4 T4SS substrates harbor C-terminal hydrophilic consensus motif R-X(7)-R-X-R-X-R-X-X(n)> (Li, et al. 2019, Vergunst, et al. 2005). On the other hand, the signal of the T4SS-depdendent antibacterial toxins is the *Xanthomonas* VirD4-interacting proteins with a conserved C-terminal domain (XVIPCD) (Sgro, et al. 2019, Souza, et al. 2015).

1.1.5 Type V secretion system (T5SS)

The Type V secretion system (T5SS) transfers proteins from periplasm across the OM and has relatively simple composition (Green and Mecsas 2016). The function of T5SS, however, ranging broadly from pathogenesis, adhesion, protein lysis, auto-aggregation/biofilm formation, to contact-dependent growth inhibition (CDI) (Meuskens, et al. 2019). The composition of the T5SS is the beta-barrel part that spans the OM and the passenger part that lies in the extracellular region (Meuskens, et al. 2019). The T5SS can be divided into several subtypes according to their composition. The class A T5SS, or the T5aSS, is the classical autotransporter type that consists of one large protein with beta-barrel part and the passenger part. The T5bSS is known as the two-partner secretion system, where different genes encode the beta-barrel part and the passenger part. The T5cSS is the trimeric autotransporter adhesins (TAAs), where three TAA monomers comprised one beta-barrel with three passenger part. The T5dSS is a hybrid of the T5aSS and the T5bSS. The T5eSS is an inverse autotransporters, where the C-N orientation is the opposite of the T5aSS.

doi:10.6342/NTU202000295

1.1.6 Type VI secretion system (T6SS)

The type VI secretion system (T6SS) is often regarded as the 'armed force' of a bacterium for its anti-prokaryotic and anti-eukaryotic activities delivered in a contact-dependent manner (Cianfanelli, et al. 2015, Hachani, et al. 2016, Hood, et al. 2010, Lien and Lai 2017, MacIntyre, et al. 2010, Pukatzki, et al. 2006). T6SS gene homologs can be found in more than a quarter of the sequenced Gram-negative bacteria, which contains many plant-associated bacteria (Abby, et al. 2016, Coulthurst 2013). T6SS is encoded by 13-14 *type six secretion* (*tss*) core genes, namely *tssA-tssM*. The T6SS structure is highly similar to a reversed contractile phage tail and can be divided into the membrane complex (MC), the baseplate (BP), the spike complex (SC), the sheath complex, the Hcp inner tube, the TssA cap, and the ClpV ATPase (TssH) (Chang, et al. 2017, Costa, et al. 2015, Rapisarda, et al. 2019, Zoued, et al. 2014). The current working model of the T6SS starts from the formation of the MC, followed by the recruitment of the BP and the effector-containing SC (Brunet, et al. 2015, Wang, et al. 2019). After loaded with a protein toxin, the TssA cap initiates the polymerization of the sheath complex (Schneider, et al. 2019, Zoued, et al. 2016, Zoued, et al. 2017). The outer sheath contracts and pushes the inner tube that tipped with the SC out to the extracellular space or the recipient cell (Basler, et al. 2013, Basler, et al. 2012).

The MC, consist of (TssJ-)TssL-TssM, forms a scaffolded pathway that spans both IM and OM that allows translocation of the effector-containing SC and inner tube extracellularly (Felisberto-Rodrigues, et al. 2011, Rapisarda, et al. 2019, Robb, et al. 2013). Of note, TssJ homologs are missing in some T6SS-harboring species like *Agrobacterium tumefaciens* and genus of *Bartonella* and *Hypomicrobiaceae* (Lin, et al. 2013, Szklarczyk, et al. 2018). The BP resembles the phage baseplate and consists of

doi:10.6342/NTU202000295

TssE, TssF, TssG, and TssK (Brunet, et al. 2015, Wang, et al. 2019). The SC is composed of the VgrG (TssI)-PAAR-(adaptor)-effectors that resembles the phage tail spike loading with effector protein (Leiman, et al. 2009, Shneider, et al. 2013). Although only VgrG was considered as a core component, interaction with its cognate effector to form a complete spike complex has recently been demonstrated critical for T6SS assembly (Bondage, et al. 2016, Liang, et al. 2019, Unterweger, et al. 2015, Unterweger, et al. 2017, Wu, et al. 2019a). The inner tube Hcp (TssD) resembles the phage tail tube, and the sheath complex TssB-TssC complex resembles the phage tail sheath (Lossi, et al. 2013, Mougous, et al. 2006, Zhang, et al. 2013).

1.1.9 Type IX secretion system (T9SS)

The type IX secretion system (T9SS), or the Por secretion system (PorSS), is found in some species of *Bacteriodetes* phylum and functions in pathogenesis and gliding ability (Lasica, et al. 2017, McBride 2019). There are 18 genes essential for a functional T9SS, but they distribute in multiple loci in the genome, instead of forming a large gene cluster. Most of the T9SS substrates contain an N-terminal peptide that enables them to translocate across the IM through the Sec system and a C-terminal domain that enable them to translocate across the OM through the T9SS (McBride 2019).

1.2 Bacterial secretion systems in plant-associated bacteria

Plant-associated bacteria indicate the bacteria that associate with plants, including endophytic, rhizospheric, and phyllospheric bacteria (Ownley and Trigiano 2016). These bacteria can be mutualism, commensalism, parasitism, depending on whether the plant host is benefited, has no effects, or harmed, respectively (Figure 1-2A)

doi:10.6342/NTU202000295

(Gnanamanickam 2006). Plant-associated bacteria can also be neutralism, in which both species are not affected by their interaction (Figure 1-2A). The majority of the plant-associated bacteria studies have focused on the mutualistic symbionts and the parasitic phytopathogens (Gnanamanickam 2006). Studies on the phytopathogens concentrated on those that make a substantial economic loss in most of the cases (Figure 1-2B, using *Agrobacterium tumefaciens*-causing crown gall disease as an example) (Mansfield, et al. 2012). Several rhizobia can form nodules with their legume hosts to fix nitrogen gas (N_2) from the atmosphere and turn it into available forms of nitrogen source (ammonia or amino acids) (Figure 1-2C) (Dreyfus, et al. 1987, Haag, et al. 2013, Jensen, et al. 2012, Zamioudis and Pieterse 2012). These symbiotic interactions have received much attention because they contribute to natural nitrogen enrichment, and have important agricultural implications for reducing the need for chemical fertilization. Accordingly, scientists have dedicated themselves from the last several decades to elucidate the underlying molecular mechanisms for expanding the host range of the rhizobia as well as transferring the endosymbiotic nitrogen-fixation capacities to major non-legume crops (Charpentier and Oldroyd 2010, Doyle 2011, Kereszt, et al. 2011, Popp and Ott 2011, Venkateshwaran 2015).

The phytopathogens are diverse in their pathogenesis, host range, and life cycle (Gnanamanickam 2006). Nevertheless, protein secretion systems play an essential role in pathogenesis as well as in host range determination in most of the cases (Bernal, et al. 2018, Filloux and Sagfors 2015, Maffei, et al. 2017, Nelson and Sadowsky 2015, Preston, et al. 2005). The secretion systems that play a pivot role in the pathogenesis of the phytopathogens are mainly contributed by the T2SS, T3SS, T4SS, and the T5SS (Filloux and Sagfors 2015, Gnanamanickam 2006, Preston, et al. 2005). The role of the

doi:10.6342/NTU202000295

T1SS in pathogenesis is relatively minor as compared to other protein secretion systems (Ownley and Trigiano 2016). Albeit T6SS widely exists in the genome of the phytopathogens, their role in pathogenesis in the phytopathogens is less pronounced (Haapalainen, et al. 2012, Wu, et al. 2008).

Rhizobia also use T3SS, T4SS, and T6SS during legume-rhizobium symbiosis in either host-range determination or symbiotic effectiveness (Bladergroen, et al. 2003, Hubber, et al. 2004, Nelson, et al. 2017, Okazaki, et al. 2013, Okazaki, et al. 2009). The presence of T3SS affects the host-specificity in many rhizobia. The effects can be both positive and negative and no conclusive rules have been determined (Nelson and Sadowsky 2015). For example, the T3SS of *Bradyrhizobium elkanii* USDA61 positively regulates its symbiotic ability to *Glycine max* ev. Clark and *Glycine max* cv. Enrei but negatively regulates to *Glycin max* cv. Hill and *Vigna radiata* (Nelson and Sadowsky 2015, Okazaki, et al. 2013, Okazaki, et al. 2009). Recently, an T3SS effector of the *B. elkanii* USDA61, the Effector required for nodulation-A (ErnA), that enables the bacteria to form a symbiotic relationship with *Aeschynomene indica* has been demonstrated (Teulet, et al. 2019).

Aside from the plant-microbe interaction, the T4SS and the T6SS of the plant-associated bacteria also play a role in interbacterial competition (Bernal, et al. 2017, Ma, et al. 2014, Souza, et al. 2015). The interbacterial competition activities of the T1SS and T5SS in plant-associated bacteria have not been demonstrated.

doi:10.6342/NTU202000295

1.3 Type VI secretion system in plant-associated bacteria

1.3.1 Roles of the T6SS in bacteria-plant interactions

T6SS exists in many plant-associated bacteria, including symbionts, pathogens, and commensal bacteria (Abby, et al. 2016, Coulthurst 2013). Before the term 'T6SS' was coined in 2006 (Bladergroen, et al. 2003), a gene cluster in legume symbiont *Rhizobium leguminosarum,* later found to encode core components of T6SS, was suggested to be involved in host range-determination (Bladergroen, et al. 2003). *R. leguminosarum* had been classified into various biovar (bv.) by their host range (Hooykaas, et al. 1981, Long 1989). The authors found a Tn5-inserted *R. leguminosarum* strain, RBL5787, that showed broaden host range compared to its mother strain RBL5523. The insertion site of this Tn5 mutant was designated *imp* (*impaired in nodulation*) locus. After the discovery of T6SS, the *imp* locus turned out to be the T6SS gene cluster, and the specific insertion site of the mutant was *tssK* (*impJ*, *pRL120484*) (Bingle, et al. 2008). RBL5523 was a hybrid strain generated from introducing the symbiosis plasmid, Sym, pRL1JI of *R. leguminosarum* bv. *viciae* 3841 into a cured *R. leguminosarum* bv. *trifolii* RCR5 (Roest, et al. 1997). Therefore, it was widely accepted that the T6SS cluster in the pRL1JI Sym plasmid, which derived from *R. leguminosarum* bv. *viciae* 3841, plays a role in host-range limitation (Bingle, et al. 2008, Filloux, et al. 2008, Panagiotis F. Sarris, et al. 2012, Ryu 2015). Whole-genome sequencing analysis revealed that *R. leguminosarum* bv. *viciae* 3841 harbors six plasmids, and the T6SS lies in a different plasmid (pRL12) other than the Sym plasmid (pRL10) (Young, et al. 2006), so the pRL1JI might be a plasmid mixture containing both pRL12 and pRL10. A recent study tested the T6SS activity, monitored by the secretion of the inner tube Hcp protein, of the *R. leguminosarum* bv. *viciae* 3841 failed to detect a positive signal (Salinero-Lanzarote,

doi:10.6342/NTU202000295

et al. 2019). Therefore, the biological function of T6SS in *R. leguminosarum* RBL5523 remains elusive.

Although how T6SS of the *R. leguminosarum* participates in symbiosis is still unknown, the idea that "T6SS affects symbiosis" has inspired many studies to focus on the biological functions of T6SS in *Rhizobium* and the results started to come out recently (de Campos, et al. 2017, Salinero-Lanzarote, et al. 2019). The T6SS of *Paraburkholderia phymatum* increases its symbiotic competitiveness against *Paraburkholderia diazotrophica*, *Paraburkholderia mimosarum*, and *Paraburkholderia sabiae* on cowpea (*Vigna unguiculata*) (de Campos, et al. 2017). The increase of the T6SS-dependent symbiotic competitiveness is partially attributed to the antibacterial activity against *P. diazotrophica* and *P. mimosarum*. The T6SS mutants of *Rhizobium etli* Mim1 significantly reduced its ability to form root nodules with common bean (*Phaseolus vulgaris*) and resulted in reduced plant dry weight (Salinero-Lanzarote, et al. 2019). It becomes evident that rhizobial T6SS is involved in symbiosis.

T6SS is involved in pathogenesis in plant pathogens. The presence of T6SS cluster II and cluster III increased the survival of *Pseudomonas aeruginosa* 100 times more than that of a T6SS mutant in an *Arabidopsis* infiltration assay (Lesic, et al. 2009). The *Pantoea ananatis* T6SS cluster I, but not cluster III, also participates in pathogenesis toward onion (Shyntum, et al. 2015). The T6SS mutant of *Ralstonia solanacearum* also had delayed disease symptoms and reduced bacterial titer on tomato (Zhang, et al. 2014). The above examples showed an influence of T6SS in pathogenesis in the plant-associated bacteria. Tumorigenesis of the potato tuber disks infected with *A. tumefaciens* was Hcp-dependent under low bacteria concentration, but a mutation in the

doi:10.6342/NTU202000295

t6ss gene cluster or *tssM* (*icmF*) had no subvert effects (Wu, et al. 2008). On the other hand, the dysfunction of T6SS did not affect the pathogenesis in *Pseudomonas syringae* pv. *syringae* B728a, *Pectobacterium atrosepticum*, and *Pseudomonas syringae* pv. tomato DC3000 (Haapalainen, et al. 2012, Mattinen, et al. 2007, Records and Gross 2010). In summary, even though T6SS of some phytopathogens showed an impact on disease development, whether T6SS plays a direct role in pathogenesis remains elusive.

1.3.2 Roles of the T6SS in interbacterial competition

The antibacterial activity of T6SS has been demonstrated in plant pathogens *A. tumefaciens*, *Pseudomonas syringae* pv. tomato DC3000, *Pantoea ananatis*, legume symbiont *Paraburkholderia phymatum*, plant growth-promoting bacterium *Pseudomonas putida*, and soil bacterium *Pseudomonas protegens* (Bernal, et al. 2017, de Campos, et al. 2017, Haapalainen, et al. 2012, Ma, et al. 2014, Shyntum, et al. 2015, Whitney, et al. 2013). In most of the cases, the T6SS-dependent interbacterial-killing outcome depends highly on their competitor or their recipient cells. For example, *A. tumefaciens* was able to kill its T6SS-sensitive siblings and *Pseudomonas aeruginosa in planta* but cannot exhibit antibacterial activity at the intra-species competition during *in vitro* (Ma, et al. 2014). More recently, it has been shown that *A. tumefaciens* intra-species T6SS killing *in planta* is highly linked to their evolutional linage, the genomospecies (Wu, et al. 2019b). The T6SS killing of the *Paraburkholderia phymatum* against *P. diazotrophica* and *P. sabiae* is more pronounced than against *P. mimosarum* (Shyntum, et al. 2015). Similarly, *P. putida* showed stronger T6SS killing activity to *P. syringae* and *Xanthomonas campestris* than to *Pectobacterium carotovorum* or *A. tumefaciens* (Bernal, et al. 2017).

doi:10.6342/NTU202000295

1.4 *Azorhizobium caulinodans* biology

1.4.1 Discovery and the stem nodules of the *A. caulinodans*

Azorbizoium caulinodans ORS571 was isolated from the stem nodule of the tropical waterlogged legume *Sesbania rostrata* in Senegal, Sahel region of West Africa (Dreyfus, et al. 1988, Dreyfus and Dommergues 1981a, Elmerich, et al. 1982). Stem nodules, like the root nodules, are plant nitrogen-fixing symbiosis organs where symbiotic bacteria live intracellularly and fix gaseous nitrogen into ammonia (Dreyfus and Dommergues 1981a, Ronson, et al. 1981, Tsien, et al. 1983). This legume-*rhizobial* symbiosis system is beneficial to both players as the fixed nitrogen provides nitrogen source to the host plant while the plant provides carbon source to the symbiotic bacteria (Lodwig, et al. 2003, Mulley, et al. 2011, Poole and Allaway 2000, Prell, et al. 2010). The isolated *A. caulinodans* had strong specificity and formed effective nodules with *S. rostrata* but not with other closely related *Sesbania* genus like *Sesbania pachycarpa* or *Sesbania aculeata,* nor with *Aeschynomene* sp. (Dreyfus and Dommergues 1981a). Legume *Aeschynomene* sp. was one of the two species that forms nitrogen-fixing stem nodules at that time (Dreyfus and Dommergues 1981a). *S. rostrata,* on the other hand, only forms effective nodules with *A. caulinodans* and only formed ineffective nodules with *Rhizobium* (*Agrobacterium*) strain IRBG74, which formed effective nodules with other *Sesbania* genus plant like *S. cannabina* (Cummings, et al. 2009, Dreyfus and Dommergues 1981a).

The stem nodule system is an adaptation of *S. rostrata* to its temporarily flooded habitat, and this system does not exist in many other legume symbiosis systems like the *Medicago truncatula-Sinorhizobium meliloti* or *Lotus japonicus-Mesorhizobium loti* systems (Capoen, et al. 2010, de Bruijn 2020, Dreyfus and Dommergues 1981b, Pajuelo

doi:10.6342/NTU202000295

and Stougaard 2005). The stem of the *S. rostrata* is occupied by rows of dormant adventitious root primordia, which forms new root at the air-waterlogged junction during the flooding season (Dreyfus and Dommergues 1981a, Dreyfus and Dommergues 1981b). The *A. caulinodans*, which dwells on the leaves of the *S. rostrata*, can form stem nodules on the bases of the adventitious root primordia via the crack entry pathway (for decent electron micrographs of the stem nodule morphogenesis, please refer to Tsien, et al. 1983) (Adebayo, et al. 1989, Capoen, et al. 2010, Tsien, et al. 1983). The crack entry pathway starts from *A. caulinodans* colonizing and multiplying at the base of the adventitious root primordia, which induces localized plant cell death and forms an infection pocket heavily occupied by *A. caulinodans* (Capoen, et al. 2010, Tsien, et al. 1983). *A. caulinodans* is then able to form an infection thread that penetrates and infects the *S. rostrata* cell after 3-4 days post-infection (dpi). At 5-6 dpi, the infected plant cell will be filled with proliferated *A. caulinodans*, and the nodule phenotype can be easily distinguished from the uninfected adventitious root primordia. Nitrogen fixation is detectable at this stage. The maximum nitrogen fixation of the stem nodule is at about seven days post infection (dpi), and the nodule will undergo senescence after 14 dpi (Capoen, et al. 2010, Chien, et al. 2019, Liu, et al. 2011).

1.4.2 *A. caulinodans* as a favorable research model as a symbiont and endophyte

After its discovery, *A. caulinodans* soon became one of the heavily investigated legume symbionts as it has much scientific and agronomical importance (Bergersen, et al. 1986, Dreyfus and Dommergues 1981b, Gebhardt, et al. 1984, Kitts and Ludwig 1994, Scott and Ludwig 2004). *S. rostrata-A. caulinodans* green manure system was able to double to triple the rice yield without applying any nitrogen fertilizer (Rinaudo, et al. 1983). Under nitrogen supply condition, when most legume nodule systems lose their ability to

doi:10.6342/NTU202000295

fix nitrogen, the *S. rostrata-A. caulinodans* stem nodule was not affected (Bergersen, et al. 1986, Dreyfus and Dommergues 1981b). *A. caulinodans* also fixes nitrogen under free-living state without any nitrogen supply, under ambient oxygen condition (10 μM, which is 1000 times higher than that of legume nodules), and had the highest nitrogen-fixing ability known at that time (300-400 nmol N (mg dry weight)$^{-1}$ h^{-1}) (Bergersen, et al. 1986, Dreyfus and Dommergues 1981b, Gebhardt, et al. 1984, Kitts and Ludwig 1994, Scott and Ludwig 2004). This diazotrophic nature has been demonstrated to provide nitrogen sources to many agriculturally vital crops like rice, maize, tomato, or even to *Arabidopsis* (Cocking 2001, Cocking 2005, Cocking, et al. 2005, Gopalaswamy, et al. 2000, Stone, et al. 2001). More recently, this endophytic activity makes *A. caulinodans* the most promising material for engineering nitrogen fixation bacteria that associate with cereals (Ryu, et al. 2019).

Aside from agronomy importance and advantages mentioned above, other characters also make *A. caulinodans* an excellent model system for scientific studies. First, the *A. caulinodans*-induced stem nodules are visible without any processing, and their development is synchronized, which is nearly impossible in the root nodule system (Dreyfus and Dommergues 1981a, Liu, et al. 2011, Suzuki, et al. 2007). Second, the whole genome sequence of *A. caulinodans* ORS571^{T} is available (GeneBank AP009384) (Dreyfus, et al. 1988, Lee, et al. 2008). Third, an *A. caulinodans* mutant library that induced ineffective stem nodules is available (Suzuki, et al. 2007). Genome analysis by STRING 9.1 identified a potential T6SS gene cluster in *A. caulinodans* ORS571 genome, and transcriptomic analysis uncovered the T6SS genes are expressed in both free-living and symbiosis condition (Franceschini, et al. 2013, Kanehisa and Goto 2000, Lee, et al. 2008, Tsukada, et al. 2009).

doi:10.6342/NTU202000295

1.5 *Agrobacterium tumefaciens* biology

1.5.1 Discovery and pathogenesis of the *A. tumefaciens*

Agrobacterium tumefaciens was first described in 1907 as the gall-causing bacterium in marguerite (Smith and Townsend 1907). To date, more than 90 families of the plants are found susceptible to *A. tumefaciens* and result in the Crown Gall disease (Kado 2010, Kado 2014). In nature, however, the host range of *A. tumefaciens* is mainly on woody plants, plants from the Rosaceae family, the Vitaceae family, and the Juglandaceae family (Kado 2010). The most studied *A. tumefaciens* strain, strain C58, contains four DNA replicons in its genome: the circular chromosome (GeneBank NC_003062), the linear chromosome (GeneBank NC_003063), the cryptic At plasmid pAtC58 (GeneBank NC_003064), and the tumor-inducing (Ti) plasmid pTiC58 (Genebank NC_003065) (Wood, et al. 2001). The T6SS gene clusters lie in the linear chromosome (Wu, et al. 2008). There are three T4SS in *A. tumefaciens* C58: the virulence system (Vir) that transfers DNA into the plant host and causes the Crown Gall disease, the Trb system for pTiC58 conjugation, and the AchB system for pAtC58 conjugation (Chen, et al. 2002, Chilton, et al. 1977, Lai and Kado 1998, Lai and Kado 2000, von Bodman, et al. 1989). The most studied T4SS of *A. tumefaciens* C58 is the Vir system due to its trans-kingdom DNA transformation ability, which has been widely applied in plant genetic engineering (Hwang, et al. 2017).

A. tumefaciens pathogenesis can be divided into several steps: (1) recognition and attachment of *A. tumefaciens* to the plant cell, (2) activation of the *A. tumefaciens* virulence genes, (3) generation and transportation of the transfer-DNA (T-DNA) into the plant cell, (4) T-DNA integration into the plant chromosome, and (5) expression of the plant genome-integrated T-DNA (reviewed in Hwang, et al. 2017). *A. tumefaciens* is

doi:10.6342/NTU202000295

attracted by the plant's wounded sap, an acidic (pH 5.0-5.8) liquid rich in phenolic compounds, and attached to the wounded site (Gao and Lynn 2005, Gohlke and Deeken 2014, Stachel, et al. 1985). The mechanism underlies the attraction is the recognition of the wounded sap by the chromosome virulence proteins ChvE, and ChvG-ChvI two-component system and the VirA-VirG two-component system that is encoded by the pTiC58 (Charles and Nester 1993, Winans 1992). The activated VirG then transcriptionally activates the *virulence* (*vir*) genes on the pTiC58 (Pazour and Das 1990). The Vir proteins then produce the single strand transfer-DNA (T-DNA), which is transferred through the Vir T4SS into the plant cell (reviewed in Gelvin 2012, Hwang, et al. 2017). The T-DNA is further integrated into the plant chromosome, and the T-DNA genes encoding proteins involved in the production of phytohormones cytokinin and auxin that lead to tumorigenesis (Akiyoshi, et al. 1983, Barry, et al. 1984, Buchmann, et al. 1985, Chilton, et al. 1980, Inzé, et al. 1984, Schröder, et al. 1984, Willmitzer, et al. 1980). The consequences of the Crown Gall disease are more than energy quenching for tumorigenesis, but also the production and secretion of the opines that provide carbon and nitrogen source to support the growth of the intercellular *A. tumefaciens* (reviewed in Vladimirov, et al. 2015).

1.5.2 *Agrobacterium tumefaciens* T6SS

The T6SS hallmark protein, Hcp, was found secreted by *A. tumefaciens* C58 grown under plant environment-mimicking medium AB-MES (pH5.5) (Wu, et al. 2008). Hcp was secreted in the presence and absence of acetosyringone (AS), a phenolic compound known to induce *vir* genes, although Hcp secretion levels were suppressed by AS (Stachel, et al. 1985, Wu, et al. 2012, Wu, et al. 2008). The deletion of *hcp* did not block the tumorigenesis ability of *A. tumefaciens* on the stems of tomato, tobacco, and white

doi:10.6342/NTU202000295

radish (Wu, et al. 2008). However, quantitative tumorigenesis assay using potato tuber demonstrated that *A. tumefaciens* Δ*hcp*, but not Δ*tssM* or Δ*tssA-tssM* (Δ*t6ss/imp* operon), reduced tumorigenesis efficiency compared to that of wild type (Wu, et al. 2008). The results suggest that the T6SS of *A. tumefaciens* C58 does not play an important role in tumorigenesis.

The T6SS of *A. tumefaciens* C58 consists of three gene clusters: the *imp* cluster (*atu4343-atu4330*), the *hcp* cluster (*atu4344-atu4352*), and the *vgrG2* cluster (*atu3642-atu3639*) (Lin, et al. 2013, Ma, et al. 2014). The T6SS genes that encode a specific part of the T6SS tend to cluster together. For example, the membrane complex is encoded by *atu4333* (*tssL*) and *atu4332* (*tssM*), the baseplate is encoded by *atu4338-atu4336* (*tssE-tssF-tssG*) and *atu4334* (*tssK*), the sheath complex is encoded by *atu4342-atu4340* (*tssB-tssC*$_{41}$*-tssC*$_{40}$). Other genes scatter in between the T6SS cluster, like the atu4345 (tssD) that encodes the inner tube, the *atu4343* (*tssA*) that encodes the cap protein, and the *atu4344* that encodes the ClpV ATPase. Current evidence suggests at least two types of spike complex in *A. tumefaciens* C58: VgrG1 (TssI1) spike that consists of VgrG1-Tap1-Tde1-Tdi1-PAAR (Atu4348-Atu4352) and VgrG2 (TssI2) spike that consists of VgrG2-DUF2169-Tde2-Tdi2 (Atu3642-Atu3639) (Bondage, et al. 2016, Ma, et al. 2014). The Tde1-Tdi1 and Tde2-Tdi2 are the effector-immunity protein pairs, and the Tap1 and DUF2169 are the chaperone/adaptor proteins that facilitate the loading of the genetically linked effector-immunity pair (Bondage, et al. 2016, Wu, et al. 2019a). The third effector-immunity pair is the Tae-Tai (Atu4347-Atu4346), and the secretion of the Tae is likely mediated by Hcp (Bondage, et al. 2016, Lin, et al. 2013). The Tde1 and Tde2 are DNase, and the Tae is a putative peptidoglycan amidase (Ma, et al. 2014). Some of the regulatory proteins are also known: the PpkA (Atu4330) and the Fha

doi:10.6342/NTU202000295

(TagH, Atu4335) that positively regulate T6SS and the TagF-PppA (Atu4331) that negatively regulates T6SS (Lin, et al. 2018, Lin, et al. 2014).

The T6SS assembly is highly regulated in *A. tumefaciens* C58, and the current knowledge is summarized below. Upon sensing an acidic environment (e.g., pH 5.5 that resembles the acidic of a wounded plant cell wall and apoplast), the negative regulator ExoR degrades and then alleviates the repression of the ChvG-ChvI two-component system for transcriptional activation of the T6SS of the *A. tumefaciens* C58 (Wu, et al. 2012). After assembly of the T6SS membrane complex TssML, the positive regulator PpkA phosphorylates the TssL by its Ser/Thr kinase activity (Lin, et al. 2014, Ma, et al. 2009). Phosphorylated TssL triggers ATP binding to TssM as well as a conformational change of the complex (Ma, et al. 2012). This conformational change may enable the binding of the Fha to the phosphorylated site of the TssL, forming the TssM-p-TssL-Fha complex (Lin, et al. 2014, Ma, et al. 2012). At some point in the TssM-p-TssL-Fha complex formation, loading the baseplate and the spike complex onto this membrane complex is enabled. This statement comes from the observation that the TssM-p-TssL-Fha complex can recruit the Hcp inner tube, and that inner tube formation forms after baseplate and spike complex formation (Brunet, et al. 2015, Lin, et al. 2014, Wang, et al. 2019). The assembly of the spike complex onto the membrane-baseplate structure is also highly regulated. First, each VgrG loads its effector with specificity: the VgrG1 explicitly loads Tde1, and VgrG2 only loads Tde2 (Bondage, et al. 2016). Second, only effector-loaded spike complexes can successfully trigger sheath complex formation (Wu, et al. 2019a).

doi:10.6342/NTU202000295

The T6SS activity is also highly regulated transcriptionally and post-translationally in *A. tumefaciens* C58 (Lin, et al. 2018, Ma, et al. 2014, Wu, et al. 2012). The membrane complex is in the TssM-p-TssL-Fha state mentioned above under T6SS ON state. The T6SS OFF state resulted from the high accumulation of the TagF-PppA protein binding to the Fha protein, preventing it from forming an active membrane complex (Lin, et al. 2018). The sensing signal that induces the accumulation of the TagF-PppA remains elusive. The T6SS activity can also be fine-tuned by pH or by endogenous cyclic-di-GMP (c-di-GMP) level (Ma, et al. 2014, McCarthy, et al. 2019, Wu, et al. 2012). Under a high c-di-GMP level, both T6SS and the T4SS are turned down transcriptionally (McCarthy, et al. 2019). The T6SS is transcriptionally upregulated under pH 5.5, which resembles plant cell wall acidity (Wu, et al. 2012). Similarly, the antibacterial activity of *A. tumefaciens* C58 T6SS against *P. aeruginosa* was observed *in planta* but not on LB agar, pH 7.0 (Ma, et al. 2014). The T6SS-mediated killing outcome is also recipient cell-dependent (Ma, et al. 2014, Wu, et al. 2019b). *A. tumefaciens* T6SS was unable to antagonize its T6SS-sensitized siblings but was able to antagonize other species like *E. coli* on LB agar (Ma, et al. 2014). The within-genomospecies antibacterial competition of *A. tumefaciens* was not observed *in planta*, despite the two competing *A. tumefaciens* harbor incompatible effector-immunity pairs (Wu, et al. 2019b). Although it is well established that the T6SS killing is recipient cell-dependent in *A. tumefaciens* C58, the factors involved are unknown.

1.6 Scientific questions addressed in this thesis

Our knowledge of how the bacterial protein secretion systems participate in plant-associated bacteria has expanded, as reviewed above. The T2SS, T3SS, and T5SS play

doi:10.6342/NTU202000295

an essential role in pathogenesis in many phytobacteria, while the T3SS, T4SS, and more recently discovered, T6SS in rhizobia are involved in legume symbiosis. On the other hand, T4SS and T6SS participate in bacterial competition in plant-associated bacteria. While much has been known in how these secretion systems participate in gaining environmental fitness of the plant-associated bacteria, the following questions about the involvement and the biological significance of T6SS in plant-associated bacteria were still unanswered when this project started.

First, the biological function(s) of the T6SS in legume-symbiotic rhizobia was mostly unknown. The only publication about rhizobial T6SS when this project started was the 2003 paper, which suggested that T6SS participates in host range-determination (Bladergroen, et al. 2003). It was not characterized whether rhizobial T6SS harbors anti-prokaryotic or anti-eukaryotic activities, nor was direct evidence that T6SS participates in legume-rhizobium symbiosis available.

Second, although evidence showed that the T6SS killing outcome of *A. tumefaciens* C58 is recipient cell-dependent (Ma, et al. 2014, Wu, et al. 2019b), the recipient factors involved in T6SS killing outcomes were unclear.

This thesis addressed these questions by genetic and biochemical approaches as well as a high-throughput screening technique.

doi:10.6342/NTU202000295

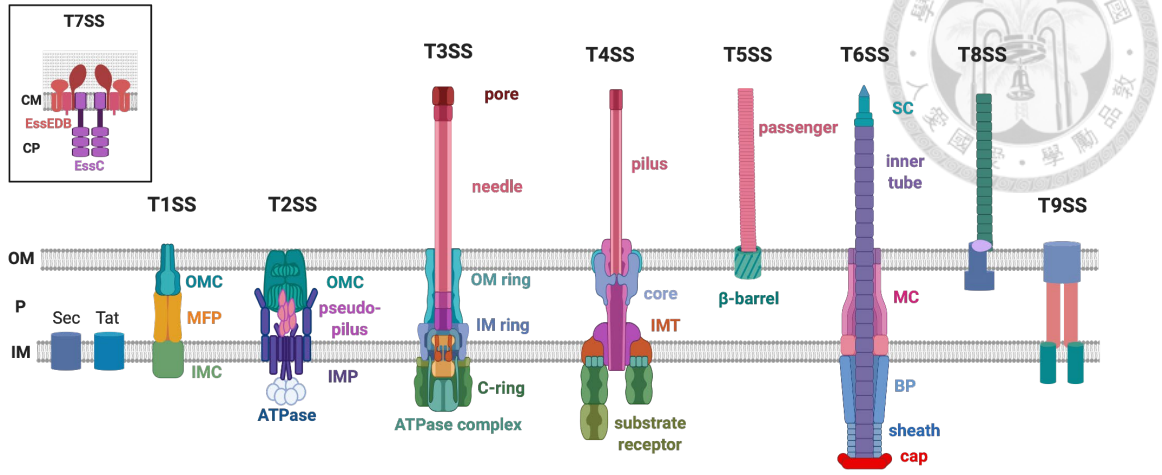

Figure 1-1. Bacteria secretion systems and the Sec and Tat export systems.

Schematic of the type I to type IX secretion systems as well as the Sec and Tat export systems, which transport substrates of type II, type V, type VIII, and type IX secretion systems. The type I secretion system (T1SS) is composed of three major proteins: the inner membrane component (IMC), the membrane fusion protein (MFP), and the outer membrane protein channel (OMP). The type II secretion system (T2SS) consists of 12-15 proteins that can be divided into the cytoplasmic ATPase, the inner membrane platform (IMP), the pseudopilus, and the outer membrane complex (OMC). The type III secretion system (T3SS) consists of more than 20 components and can be divided into the cytosolic ATPase complex, the cytoplasmic ring (C-ring), the inner membrane ring (IM ring), the outer membrane ring (OM ring), the needle, and the translocation pore (pore). The type IV secretion system (T4SS) is composed of 12 components that can be divided into the substrate receptor, the inner membrane translocase (IMT), the transmembrane core complex (core), and the extracellular pilus (pilus). The type V secretion system (T5SS) consists of 1-3 proteins that contain the beta-barrel part that spans the outer membrane and the extracellular passenger part. The type VI secretion system (T6SS) is composed of 13-14 core proteins, and the structure can be divided into

doi:10.6342/NTU202000295

the TssA cap (cap), the sheath complex (sheath), the baseplate (BP), the membrane complex (MC), the Hcp inner tube, and the spike complex (SC). The type VII secretion system (T7SS) exists in Gram-positive bacteria that harbor one lipid bilayer. The type VIII secretion system (T8SS) only spans the outer membrane, and the type IX secretion system (T9SS) consists of 18 proteins that span both the inner and outer membrane. This figure was created with BioRender (https://biorender.com/).

doi:10.6342/NTU202000295

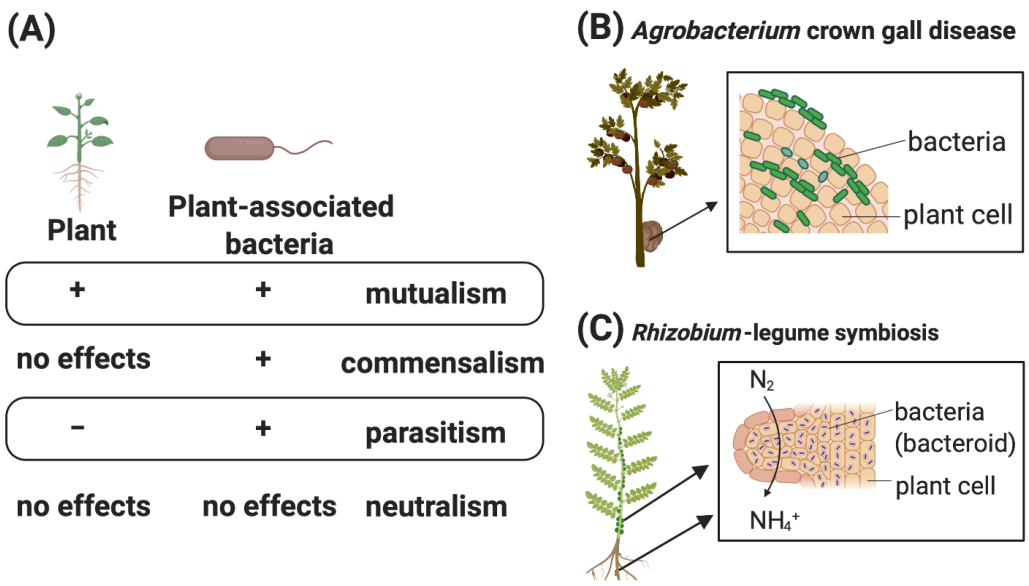

Figure 1-2. Interactions between plant and plant-associated bacteria.

(A) Relationships between plant and plant-associated bacteria. **(B)** Parasitism using *Agrobacterium tumefaciens*-host plant as an example. *A. tumefaciens* causes crown gall disease by forming a tumor on the stem of its plant host. The tumor will become a huge nutrient sink that takes away the nutrient of the plant not only to sustain the crown gall growth, but also to provide intercellular dwelled *A. tumefaciens* cells with both nitrogen and carbon source. Therefore, this interaction is harmful to the host plant but beneficial to the bacteria. **(C)** Mutualism exemplified by the *Rhizobium*-legume symbiotic system. Some of the *Rhizobia* are able to infect legume plants and dwell intracellularly in stem/root nodules, where they transform gaseous nitrogen into biocompatible ammonium that can be used by its host plant. In return, the host plant provides the *Rhizobium* with carbon source so that both members benefit from this interaction. Created with BioRender (https://biorender.com).

1

doi:10.6342/NTU202000295

Chapter 2. Type VI secretion system in *Azorhizobium caulinodans* ORS571

Most of the results described in this chapter has been published as part of a peer reviewed article in the *Molecular Plant-Microbe Interactions*, USA:

Hsiao-Han Lin, Hsin-Mei Huang, Manda Yu, Erh-Min Lai, Hsiao-Lin Chien, and Chi-Te Liu (2018). Functional exploration of the bacterial type VI secretion system in mutualism: *Azorhizobium caulinodans* ORS571–*Sesbania rostrata* as a research model. *Molecular Plant-Microbe Interactions*, **31**: 856-67.doi: 10.1094/MPMI-01-18-0026-R

Contributions:

Hsiao-Han Lin and Chi-Te Liu conceived and designed the experiments. Hsiao-Han Lin performed most of the experiments assisted by Hsin-Mei Huang in mutant construction, mutant confirmation, and nodule staining, by Manda Yu in protein secretion assay and interbacterial competition assay, by Hsiao-Lin Chien in nodulation assay and nitrogen fixation assay. Chi-Te Liu and Erh-Min Lai supervised the execution of the experiments and data analysis assistance.

doi:10.6342/NTU202000295

2.1 Summary

The bacterial type VI secretion system (T6SS) has been considered the armed force of bacteria because it can deliver toxin effectors to prokaryotic or eukaryotic cells for survival and fitness. Although many legume symbiotic rhizobacteria encode T6SS in their genome, the biological function of T6SS in these bacteria is still unclear. To elucidate this issue, we used *Azorhizobium caulinodans* ORS571 and its symbiotic host *Sesbania rostrata* as our research model. By using T6SS gene deletion mutants, we found that T6SS provides *A. caulinodans* with better symbiotic competitiveness when co-infected with a T6SS-lacking strain, as demonstrated by two independent T6SS-deficient mutants. Meanwhile, the symbiotic effectiveness was not affected by T6SS because the nodule phenotype, nodule size, and nodule nitrogen fixation ability did not differ between the T6SS mutants and the wild-type when infected alone. Our data also suggest that under several lab culture conditions tested, *A. caulinodans* showed no T6SS-dependent interbacterial competition activity. Therefore, instead of being an antihost or antibacterial weapon of the bacterium, the T6SS in *A. caulinodans* ORS571 seems to participate specifically in symbiosis by increasing its symbiotic competitiveness.

Keywords: Type VI secretion system, *Rhizobium*-legume symbiosis, symbiotic competitiveness, *Azorhizobium caulinodans*

doi:10.6342/NTU202000295

2.2 Introduction

Gram-negative bacteria have evolved various secretion systems that can deliver specific proteins, polysaccharides, or transferable DNA to the environment or directly into recipient cells to help them gain better fitness in the complex, ever-changing living niche (Tseng, et al. 2009). The Type VI secretion system (T6SS) is one of the systems and can be found in more than a quarter of the sequenced Gram-negative bacterial genome (Coulthurst 2013). T6SS has been considered a nano-weapon able to attack other organisms in a contact-dependent manner (Alcoforado Diniz, et al. 2015, Cianfanelli, et al. 2015, Hachani, et al. 2016). Recent findings also showed its participation in metal ion sequestration in a contact-independent manner (Lin, et al. 2017, Si, et al. 2017).

The T6SS is composed of 13 type six secretion (Tss) core proteins, namely TssA to TssM, which span the double membranes of a Gram-negative bacteria (Basler 2015, Zoued, et al. 2014). The core apparatus can be further divided into the non-secreted and secreted modules. The non-secreted module is composed of the membrane spanning TssJLM complex, the baseplate TssAEFGK complex, and the cytoplasmic contractile sheath TssBC complex. The secretion module of T6SS contains VgrG (or TssI) and Hcp (or TssD), similar to the T4 phage tail tip and tail tube, respectively (Leiman, et al. 2009). The tail tube-like structure is surrounded by the TssBC complex; and when triggered, the TssBC complex will contract and inject the secretion module into the recipient cell (Brackmann, et al. 2017). After injection, ClpV (or TssH) can disassemble the TssBC complex through its AAA+ ATPase, which energizes the disassociation of T6SS (Basler, et al. 2012, Bönemann, et al. 2009). Because the Hcp–VgrG complex is sent outside of the cell when T6SS is in action, the secretion of Hcp or VgrG to the

doi:10.6342/NTU202000295

medium has been widely considered an effective indicator of T6SS activity (Lin, et al. 2013, Schell, et al. 2007, Zheng and Leung 2007). Because of stoichiometric differences, Hcp is more broadly used as a T6SS activity indicator than VgrG.

The outcome of T6SS activity in a contact-dependent manner is the delivery of toxic effector proteins into the recipient cell via the secreted module mentioned previously (Basler, et al. 2013). After the effector proteins reach the recipient cell, the toxicity could lead to cell death if the recipient cell does not synthesize the cognate immunity protein for neutralization (Lien and Lai 2017). These recipient cells can be prokaryote or eukaryote cells. For example, *Vibrio cholera* can use its T6SS to kill bacteria such as *Escherichia coli* or eukaryotic cells such as amoeba (Pukatzki, et al. 2006). Depending on the types of a recipient cell, T6SS-dependent killing activity is referred to as antibacterial activity or anti-eukaryotic activity (Cianfanelli, et al. 2015). However, because of its energy-consuming nature, T6SS is tightly regulated in many species, and its activity can be observed only under certain conditions (Miyata, et al. 2013, Silverman, et al. 2012). For example, secretion of the T6SS-associated Hcp proteins in the plant pathogen *Agrobacterium tumefaciens* was silent with growth in neutral minimal medium (pH 7.0) but activated at acidic pH 5.5 (Wu, et al. 2012), the environment present in the intercellular space and the cell wall of plants (Rayle and Cleland 1992). Furthermore, the T6SS-dependent interbacterial competition among *A. tumefaciens* siblings was evident only inside plant leaves but significantly reduced on an agar surface (Ma, et al. 2014). In the study of a plant growth-promoting bacteria, *Pseudomonas fluorescens* MFE01, the Hcp secretion and antibacterial activity of MFE01 could be observed at 28°C but not 37°C. Because MFE01 is an environmental strain that grows better at 30°C than 37°C, the above results suggest that T6SS has

doi:10.6342/NTU202000295

stronger activity under conditions that resemble its natural habitat (Decoin, et al. 2014). Activation of T6SS was also found in the mammalian gastrointestinal pathogen *Salmonella typhimurium*, in which T6SS-dependent antibacterial activity was observed in the presence of bile salt (Sana, et al. 2016). Therefore, T6SS is more likely to be activated when the bacteria accommodate in their ecological niches for better fitness.

Apart from pathogenic bacteria, T6SS gene homologs are also widely found in legume symbionts (Nelson and Sadowsky 2015). Before T6SS was documented in 2006 (Pukatzki, et al. 2006), insertion of a transposon insertion in *impaired in nodulation J* (*impJ*), later known as *tssK*, in *Rhizobium leguminosarum* RBL5523, enabled the bacterium to establish a successful symbiosis relationship with its non-host legume *Pisum sativum* (Bladergroen, et al. 2003, Roest, et al. 1997). The above results suggest a role of T6SS in *Rhizobium* symbiotic ability. Since the symbiotic relationship between *Rhizobium* and legumes is highly specific, elucidation of how legume plant recognize its microsymbionts from non-symbionts could provide ways to broaden the host range of critical crops in agriculture (Venkateshwaran 2015). Accordingly, T6SS may be one of the factors involved in the symbiotic ability. However, whether and how T6SS impacts symbiotic ability and whether it participates in the antibacterial activity in rhizobia remain to be elucidated.

In this study, we used *Azorhizobium caulinodans* ORS571 as a rhizobium model to reveal the biological function of T6SS. This bacterium can form both root and stem nodules with its tropical legume host *Sesbania rostrata* (Dreyfus and Dommergues 1981a). Our analysis revealed that *A. caulinodans* harbors a complete T6SS gene cluster homolog. Furthermore, transcriptomic data demonstrated that these T6SS gene

doi:10.6342/NTU202000295

homologs in *A. caulinodans* ORS571 are expressed in both free-living and symbiotic conditions (Tsukada, et al. 2009). A successful symbiotic relationship can be evaluated by two important factors: symbiotic effectiveness and symbiotic competitiveness. Symbiotic effectiveness describes how efficient a strain is to form nodules with its host plant, while symbiotic competitiveness describes the ability of a strain to outcompete other strains during infection (Bromfield and Jones 1979). Here, we address whether symbiotic effectiveness and symbiotic competitiveness are affected by T6SS in ORS571. We also performed the antibacterial competition assay to address whether T6SS of *A. caulinodans* harbors antibacterial activity like that of many bacteria. The results show that T6SS provides *A. caulinodans* with better symbiotic competitiveness but not effectiveness.

2.3 Materials and methods

Bacterial strains, media, and growth condition

The bacterial strains used in this study are in Table 2-1. *A. caulinodans* ORS571 was used as a parental strain for constructing mutants. Wild-type and mutant *A. caulinodans* strains were cultured at 37°C in rich tryptone yeast extract medium (TY), minimal medium MMO (Dreyfus, et al. 1983), *nod* gene-inducing medium (MMO with 20 μM naringenin) (Goethals, et al. 1989), or nitrogen-fixing medium L2 (MMO without ammonium sulfate) (Dreyfus, et al. 1983) with appropriate antibiotics unless specified (Liu, et al. 2011). *A. tumefaciens* strains were cultured at 25°C in 523 medium (Kado and Heskett 1970). *E. coli* strains were cultured under 37°C in Luria-Bertani (LB) medium (Bertani 1951). The working concentrations of antibiotics were nalidixic acid 25 μg ml^{-1}, kanamycin 50 μg ml^{-1}, ampicillin 100 μg ml^{-1}, gentamycin 50 μg ml^{-1}, and

doi:10.6342/NTU202000295

streptomycin 12.5 μg ml^{-1}. For doubling time and competitive activity in liquid medium measurements, *A. caulinodans* strains were grown in TY medium either singly or mixed in 1 : 1 ratio with starting optical density (OD_{600}) equals 0.01. Colony forming units were counted. Three biological replicates were performed. Statistical analysis involved single factor ANOVA for each time point. The significance threshold was $p<0.05$.

Plant growth and bacterial inoculation

To facilitate germination, *S. rostrata* seeds were treated with concentrated sulfate for 7 min, followed by tap water flushing for 1 h. The seeds were then washed with sterile water several times, sprayed on trays, covered by sterile vermiculite, then some sterile water was used to wet vermiculite. The seed-containing trays were placed in dark for 3 days at 37°C to germinate. For stem nodule test, the germinated *S. rostrata* were transferred to horticulture soil and grown for another 18 days at 35°C under 24 h light, as described previously (Liu, et al. 2011). The plants were then inoculated with mid-log phase *A. caulinodans* strains with adjustment to OD_{600} 0.5. The stem inoculation was performed by wiping the bacteria onto *S. rostrata* stems using a *A. caulinodans*-soaked kimwipes. Stem nodules were collected at 7 days post inoculation (7dpi). For mixed inoculation assay, two strains of *A. caulinodans* were adjusted to OD_{600} 0.5, mixed at ratio 1 : 1, then the mixture was diluted 50-fold before inoculation. For the root nodule test, the germinated *S. rostrate* were grown in the modified Leonard jars supplied with nitrogen-free Norris medium as described previously (Fernández-López, et al. 1998). *A. caulinodans* strains were adjusted to OD_{600} 0.01, and 50 ml of each strains was used for inoculating the 7-days-post-germination *S. rostrata* seedlings by pouring the bacteria into the soil. Shoot fresh weight and the nodule number were determined at 20 dpi.

doi:10.6342/NTU202000295

Bioinformatics and phylogenetic analysis

The whole genome of *A. caulinodans* ORS571 was obtained from NCBI (accession AP009384.1). We searched T6SS homologous genes by using KEGG pathway (release 68.1) (Kanehisa and Goto 2000) and STRING (v 9.1) (Franceschini, et al. 2013). For the genes lying in the T6SS gene cluster but could not be identified to be related to T6SS, we used Protein Homology/analogY Recognition Engine v2.0 (Phyre2) (Kelley, et al. 2015) and NCBI's Conserved Domain search (CD-Search) (September 2017) (Marchler-Bauer, et al. 2017) to identified conserved domains. Phylogenetic analysis was conducted with MEGA6 (Tamura, et al. 2013). The statistic model used to build the Maximum-likelihood (ML) tree was GTR+G+I based on the partial *tssC* gene (1,400 bp) of Rhizobial symbionts and selected pathogens. ML bootstrap support is indicated. Scale bar indicate the number of substitutions per site for genes. i1 to i5 represent the subgroups of T6SS suggested by Boyer, et al. 2009.

Construction and confirmation of T6SS gene-deletion mutants

Gene-deletion mutants were constructed as described (Liu, et al. 2011). In brief, about 500 bp immediately upstream and downstream of the deleted codons were amplified and combined by using splicing by overlap extension (SOEing) PCR. Primers used in this study are listed in Table 2-2. The products were then cloned into pK18mobsacB. After sequencing the product, the plasmids were transformed into *E. coli* S17-1 as a conjugation donor to ORS571. After conjugating plasmid-harbor *E. coli* S17-1 and ORS571, the single crossover strains were selected by kanamycin. The strains were then grown on TY medium without antibiotics at 37°C for 24 h, and then plated onto a 10% sucrose-containing TY plate for selection of the second crossover strain. The gene deletion in the strains was confirmed by sequencing and by Southern hybridization. For

doi:10.6342/NTU202000295

sequencing, the genomic DNA was first amplified using primers flanking the deleted regions and then subjected to DNA sequencing to ensure complete missing in the deletion codons. Southern blotting and DIG-labeling were conducted according to the DIG Application Manual (Roche, Germany), except adoption of alkaline transfer method in capillary transfer step (Reed and Mann 1985). The following DIG-labeled PCR probes were prepared using primer pairs shown in the parentheses: probe-tssJ (Azc_2586-P5 plus Azc_2586-P6), probe-vgrG (imp_operon-P1 plus Azc_2592-P6), probe-tssL (Azc_2596-P5 plus Azc_2596-P7), probe-tssB (Azc_2599-P8 plus Azc_2599-P9), probe- nodD (nodD-P5 plus nodD -P7), and probe-G (Azc_0874-P3 plus Azc_0874-P4).

Antibody generation

The *hcp2*(*azc_2591*) was amplified using primers Azc_2591-fw and Azc_2591-rv (Table 2-2) and constructed into pET29a upstream of the C-terminal His-tag. pET29a-Hcp2-His(BL21(DE3)) was used for Hcp-His purification. Briefly, the cells were cultured overnight until the stationary phase, and then sub-cultured for another 3 h to reach the mid-log phase. The mid-log phase cells were induced with 0.4 mM isopropyl β-D-1-thiogalactopyranoside (IPTG) for 3 h at 37°C before disruption by using the EmulsiFlex-C3 homogenizer (Avestin Inc., Canada) under 18,000 pounds per square inch (psi). The harvested crude proteins were then purified by using a Ni Sepharose 6 Fast Flow column (GE healthcare, USA). For antibody production, the Ni column-purified proteins were further purified by using HiTrap Q FF (GE healthcare, USA) following the user manual. The purified proteins were then used for antibody production in rabbits (Yao-Hong Biotechnology Inc., Taiwan).

doi:10.6342/NTU202000295

Protein secretion assay

The secretion assay for *A. caulinodans* and *A. tumefaciens* strains was performed as described (Lin, et al. 2014) unless specified. *A. caulinodans* strains were adjusted to OD_{600} 1.0 with TY medium, and then grown at 37°C for another 6 h before they were harvested at 4°C, 8000 rcf for 10 min. The pellet was used as a cellular protein sample and the supernatant as an extracellular protein sample. The pellet was mixed with 2x protein sample buffer directly, boiled for 10 min, and then centrifuged at 4°C, 10,000 rcf for 10 min to remove cell debris. Supernatant was passed through a 0.22-μm filter (Millipore, USA) first, then each milliliter of sample was mixed with 30 μL of 1% sodium deoxycholate and incubated on ice for 10 min before the addition of 150 μL trichloroacetic acid (TCA) in each sample for overnight incubation at 4°C. The TCA-precipitated supernatant was centrifuged at 4°C, 16,000 rcf for 30 min, and then all liquid was carefully removed. The remaining protein pellet was resuspended with 10 μL of 1 M Tris-base (original pH), followed by adding 10 μL of 2x protein sample buffer.

Western blot analysis

Proteins resolved by 12.5% SDS-PAGE were transferred to the nitrocellulose membrane (Millipore, USA), and then incubated at room temperature for 1 h with the primary polyclonal antibody against Hcp encoded by *A. tumefaciens* (anti-C58Hcp, dilution 1:2500) as described in Lin, et al., 2014 and against Hcp2-His (anti-AcHcp, dilution 1:5000) generated by rabbit immunization (Yao-Hong Biotechnology Inc., Taiwan), then the horseradish peroxidease-conjugated goat anti-rabbit secondary antibody (dilution 1:10000) (Millipore, USA) at room temperature for 1 h. Chemiluminescent was used for signal development and visualization by the BioSpectrum AC Imaging system (UVP, USA).

doi:10.6342/NTU202000295

Nitrogen-fixing activities of bacteria cultures

Nitrogen fixing activities of free-living bacteria were determined by acetylene reduction assay (ARA) and defined as C_2H_4 produced per hour per OD_{600}. Bacteria were grown in TY until mid-log phase (OD_{600} 0.5-0.7), and then washed by L2 medium for three times. The L2-mdeium resuspended bacteria were adjusted to OD_{600} 0.1, and 2 mL were put into an 18-mL Hungate type tube. The air in the headspace of tube was replaced with 10% C_2H_2, 3% O_2, and 87% N_2. The samples were incubated at 37°C, 180 rpm, for 1 h, and then 500 μL of the sample was injected into a gas chromatography G3000 (HITACHI, Japan) equipped with a HayeSep T 80/100 volume (Supelco, USA). Statistical analysis involved single factor ANOVA followed by Tukey's HSD. The significance threshold was $p<0.05$.

Symbiotic nitrogen-fixing activities of stem nodules

Nitrogen fixing activities of stem nodules were determined by acetylene reduction assay (ARA) and defined as C_2H_4 produced per hour per gram nodule fresh weight. Stem nodules were peeled from plants and placed into 18-mL Hungate type tubes. The air in the headspace of tube was replaced with 10% C_2H_2. The samples were then incubated at 37°C for 1 h. Then 500 μL of the sample was injected into a gas chromatography G3000 (HITACHI, Japan) equipped with a HayeSep T 80/100 volume (Supelco, USA). Fresh weight of the stem-nodule was measured. Statistical analysis involved single factor ANOVA. The significance threshold was $p<0.05$.

Antibacterial competition assay

A. caulinodans ORS571 and its derivative strains, *A. tumefaciens* C58, and *E. coli* strain DH10B harboring pRL662 were used for antibacterial competition assay. Bacterial

doi:10.6342/NTU202000295

cultures were washed with 0.9% NaCl (w/v) and adjusted to OD_{600} 1.0 for *A. caulinodans* and 0.01 for *A. tumefaciens* or *E. coli*. Then cultures were mixed at equal volume (ratio 100 : 1), and 10 μL of the mixture was spotted on MMO or TY plates. The incubating temperature for *A. cauilinodans* and *E. coli* competition was 37°C, with 25°C used for competition between *A. caulinodans* and *A. tumefaciens*. After incubation for 6 h, bacterial colonies were collected and resuspended in 1 mL 0.9% NaCl (w/v). The suspension was then serially diluted, and then 100 μL of each dilution was spread on 523 agar for *A. tumefaciens* and on Luria-Bertani agar for *E. coli* with appropriate antibiotics for recovery. The procedure used for *A. caulinodans* ORS571 against the T6SS-deficient derivatives were the same as mentioned above with minor modifications. The ratio was 50 : 1 and the incubation time was 16 h. Fifteen parts per million (ppm) streptomycin was used for *A. tumefaciens* recovery and 20 ppm gentamycin for *E. coli* and *A. caulinodans* recovery. All results were obtained from at least two independent experiments. Statistical analysis involved single-factor ANOVA with $p<0.05$ for statistical significance.

Mixed inoculation assay

To determine nodule occupancy of respective pairwise inoculation, we tagged ORS571 and Δ*imp* with β-glucuronidase (GUS) or β-galactosidase (LacZ) reporter and named the counterparts ORS571(pGusA), ORS571(pLacZ), Δ*imp*(pGusA), and Δ*imp*(pLacZ), respectively (Table 2-3). For any pairwise strain combination, they were mixed equally before inoculating on the stem of *S. rostrate*. *S. rostrata* was infected as described in the plant growth and bacterial inoculation section. The 7-dpi nodule was cut in half, immersed in phosphate buffer (pH 7.5) before all samples were collected. For GUS staining, nodules were fixed with acetone for 1 h, then washed by phosphate buffer for

doi:10.6342/NTU202000295

three times. Then the nodules were stained with GUS substrate solution [$K_3Fe(CN_6)$ 2.5 mM, $K_4Fe(CN_6)$ 500 mM, 0. 5% (v/v) Triton X-100, phosphate buffer 0.1 M (pH 7.5), 0. 5 mg mL^{-1} 5-bromo-4-chloro-3-indolyl-β-D-glucuronic acid (X-Gluc)]. For LacZ staining, the nodules were fixed with 1.25% (v/v) glutaraldehyde for 1 h, washed with phosphate buffer for 3 times, then stained with LacZ substrate solution [$K_3Fe(CN_6)$ 2.5 mM, $K_4Fe(CN_6)$ 500 mM, 0. 5% (v/v) Triton X-100, phosphate buffer 0.1 M (pH 7.5), 0.8 mg ml^{-1} 5-bromo-4-chloro-3-indolyl-β-D-galactopyranoside (X-Gal)]. Both GUS and LacZ staining was performed overnight before observation. Each data point represents the nodule occupancy from all of the nodule infection zones of a single plant, and each group contains 15 plants. As the population distribution was not normally distributed, we used non-parametric statistics. Wilcoxon signed rank test with continuity correction test was used for statistical analysis with $p<0.01$ for statistical significance.

S. rostrata seedling colonization assay

The *S. rostrata* seedling colonization assay was performed as described by Liu, et al. (Liu, et al. 2017) with a few modifications. In brief, bacterial were grown separately and adjusted to OD_{600} 0.5, then mixed in 1 : 1 ratio, and used for immersing 2-day-old *S. rostrata* seedlings for 24 h. At 24 hours post inoculation, the seedlings were taken out, washed by sterile water for four times to remove the unattached bacteria, homogenized and suspended in sterile water. The suspensions were serially diluted and then spread on plate for colony counting. Three independent experiments were performed.

doi:10.6342/NTU202000295

2.4 Results

Gene cluster of T6SS in *A. caulinodans* is closely related to those in *R. leguminosarum* and *A. tumefaciens*

We used KEGG pathway (Kanehisa and Goto 2000), STRING 9.1 (Franceschini, et al. 2013), Phyre2 (Kelley, et al. 2015), and NCBI's Conserved Domain Search (Marchler-Bauer, et al. 2017) to search for the homologs of T6SS in the *A. caulinodans* ORS571 genome (NCBI accession AP009384.1). The genome harbors one deduced T6SS gene cluster (*azc_2586* to *azc_2605*) (Figure 2-1A and Table 2-3). Two *hcp* homologs were found in the T6SS gene cluster (*azc_2589* and *azc_2591*), but only one *vgrG* homolog (*azc_2592*) was identified in ORS571. We also identified an *hcp* homolog (*azc_0275*) that lies outside of this T6SS cluster (Figure 2-1A and Table 2-3). For clarity, we annotated the *hcp* homologs residing in the main cluster as *hcp1* (*azc_2589*) and *hcp2* (*azc_2591*) and the one that resides outside the main cluster as *hcp3* (*azc_0275*). The sequences of *hcp1*, *hcp2*, and *hcp3* share 57%, 56%, and 54% amino acid identity, respectively, with the *hcp* of *A. tumefaciens* C58 (*atu4345*). Some genes within the cluster did not show homology to T6SS core apparatus components, T6SS-associated genes (*tag*), or any known T6SS effectors or immunity proteins. These genes are *azc_2588*, *azc_2590*, and *azc_2593* (Figure 2-1A and Table 2-3). Bioinformatics analysis revealed that *azc_2588* is a putative SAM-dependent methyltransferase, but no reliable conserved domain could be identified in *azc_2590* and *azc_2593*. Intriguingly, although we could not find any conserved domain in *azc_2590*, it showed homology to *azc_0274*, which lies downstream of *hcp3* (Figure 2-1A). We also analyzed the two genes that lie downstream of the T6SS main cluster: *azc_2606* and *azc_2607*. Although the *azc_2606* was annotated as *ubiE* previously (Lee, et al. 2008), we conducted a protein BLAST search and found the alignment coverage between Azc_2606 (UniProt

doi:10.6342/NTU202000295

A8IB41) and *E. coli ubiE* (UniProt P0A887) was 22%, and only 24% identity in the aligned region (data not shown). We further analyzed this gene by NCBI Conserved Domain Search and found that the *azc_2606* harbored a SAM-dependent methyltransferase domain (E-value 1.14e-33) and a methyltransferase regulatory domain (E-value 7.07e-12). On the other hand, the *azc_2607* encodes a putative *thiC* gene involved in thiamine biosynthesis (Suzuki, et al. 2007).

We then performed phylogenetic clustering of T6SS of ORS571 by using conservative *tssC* genes against selected nodule-forming symbionts and some pathogens (Figure 2-1B). The *tssC* gene was chosen for the comparison because it is more conserved than the other T6SS genes, such as *tssF*, *tssG*, and *tssM* (Barret, et al. 2013). T6SS subgroups (group i1 to i5) defined by genome-wide analyses with sequenced bacteria (Barret, et al. 2013) were also included (Figure 2-1B). Unlike the phylogenetics results previously reported with 16S rDNA, showing that *A. caulinodans* ORS571 is related more to *Bradyrhizobium japonicum* USDA110 than to *Rhizobium leguminosarum* or *Mesorhizobium loti* (Lee, et al. 2008), the T6SS of *A. caulinodans* ORS571 is separated from that of *B. japonicum* and *M. loti*. Meanwhile, the T6SS of ORS571 was grouped with those of *R. leguminosarum*, the well-known plant growth promoting bacterium (PGPB) *Azospirillum lipoferum* 4B, and the plant pathogen *Agrobacterium tumefaciens* C58, all belonging to T6SS group V (i5) according to (Boyer, et al. 2009) (Figure 2-1B).

T6SS hallmark protein Hcp detected in the cellular but not extracellular fraction of *A. caulinodans* ORS571

The T6SS homologous genes in *A. caulinodans* ORS571 were expressed when cultured in rich tryptone-yeast medium (TY), minimal medium (MMO), *nod* gene-inducing

doi:10.6342/NTU202000295

medium (MMO with 20 μM naringenin), and in the symbiotic state (bacteroid) (Tsukada, et al. 2009). Because Hcp is considered the hallmark protein of T6SS and its secretion reflects T6SS activity (Haapalainen, et al. 2012, Lin, et al. 2013, Murdoch, et al. 2011), we first tried to detect Hcp protein levels in *A. caulinodans* ORS571 by using the Hcp-specific antibody generated against *A. tumefaciens* C58 (anti-C58Hcp) (Wu, et al. 2008). The recombinant *A. caulinodans* Hcp2 and Hcp3 were detectable by anti-C58Hcp (Figure 2-2A), indicating the cross-reactivity of this antibody against azorhizobial Hcp(s). By using this antibody, the azorhizobial Hcp proteins were detected in the cellular fraction under various culture conditions, such as TY, MMO, *nod* gene-inducing medium (MMO with naringenin), and free-living nitrogen-fixing situation (L2 medium) (Figure 2-2A).

To determine the secretion activity and biological functions of T6SS in *A. caulinodans*, we constructed various T6SS in-frame deletion mutants: Δ*tssJ* (Δ*azc_2586*), Δ*tssL* (Δ*azc_2596*), Δ*tssB* (Δ*azc_2599*), and Δ*vgrG* (Δ*azc_2592*). These strains are deficient in the outer-membrane protein TssJ, inner-membrane protein TssL, cytosolic tube sheath component TssB, and spike protein VgrG of T6SS, respectively. In addition, we also disrupted the whole *imp* operon (from *azc_2594* to *azc_2605*) and designated it as Δ*imp* mutant. All mutations were confirmed by both sequencing and Southern hybridization (Appendix Figure 1). As a control for secretion assay, the extracellular Hcp of *A. tumefaciens* C58 was detected in high abundance as reported (Lin, et al. 2014) while Hcp(s) of *A. caulinodans* ORS571 was hardly detectable. The absence of signals could be due to the significantly weaker reactivity of the anti-C58Hcp antibody against Hcp(s) of ORS571 (Figure 2-2A and 2-2B). Hence, we then generated a Hcp antibody against ORS571 (anti-AcHcp) and repeated the secretion assay using anti-

doi:10.6342/NTU202000295

AcHcp.Although signals using anti-AcHcp were improved for cellular Hcp proteins, no Hcp proteins were detected in the extracellular fraction of wild-type or Δ*tssL* grown in any of the media tested (Figure 2-2C). These results suggest that T6SS component Hcp(s) is expressed but not secreted under the *in vitro* growth condition tested.

Free-living nitrogen fixing ability and the cell morphology or growth rate were not altered in T6SS mutants

We then observed the phenotypes of T6SS mutants of ORS571 cultured in rich medium (TY), as well as in nitrogen-fixing state (L2). There were no significant differences in morphology (Figure 2-3A, upper panel) and growth rate (Appendix Figure 2) between the T6SS mutants and wild-type when cultured in rich medium. Under free-living nitrogen-fixing state, cell morphology (Figure 2-3A, lower panel) showed no significant difference between wild-type and the T6SS mutants as well. The free-living nitrogen fixing activities of the T6SS mutants, which were measured by Acetylene Reduction Assay (ARA), were not significantly different from that of the wild type (Figure 2-3B). The free-living nitrogen fixing activity of the Δ*nodD* was significantly higher than that of the Δ*tssL* but not Δ*imp* (Figure 2-3B). We also measured the OD_{600} of the bacteria that were performing nitrogen fixation, and found there was no significant difference among them (data not shown). Overall, these results indicated that lack of T6SS does not seem to affect the vegetative growth of *A. caulinodans*.

T6SS-dependent antibacterial activity was not observed in *A. caulinodans*

No Hcp secretion could be detected under the growth conditions tested, but the T6SS machine may be assembled for effector delivery only when interacting with recipient cells. To examine the T6SS-mediated antibacterial activity of ORS571, we used *E. coli*

doi:10.6342/NTU202000295

DH10B or *A. tumefaciens* as the recipient cells in the interbacterial competition assay. *E. coli* DH10B was chosen because it has been widely used as a susceptible recipient in T6SS-mediated antibacterial competition assays, and it can also be cultured under 37°C (Basler, et al. 2013, Decoin, et al. 2014, Ma, et al. 2014). *A. tumefaciens* was chosen because it is a soil-borne plant pathogen but also because its antibacterial activity has been well demonstrated (Ma, et al. 2014). *E. coli* survival did not differ under co-culture with ORS571, or with any T6SS-deficient mutants, or *E. coli* only (labeled in --) in either MMO (Figure 2-4A) or rich medium (Figure 2-4B). Therefore, *A. caulinodans* may not have antibacterial activity against *E. coli*. For interbacterial competition assay against *A. tumefaciens*, we used MMO (Figure 2-4C), TY (Figure 4D), or tobacco leaves (i.e., *in planta* situation) (Figure 4E) as the competition environments. Similar to the results of *E. coli*, the survival of *A. tumefaciens* C58 cells remained at similar levels under co-culture with ORS571, with any T6SS-deficiency mutants, or *A. tumefaciens* itself under all conditions tested. In addition to the above-mentioned interbacterial competitive assays with attacker to recipient as 100 : 1 ratio, no T6SS-dependent antibacterial activity could be observed in *A. caulinodans* under co-culture at various ratios of attacker to recipient, including 1 : 1, 10 : 1 (data not shown). Thus, we conclude that no direct antibacterial activity of T6SS of *A. caulinodans* is present at least in our tested conditions.

Deletion of T6SS had no adverse effects on symbiotic effectiveness

To understand whether T6SS interferes with the ability of ORS571 to form efficient symbiotic nodules, we inoculated the ORS571 and its derivatives on either stem or root of *S. rostrata*, and observed the phenotype of stem nodules at 7 days post-infection (dpi) as well as that of root nodules at 20 dpi. The longitudinal sections of the stem nodules

doi:10.6342/NTU202000295

infected with T6SS mutants or ORS571 showed red color, which indicates active nitrogen fixation in these nodules (Figure 2-5A). Also, the symbiotic bacteria or the bacteroids fully occupied the infected plant cells in both ORS571- and Δ*imp*-infected nodules (Figure 2-5B). Moreover, the size of the nodules was comparable among the wild type and mutants (Figure 2-5C). Nitrogen-fixing ability did not differ between nodules infected with ORS571 and any of the T6SS deletion mutants (Figure 2-5D). On the other hand, root nodules cultured under nitrogen-free condition was also evaluated. All the *A. caulinodans* infected groups had shoot weight significantly higher than that of the nitrogen-free group (-N) and significantly lower than that of the nitrogen supply group (+N). However, there was no significant difference between wild type or T6SS mutant *A. caulinodans* infected groups (Figure 2-6A). Besides, there was no significant difference in the nodule number among the groups infected by the ORS571 derivatives (Figure 2-6B). Taken together, it suggests that deficient of T6SS in *A. caulinodans* does not affect its symbiotic effectiveness in *S. rostrata*.

Deletion of T6SS reduced the symbiotic competitiveness of *A. caulinodans*

In addition to symbiotic effectiveness, symbiotic competitiveness is considered as a major factor for successful nodulation (Bromfield and Jones 1979). Symbiotic competitiveness can be measured by the nodule occupancy rate of each rhizobium strain under mixed inoculation (Ji, et al. 2017, Wielbo, et al. 2010). To observe nodule occupancies, we tagged ORS571 and Δ*imp* with β-glucuronidase (GUS) or β-galactosidase (LacZ) reporter and named the counterparts ORS571(pGusA), ORS571(pLacZ), Δ*imp*(pGusA), and Δ*imp*(pLacZ), respectively (Figure 2-7A). The stem nodules were formed synchronously and fix nitrogen at 7 dpi with the pairwise strain combination (Figure 2-7B and 2-7C). The harvested stem nodules were cut in

doi:10.6342/NTU202000295

half, and the total number of GUS or lacZ hits in individual nodule were determined by histochemical staining in the equal parts of the manually dissected nodule (Figure 2-7D and 2-7E). With the mixed inoculation of ORS571(pGusA) and Δ*imp*(pLacZ), the GUS-marked nodules significantly outnumbered the LacZ-marked ones, which indicates higher nodule occupancy rate for ORS571 than Δ*imp* (p= 3.17x10^{-3}, Figure 2-7F). Although not statistically significant, we noted that bacteria tagged with *gusA* showed generally higher infection rate than those tagged with *lacZ*, whether in the ORS571(pGusA) plus ORS571(pLacZ) or Δ*imp*(pGusA) plus Δ*imp*(pLacZ) group (Figure 2-7F). To confirm the results from ORS571(pGusA) and Δ*imp*(pLacZ) was not due to reporter bias, we switched the labeling to verify the distinctive nodule occupancy rate was not derived from the experimental system itself. As shown for the ORS571(pLacZ) plus Δ*imp*(pGusA) group (Figure 2-7F), despite the Δ*imp* possessing the GusA-tagged advantage, the median nodule occupancy rate was even higher for ORS571(pLacZ) than Δ*imp*(pGusA), although the difference was less pronounced (p>0.01). We further confirmed such phenomenon by using ORS571 and another T6SS-deficient mutant, Δ*tssL*, as the competition pair. In group ORS571(pGusA) plus Δ*tssL* (pLacZ), we also found that the occupancy of ORS571 was significantly higher than that of T6SS mutant (p= 4.27x10^{-4}, Figure 2-8). Accordingly, our results suggest that T6SS enhances *A. caulinodans* in symbiotic competitiveness.

To verify whether the higher infection rate for ORS571 under symbiosis derived from its higher competitive activity under vegetative state, we tested their antibacterial activities and found no significant difference between wild type and the T6SS-deficient derivatives under either nutrient-rich (TY) or minimal nutrient (MMO) medium (Figure 2-9A). We also determined the growth of these bacteria in minimal nutrient medium

doi:10.6342/NTU202000295

either singly (Figure 2-9B) or in equimolar mixtures (Figure 2-9C and 2-9D) and found no significant difference among them. Furthermore, we attempted to study the compatibility between the individual bacterium and the host by conducting a colonization assay with *Sesbania* seedlings. As shown in Figure 2-9E, it did not differ significantly among the test groups, suggesting the recovery of ORS571 from host plant was no better than that of the T6SS-deficient derivatives.

2.5 Discussion

In this research, we identified a complete T6SS core apparatus homolog in *A. caulinodans* ORS571 genome interspersed with several unknown functional genes (*azc_2588*, *azc_2590*, and *azc_2593*) (Figure 2-1A and Table 2-3). On the other hand, although two genes (*azc_2606 and azc_2607*) lay downstream of *azc_2605* (*tssG*), the latter gene, *azc_2607*, is not likely part of the T6SS operon due to the following reasons. First, the gap between *azc_2606 and azc_2607* is 382 bp, and there would be a thiamin pyrophosphate regulon at -245 of *azc_2607*, which is located in the 5'-untranslated region of the thiamin metabolism-related gene (Novichkov, et al. 2013) according to the RegPrecise database (Dec. 2017). Second, we noted that the expression dynamics of the *azc_2607* gene were not synchronized with its upstream genes (*azc_2601- azc_2606*) under minimal medium, nod-factor induction, or bacterioid condition (Tsukada, et al. 2009). Accordingly, it suggests that the *azc_2607* is regulated separately from the *imp* operon. We deduced that four unknown functional genes: *azc_2588*, *azc_2590*, *azc_2593*, and *azc_2606*, are associated with the T6SS cluster in *A. caulinodans*.

doi:10.6342/NTU202000295

The T6SS gene cluster is widespread in legume symbionts (Nelson and Sadowsky 2015), but little is known about their biological function(s). With *A. caulinodans* used as a model, our data suggest that T6SS could confer *A. caulinodans* with better symbiotic competitiveness, which enables it to outcompete its T6SS-lacking counterparts, either Δ*imp* or Δ*tssL*, in a mixed inoculation situation (Figure 2-7 and Figure 2-8). Such outcompete was unlikely due to T6SS-dependent antibacterial activity under free-living states between ORS571 and Δ*imp* (Figure 2-9A), which meet our expectation as the genes mutated in Δ*imp* were homologs known as T6SS core apparatus rather than as putative toxin or immunity proteins (Figure 2-1 and Table 2-3). The advantage of the wild-type ORS571 in symbiotic competitiveness was also unlikely due to the superior doubling time and competitive activity in low-nutrient microenvironment as the colony forming units of ORS571 and Δ*imp* did not differ when cultured in MMO medium either singly (Figure 2-9B) or in a mixture (Figure 2-9C and 2-9D). *S. rostrata* seedling colonization assay also demonstrated that the recovery of ORS571 was no better than that of Δ*imp* (Figure 2-9E). This result suggests that the symbiotic competitiveness may not result from colonization ability, which has also been demonstrated before (Duodu, et al. 2008). The previous study that *R. leguminosarum* with T6SS disruption was able to form an effective nodule with its non-host legume *P. sativum* (Bladergroen, et al. 2003) could echo with our observations that T6SS of *Rhizobium* play an role in symbiosis. However, with *R. leguminosarum*, the T6SS seems to play a negative role in the plant–microbe interaction. *Rhizobium* may utilize the T6SS to obtain benefits from interacting with its host but have a negative role with its non-host.

doi:10.6342/NTU202000295

As no interbacterial competition advantages could be detected with the T6SS of *A. caulinodans* when interacting with *E. coli* or *A. tumefaciens* (both *in vitro* and *in planta*) (Figure 2-4), the T6SS of *A. caulinodans* is unlikely to function as an antibacterial weapon. The negative results of our interbacterial competition assay are also supported by the lack of putative bacterial toxin and immunity pairs identified in our comprehensive bioinformatics analysis. Furthermore, instead of being a bacterial nano-weapon, the T6SS could serve as an intercellular communication signal (Gallique, et al. 2017a). The cell–cell communication function of T6SS has been demonstrated in several bacteria such as *Proteus mirabilis*, *Pseudomonas fluorescens*, and *Pseudomonas aeruginosa* (Gallique, et al. 2017b, Lin, et al. 2017, Wenren, et al. 2013). In those cases, the T6SS participates in interbacterial communication and provides the bacterium with better fitness (Gallique, et al. 2017a). Therefore, rhizobium may use the T6SS as a rhizobium–plant cell communication system that consists of the recognition code, which could be achieved by secreting some yet-to-be identified T6SS-dependent effectors during the infection process.

The *azc_2588*, *azc_2590*, and *azc_2593*, which are each encoded adjacent to *hcp1* (*azc_2589*), *hcp2* (*azc_2591*), and *vgrG*/*tssI* (*azc_2592*) (Figure 2-1), could be the potential effectors. The Hcp serves as a tube component of the T6SS tail structure and also functions as a chaperone and receptor for certain effectors (Silverman, et al. 2013), and the VgrG is the tip of the T6SS and is usually associated with the adapter and effector encoded in its neighboring genes (Lien and Lai 2017). The N-terminal half of the Azc_2590 and Azc_0274 showed similarity to the T3SS effector HopM1 of *Pseudomonas syringae* B728a (bitscore 60.8) using STRING (v.9.1) (Franceschini, et al. 2013) but not STRING (v.11) (Szklarczyk, et al. 2018). Although the authors were

doi:10.6342/NTU202000295

not very confident about this result based on the inconsistency, the result points out that Azc_2590 and Azc_0274 could serve as good effector candidates. The *azc_2588* encodes a protein that contains a putative plant SAM-dependent methyltransferase domain and the *azc_2593* encode a protein of unknown function may also be good candidates of the effector. However, whether these proteins are T6SS effectors and whether they participate in rhizobium–plant cell communication remains elusive.

In this study, we were unable to detect Hcp in the extracellular fraction, a hallmark of T6SS activity, under lab culture conditions (Figure 2-2). As we were unable to observe the T6SS-dependent anti-bacterial activity of *A. caulinodans* by testing the bacterial opponents, including *E. coli*, and soilborne plant pathogen *A. tumefaciens* under various growth conditions (Figure 2-4), the T6SS of *A. caulinodans* may be assembled and executed for Hcp secretion only when sensing specific signal(s) yet to be identified. We are aware of the result that the free-living nitrogen-fixing ability of the Δ*nodD* was significantly higher than that of the Δ*tssL* (Figure 2-3B). However, as the free-living nitrogen-fixing abilities of the ORS571, Δ*tssL*, and Δ*imp* were not significantly different, we concluded that the T6SS is unlikely to participate in free-living nitrogen fixation. In a previous study, Mougous *et al.* reported that under laboratory *in vitro* culture conditions, H1-T6SS of the wild type *P. aeruginosa* PAO1 was not expressed and only activated for Hcp1 expression and secretion when a sensor kinase *retS* gene was mutated (Mougous, et al. 2006). Strikingly, Hcp1 could be detected in pulmonary secretions of cystic fibrosis patients infected with *P. aeruginosa* (Mougous, et al. 2006). Therefore, the T6SS of *A. caulinodans* seems to be repressed by a negative regulator, which awaits future genome-wide screening for identifying the mutants de-repressing Hcp secretion activity.

doi:10.6342/NTU202000295

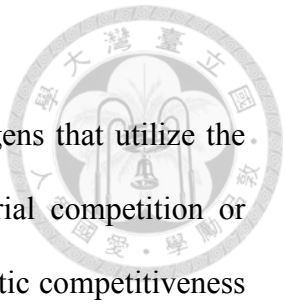

Overall, our data suggest that unlike many animal and plant pathogens that utilize the T6SS as an antibacterial or anti-host nano-weapon for interbacterial competition or pathogenesis, the T6SS of *A. caulinodans* may participate in symbiotic competitiveness but not effectiveness. Such function may be one of the rhizobium-host recognition codes for host specificity, which is an indispensable issue in legume-rhizobium symbiosis indispensable for sustainable agriculture. Thus, our results shed light on T6SS research on rhizobial symbionts and also provide new insights for future attempts at expanding the host range of rhizobium.

doi:10.6342/NTU202000295

Table 2-1. Strains and plasmids used in chapter 2.

Strain or plasmid	Relevant characteristics[a]	Source or reference
***A. caulinodans* strains**		
ORS571	Wild-type; Nx^R	(Dreyfus, et al. 1988)
Δ*imp*_operon	Entire *imp*_operon deletion mutant (from *azc_2594* to *azc_2605*); Nx^R	this study
Δ*tssJ*	Deletion from +7 to +594 of *azc_2586* (*tssJ*, 600 bp); Nx^R	this study
Δ*vgrG*	Deletion from +10 to +2037 *azc_2592* (*vgrG*, 2040 bp); Nx^R	this study
Δ*tssL*	Deletion from -4 to +1467 of *azc_2596* (*tssL*, 1485 bp); Nx^R	this study
Δ*tssB*	Deletion from +1 to +510 of *azc_2599* (*tssB*, 513 bp); Nx^R	this study
ORS571(pLacZ)	ORS571 harboring pLacZ, *lacZ*; Nx^R, Tet^r	this study
ORS571(pGusA)	ORS571 harboring pFGusA, *gusA*; Nx^R, Tet^R	this study
Δ*imp*(pLacZ)	Δ*imp*_operon harboring pLacZ, *lacZ*; Nx^R, Tet^R	this study
Δ*imp*(pGusA)	Δ*imp*_operon harboring pGusA, *gusA*; Nx^R, Tet^R	this study
***E. coli* strains**		
DH5a	*endA1 hsdR17 supE44 thi-1 recA1 gyrA96 relA1 D*(*argF-lacZYA*)*U169 Φ*80*lacZD*M15	Invitrogen
S17-1	Sp^r; RP4 *tra* region, mobilizer strain, for conjugation	(Simon, et al. 1983)
DH10B	F– *mcr*A Δ(*mrr-hsd*RMS-*mcr*BC) Φ80*lacZ*ΔM15 Δ*lac*X74 *rec*A1 *end*A1 *ara*D139 Δ(*ara leu*) 7697 *gal*U *gal*K *rps*L *nup*G λ–	Invitrogen
***A. tumefaciens* strains**		
C58	Wild-type strain containing nopaline-type plasmid pTiC58	(Lin and Kado 1977)
Δ*t6ss*	entire *t6ss* gene cluster deletion mutant	(Lin, et al. 2014)
Plasmids		
pK18mobsacB	*sacB* mobolizable cloning vector, Km^R	(Schäfer, et al. 1994)
pRL662	broad-host range vector derived from pBBR1MCS-2, Gm^R	(Vergunst, et al. 2000)
pK18-Δ*imp*	plasmid used to generate ORS571-Δ*imp*_operon, pK18mobsacB backbone, Km^R	this study
pK18-Δ*tssJ*	plasmid used to generate ORS571-Δ*tssJ*, pK18mobsacB backbone, Km^R	this study
pK18-Δ*vgrG*	plasmid used to generate ORS571-Δ*vgrG*, pK18mobsacB backbone, Km^R	this study
pK18-Δ*tssL*	plasmid used to generate ORS571-Δ*tssL*, pK18mobsacB backbone, Km^R	this study
pK18-Δ*tssB*	plasmid used to generate ORS571-Δ*tssB*, pK18mobsacB backbone, Km^R	this study
pFAJ1703	promoter assay vector, RK2-derived, with promoterless *lacZ*, Amp^R, Tet^R	(Dombrecht, et al. 2001)
pLacZ	pFAJ1703 derived, constitutive *lacZ* expression, Amp^R, Tet^R	this study
pGusA	pFAJ1703 derived, constitutive *gusA* expression, Amp^R, Tet^R	this study

[a] Nx^R, Tet^R, Km^R, Gm^R, Amp^R; Resistance to nalidixic acid, tetracycline, kanamycin, gentamycin, and ampicillin

doi:10.6342/NTU202000295

Table 2-2. Primers used in chapter 2.

Primer	Sequence (5'-3')	Restriction site
Gene deletion and Southern hybridization		
imp_operon-P1	cggaattcCCATCACCATCAAGAACAACC	*Eco*RI
imp_operon-P2	actgagcacccaggcgagGGGCACCATCAGCTTGAGAT	
imp_operon-P3	CTCGCCTGGGTGCTCAGT	
imp_operon-P4	ccgaagcttTAGAAACGGTCAGGGAGCTG	*Hin*dIII
Azc_2586-P1	cggaattcTCTCATCATCGACACCCATC	*Eco*RI
Azc_2586-P2	tagaaaatggtagcgtgcggCTCTTCCCCTTCTGAGCCG	
Azc_2586-P3	CCGCACGCTACCATTTTCTA	
Azc_2586-P4	ccgaagcttCCGTAATGAGCGAGAATGAGC	*Hin*dIII
Azc_2586-P5	CGGGCGCAGGTCATAGAA AAT	
Azc_2586-P6	GCTCAGAAGGGGAAGAGGG	
Azc_2592-P1	cggaattcATCTCAACGCCAACAGGAGA	*Eco*RI
Azc_2592-P2	ctccatcgatcccctctcaGTCACTCATGCGATCCCCTC	
Azc_2592-P3	TGAGAGGGGATCGATGGAG	
Azc_2592-P4	ccgaagcttTCCAGCACCCAGTCATTGTC	*Hin*dIII
Azc_2592-P6	CTCCATCGATCCCCTCTCA	
Azc_2596-P1	cggaattcCCGGTGGAGCAAATTCGAGA	*Eco*RI
Azc_2596-P2	ctattgcggcgtgagaacTCCCTTCCAGTGATCAGGACG	
Azc_2596-P3	GTTCTCACGCCGCAATAG	
Azc_2596-P4	ccgaagcttCGTACCAGGGCAGTTCATATT	*Hin*dIII
Azc_2596-P5	TGATGCTTCCGTCCTGATCA	
Azc_2596-P7	CGACACAGGTTGCTCATTGG	
Azc_2599-P1	gctctagagcCAACCTGCTCAACACTGTCC	*Xba*I
Azc_2599-P2	cttcagctgttcctcgttcgaGAGACTTCCCCGTTGACTG	
Azc_2599-P3	TCGAACGAGGAACAGCTGAAG	
Azc_2599-P4	ccgaagcttGTGGACTGGTCGAACTCAGA	*Hin*dIII
Azc_2599-P8	GCGTCATGGGCGATTTCTC	
Azc_2599-P9	ATCCTCCAGCGACTTAAAGC	
nodD-P1	cggaattcCTCCAGCGCCTTCATCTTCT	*Eco*RI
nodD-P2	ttctgcgctgtccaaaatcatCTCCATCTACCCAGCATCCG	
nodD-P3	ATGATTTTGGACAGCGCAGAA	
nodD-P4	ccgaagcttTTCTGTCTGGCGAGGAAGAG	*Hin*dIII
nodD-P5	CGGATGCTGGGTAGATGGAG	
nodD-P7	CTCTTCGCTGCAGATGTCAC	
Azc_0874-P3	GAAGGCCCGGACGAGATAC	
Azc_0874-P4	ccgaagcttGCGCCTGTCTCCTCCATG	*Hin*dIII
overexpressing Hcp		
Azc0275-rv	gatatacatatgGCTATCTATGTGAACTACGAC	*Nde*I
Azc0275-fw	ccgaagcttGCTCTTGGTGGTCGCGAG	*Hin*dIII
Azc2591-fw	gatatacatatgGCCATCTACGTTAAATATGAC	*Nde*I
Azc2591-rv	ccgaagcttCGAGCTCTTGGTGGTGGC	*Hin*dIII
GUS, LacZ tagged		
pNodD-fw	ggggtaccccAGCCCGTCGGTGATTATCCA	*Kpn*I
pNodD-rv	gctctagagcCTCTTCGCTGCAGATGTCAC	*Xba*I

doi:10.6342/NTU202000295

Table 2-3. Type VI secretion system gene homologous analysis in *A. caulinodans* ORS571 and their putative function.

ORF	Homologues	*tss* name	putative function	Source
azc_0274			homology to *azc_2590*	STING 9.1
azc_0275	*hcp*	*tssD*	secretion tube	KEGG
azc_2586	*vasD*	*tssJ*	membrane	KEGG
azc_2587	*clpV*	*tssH*	cytoplasmic disassembler	KEGG
azc_2588			putative SAM-dependent methyltransferases	CD-search, Phyre2
azc_2589	*hcp*	*tssD*	secretion tube	KEGG
azc_2590			homology to *azc_0274*	CD-search, Phyre2
azc_2591	*hcp*	*tssD*	secretion tube	KEGG
azc_2592	*vgrG*	*tssI*	secretion spike	KEGG
azc_2593			unknown function	CD-search, Phyre2
azc_2594	*impI*	*tagH*	T6SS-associated gene, FHA domain-containing protein	STING 9.1
azc_2595	*impJ*	*tssK*	baseplate	STING 9.1
azc_2596	*impK*	*tssL*	membrane	KEGG
azc_2597	*impL*	*tssM*	membrane	KEGG
azc_2598	*impA*	*tssA*	baseplate	STING 9.1
azc_2599	*impB*	*tssB*	cytoplasmic sheath	STING 9.1
azc_2600	*impC*	*tssC41*	cytoplasmic sheath	STING 9.1
azc_2601	*impD*	*tssC40*	cytoplasmic sheath	STING 9.1
azc_2602	*impE*	*tagJ*	T6SS-associated gene	STING 9.1
azc_2603	*impF*	*tssE*	baseplate	STING 9.1
azc_2604	*impG*	*tssF*	baseplate	STING 9.1
azc_2605	*impH*	*tssG*	baseplate	STING 9.1
azc_2606			SAM-dependent methyltransferase	CD-search
azc_2607	*thiC*		thiamine biosynthesis protein	(Lee, et al. 2008)

doi:10.6342/NTU202000295

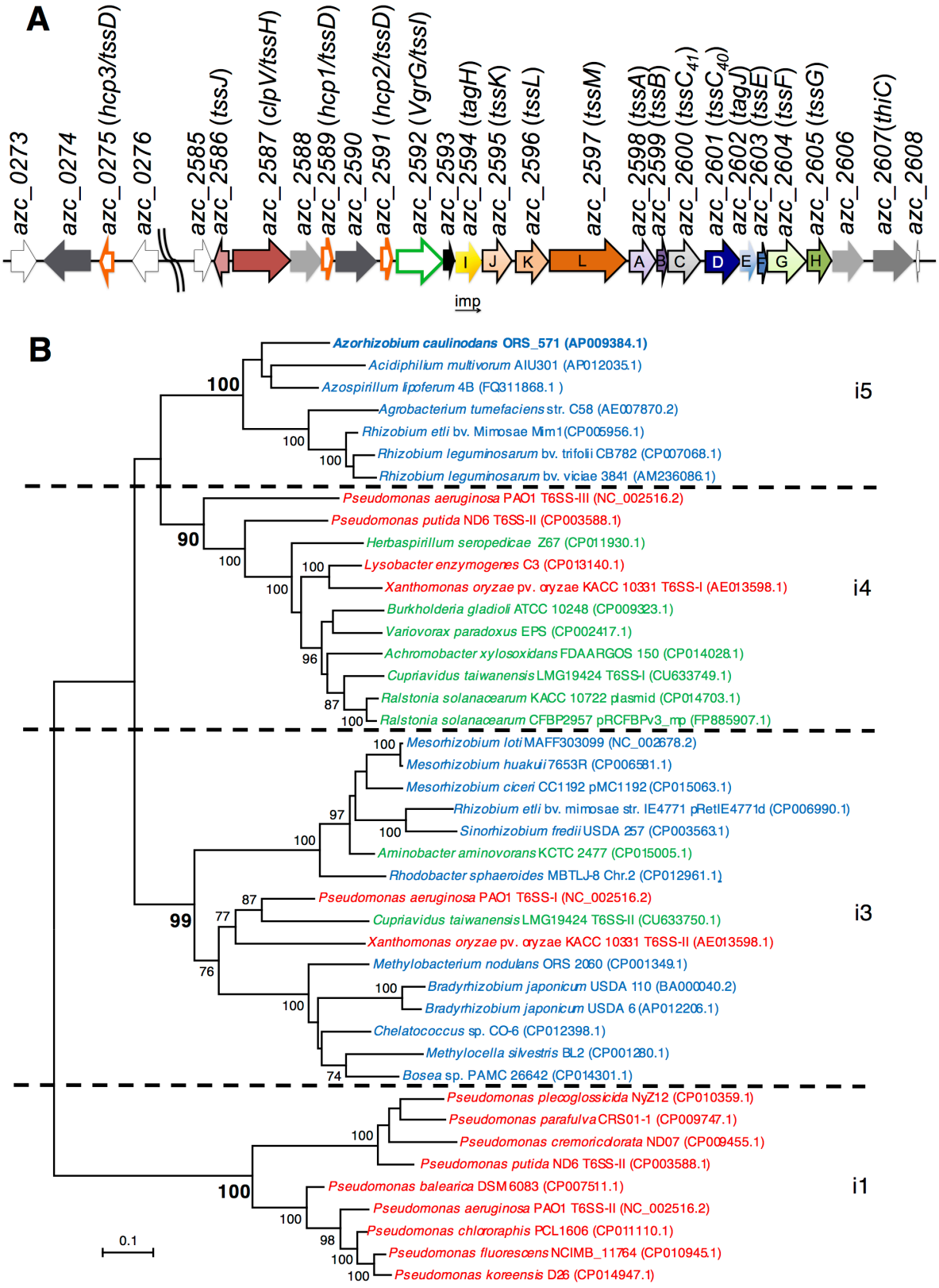

doi:10.6342/NTU202000295

Figure 2-1. T6SS gene cluster in *A. caulinodans* ORS571 and phylogenetic analysis. **(A)** T6SS gene cluster in *A. caulinodans* ORS571. The deduced T6SS conserved non-secreted genes are shown in filled color, with black boxed arrows indicating *tss* genes (type VI secretion) and non-boxed arrows indicating tag genes (type VI secretion-associated gene) based on nomenclature proposed by Shalom et al. (Shalom, et al. 2007). The secreted module *hcp* and *vgrG* genes are shown with orange and green boxed arrows, respectively. Genes with unknown functions (*azc_0274*, *azc_2588*, *acz_2590*, *azc_2593*, and *azc_2606*) are shown with gray arrows. Sequences were retrieved from the whole genome of *A. caulinodans* ORS571 in NCBI accession AP009384.1. (**B)** Maximum-likelihood (ML) tree based on the partial *tssC* gene (1,400 bp) of *Rhizobial* symbionts and selected pathogens. Bacteria that belong to α-, β-, and ɣ-proteobacteria are labeled in blue, green, and red, respectively. Statistics of the ML model used to build the tree was GTR + G + I. ML bootstrap support (≥ 70%) is indicated at each node. The phylogenic analysis involved using MEGA6 (Tamura, et al. 2013). Scale bar indicates the number of substitutions per site of the genes. i1 to i5 represent the subgroups of T6SS suggested by (Boyer, et al. 2009).

doi:10.6342/NTU202000295

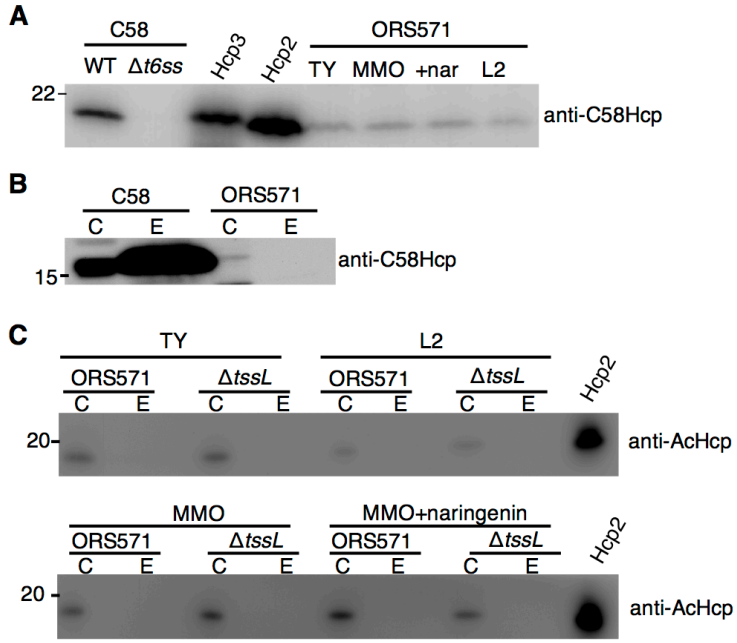

Figure 2-2. T6SS hallmark protein Hcp can be found in cellular but not extracellular fraction of *A. calinodans* ORS571.

(A) Hcp protein detected in the cellular fraction under all culture conditions tested. C58 WT: *A. tumefaciens* C58, C58 Δ*t6ss*: Δ*t6s A. tumefaciens* C58, Hcp3: pET29a-Hcp3(Azc_0275)-His/*E. coli* BL21(DE3), Hcp2: pET29a-Hcp(Azc_2591)-His/*E. coli* BL21 (DE3). *A. caulinodans* ORS571 cultured in TY: rich medium, MMO: minimal medium, MMO+naringenin: MMO with naringenin, representing *nod* gene inducing condition, and L2: the nitrogen-fixing state. **(B)** No Hcp proteins were secreted into TY medium by *A. caulinodans* ORS571 wild type; *A. tumefaciens* C58 was a positive control for Hcp secretion, with anti-C58Hcp used for detecting Hcp expression. **(C)** No Hcp secretion was detected in *A. caulinodans* ORS571 wild type or Δ*tssL* mutant in all culture conditions, with anti-AcHcp used for detecting Hcp expression. C: cellular fraction, E: extracellular fraction.

doi:10.6342/NTU202000295

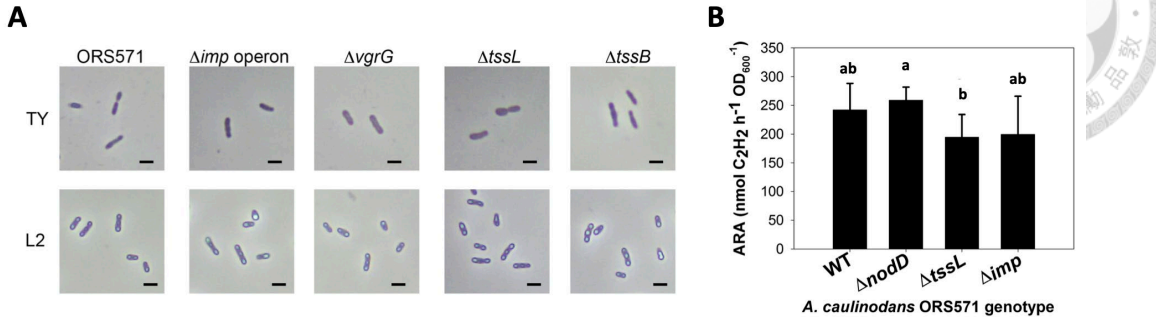

Figure 2-3. Phenotypic observation of the T6SS mutants under free-living state.

(A) Bacterial morphologies were observed either in rich medium TY or in nitrogen fixing medium L2. (**B**) Free-living nitrogen fixing ability measured with acetylene reduction assay (ARA). Figure shows the means ± SD, bars with the same letter are not significantly different at 5% level by TukeyHSD test (n=9).

doi:10.6342/NTU202000295

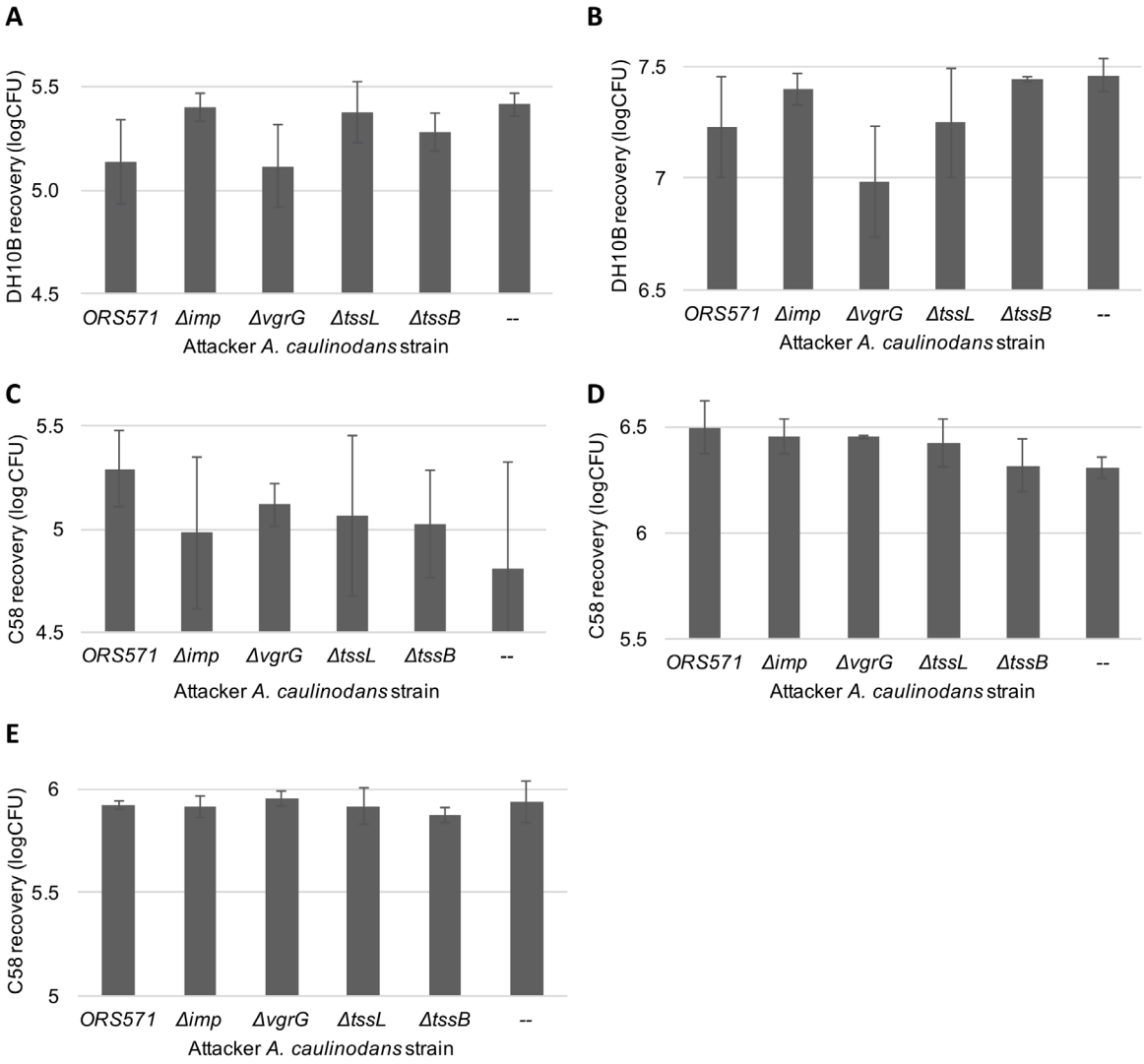

Figure 2-4. *A. caulinodans* did not show T6SS-dependent antibacterial activity.

A. caulinodans cells were co-cultured with *E. coli* DH10B harboring pRL662 plasmid at a ratio of 100 : 1 in (**A**) minimal medium or (**B**) rich medium. The same experiment was also performed between *A. caulinodans* and *A. tumefaciens* in (**C**) minimal medium, (**D**) rich medium, or (**E**) in tobacco leaves. Survival of *E. coli* or *A. tumefaciens* cells was then quantified by resistance to gentamycin and streptomycin, respectively. Group labeled in '–'represents the group without *A. caulinodans* attacker. Data are mean (±SD) results from one representative experiment and similar results were obtained from at least two independent experiments.

doi:10.6342/NTU202000295

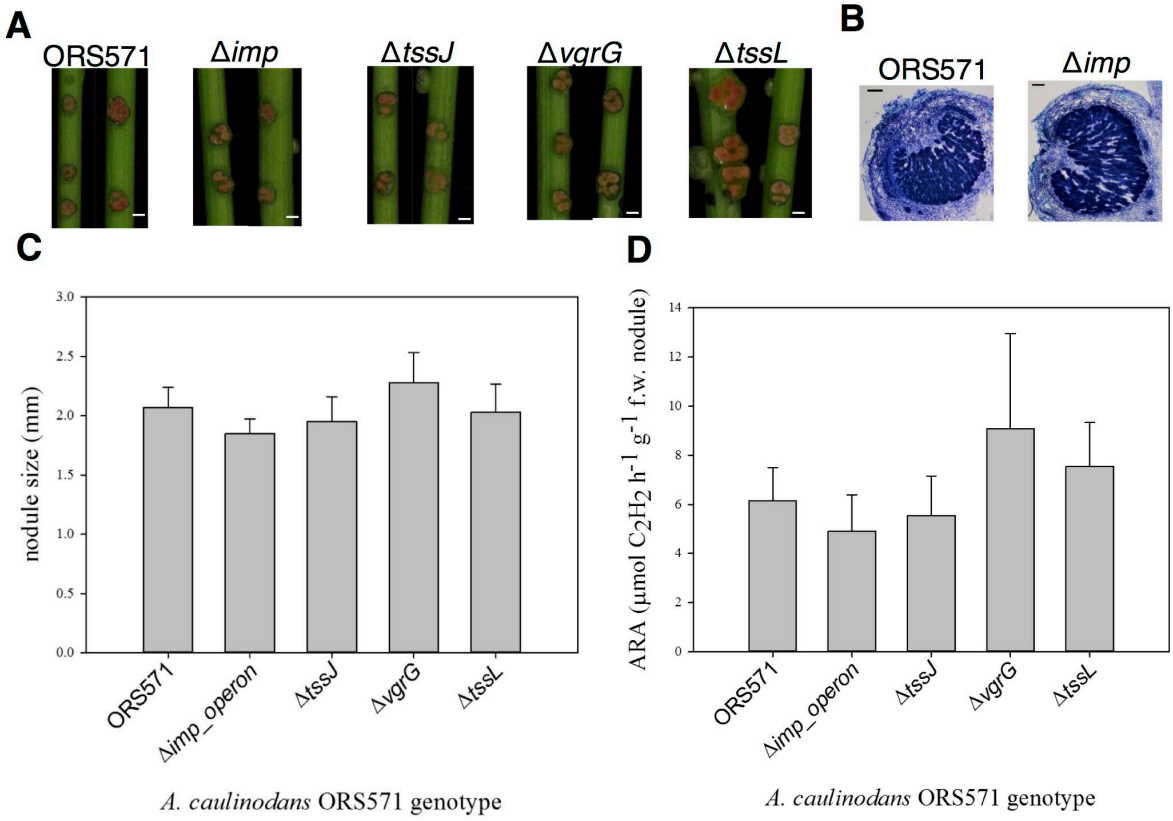

Figure 2-5. Deletion of T6SS had no adverse effects on symbiotic effectiveness.

S. rostrata stem nodules formed after infection by *A. caulinodans* observed at 7 days post-inoculation (dpi). (**A)** Shows longitudinal section of the nodule and (**B)** bacteroid occupancy. (**C)** nodule size and (**D)** nitrogen fixing ability were measured. Scale bar in A is 1 mm, and 100 μm in B. Data are mean (±SD).

doi:10.6342/NTU202000295

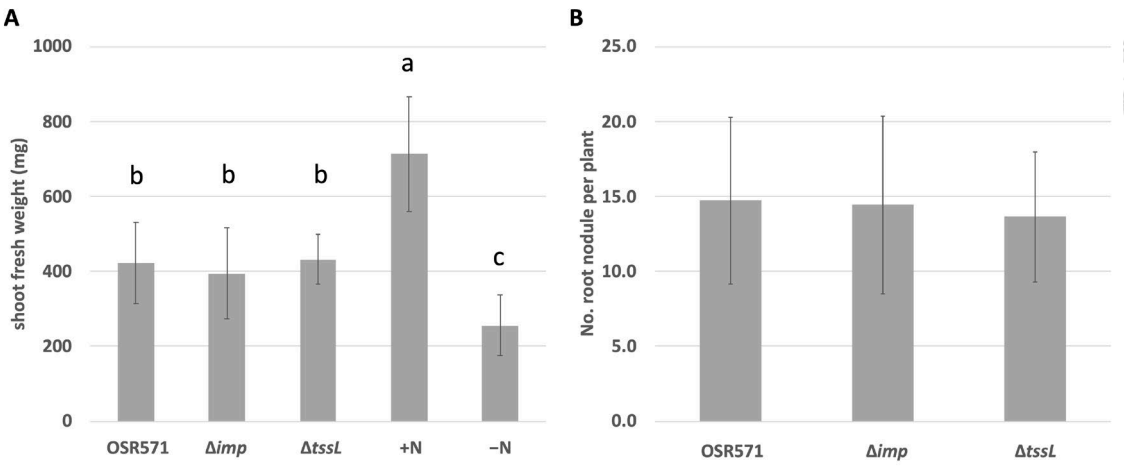

Figure 2-6. Deletion of T6SS had no adverse effects on symbiotic effectiveness in *S. rostrata* root nodules.

(A) shoot fresh weight and (**B**) nodule numbers were analyzed at 20 dpi. Data are mean (±SD) from three independent experiments. +N: supplied with nitrogen, -N: nitrogen-free and inoculation free group. One-way ANOVA with $p<0.05$ and Tukey's HSD were used for statistical analysis.

doi:10.6342/NTU202000295

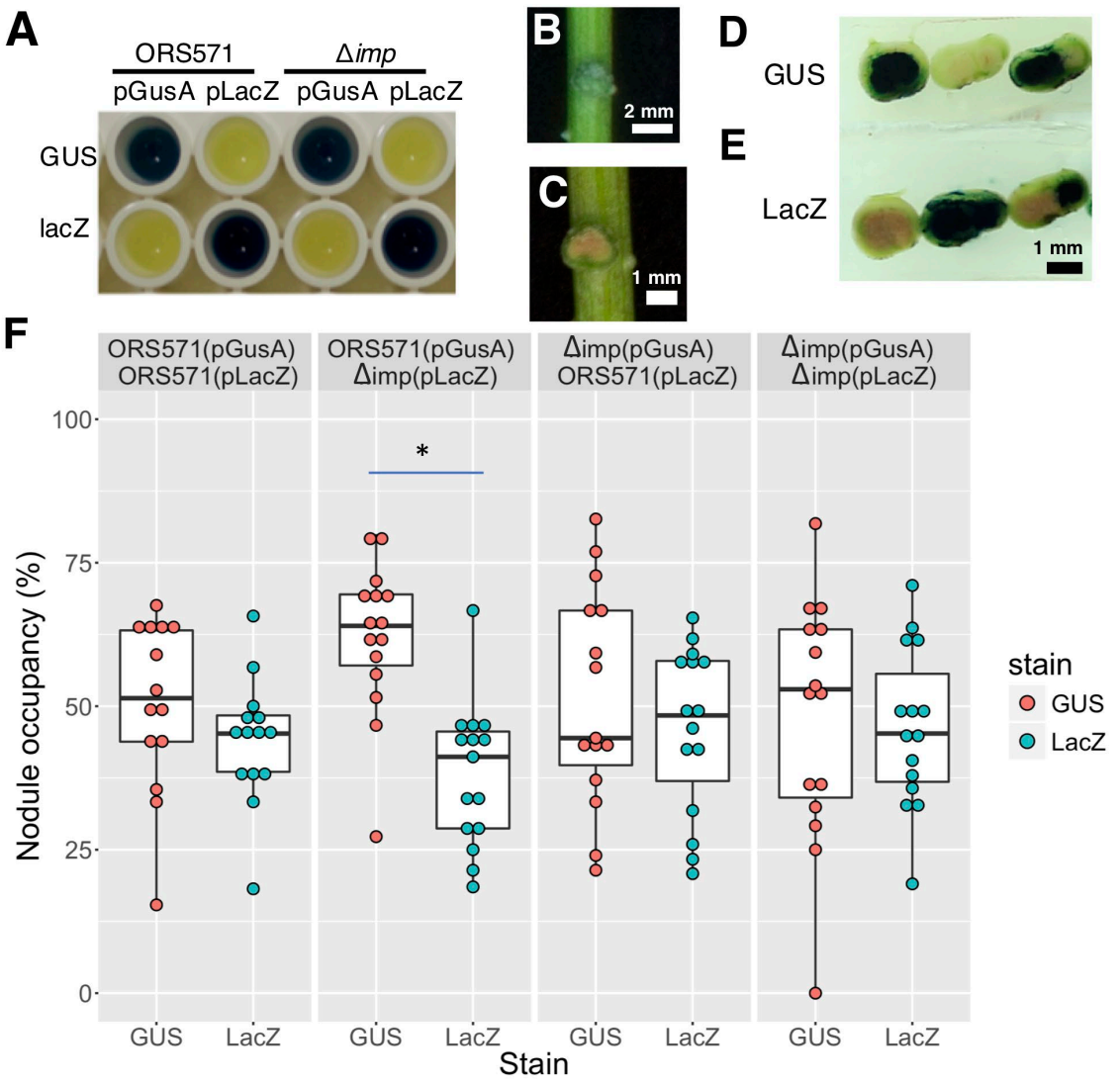

Figure 2-7. Deletion of T6SS reduced the symbiotic competitiveness of *A. caulinodans*.

(A) GUS and LacZ were constitutively expressed with strong staining signal in *A. caulinodans* ORS571 and Δ*imp* cells grown in TY medium. **(B)** Stem nodules 7 days old were **(C)** cut in half before staining. Each infection zone was stained fully with **(D)** GUS or **(E)** LacZ. **(F)** Symbiotic competitiveness indicated by nodule occupancy between ORS571 and Δ*imp*. Horizontal lines are median, box edges are quartiles 1 and 3 and whiskers are 1.5 times of the interquartile range (IQR) from the box edges.

doi:10.6342/NTU202000295

Wilcoxon signed rank test with continuity correction test was used for statistical analysis with $p<0.01$ for statistical significance. * $p= 3.17 \times 10^{-3}$.

doi:10.6342/NTU202000295

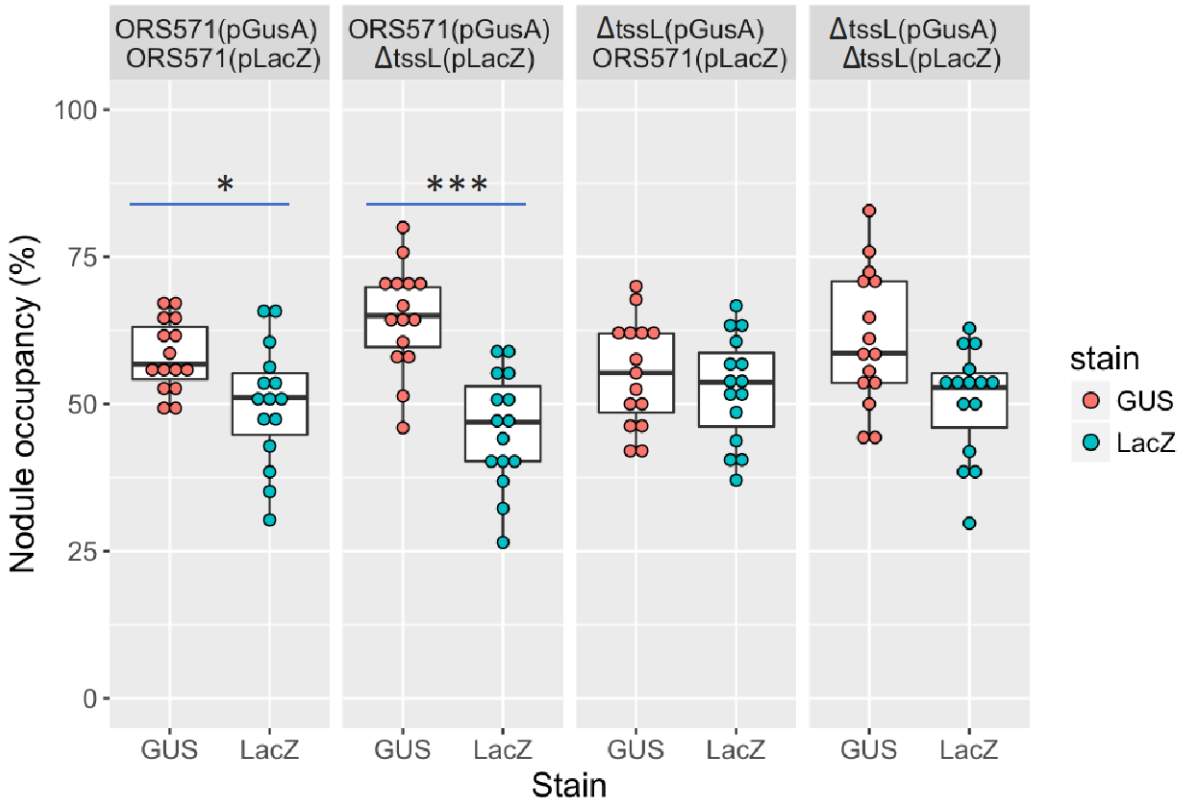

Figure 2-8. Deletion of Δ*tssL* reduced the symbiotic competitiveness of *A. caulinodans* indicated by mixed inoculation assay.

Symbiotic competitiveness indicated by nodule occupancy between ORS571 and Δ*tssL*. Horizontal lines are median, box edges are quartiles 1 and 3 and whiskers are 1.5 times of the interquartile range (IQR) from the box edges. Wilcoxon signed rank test with continuity correction test was used for statistical analysis with $p<0.01$ for statistical significance. * $p= 4.27 \times 10^{-4}$.

doi:10.6342/NTU202000295

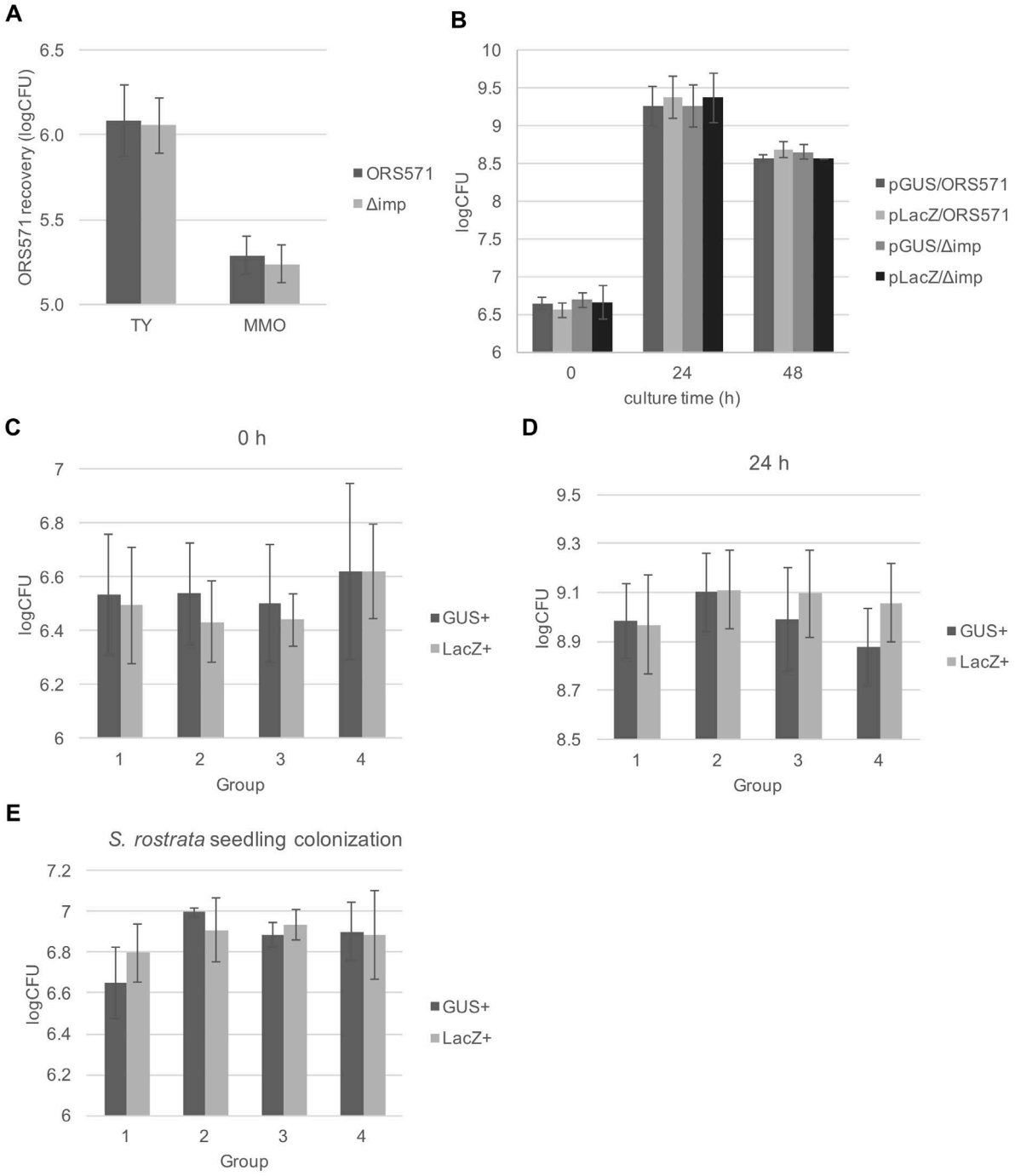

Figure 2-9. Determine antibacterial activities and evaluate the compatibility between the individual bacterium and the host.

(A) Antibacterial competition between ORS571 and *Δimp* under either nutrient-rich (TY) or minimal nutrient (MMO) medium. (**B**) *A. caulinodans* derivatives were cultured in MMO medium and CFU per ml were measured at 0, 24, and 48 hours post

doi:10.6342/NTU202000295

inoculation. Bacterial growth of *A. caulinodans* derivatives as equimolar mixtures with cells in individual groups under MMO medium was measured at (**C**) 0 h and (**D**) 24 h. (**E**) Colonization assay with *Sesbania* seedlings. Individual bacteria were recovered from three seedlings and CFU per ml were counted. Group 1: ORS571(pGusA) plus ORS571(pLacZ), Group 2: ORS571(pGusA) plus Δ*imp*(pLacZ), Group 3: Δ*imp*(pGusA) plus ORS571(pLacZ), and Group 4: Δ*imp*(pGusA) plus Δ*imp*(pLacZ). Data are mean (±SE) from 3 biological replicates.

1

doi:10.6342/NTU202000295

Chapter 3. Screening and identification of recipient cell factors involved in type VI secretion system-mediated killing of *Agrobacterium tumefaciens* C58

Most of the following chapter has been published as part of a peer reviewed article in the *Frontiers in Microbiology*, Switzerland:

Hsiao-Han Lin, Manda Yu, Manoj Kumar Sriramoju, Shang-Te Danny Hsu, Chi-Te Liu, Erh-Min Lai (2020). A high-throughput interbacterial competition screen identifies ClpAP in enhancing recipient susceptibility to type VI secretion system-mediated attack by *Agrobacterium tumefaciens*. Frontiers in Microbiology, **10**. doi: 10.3389/fmicb.2019.03077

Contributions:

Hsiao-Han Lin, Manda Yu, and Erh-Min Lai conceived and designed the experiments. Hsiao-Han Lin performed most of the experiments and Manoj Kumar Sriramoju contributed to the protease activity assay. Manoj Kumar Sriramoju and Shang-Te Danny Hsu provided the materials and tools for the protease activity assay. Shang-Te Danny Hsu, Chi-Te Liu, and Erh-Min Lai supervised the execution of the experiments.

doi:10.6342/NTU202000295

3.1 Summary

The type VI secretion system (T6SS) is an effector delivery system used by Gram-negative bacteria to kill other bacteria or eukaryotic hosts to gain fitness. The plant pathogen *Agrobacterium tumefaciens* utilizes its T6SS to kill other bacteria, such as *Escherichia coli*. We observed that the *A. tumefaciens* T6SS-dependent killing outcome differs when using different T6SS-lacking, K-12 E. coli strains as a recipient cell. Thus, we hypothesized that the *A. tumefaciens* T6SS killing outcome not only relies on the T6SS activity of the attacker cells but also depends on the recipient cells. Here, we developed a high-throughput interbacterial competition platform to test the hypothesis by screening for mutants with reduced killing outcomes caused by *A. tumefaciens* strain C58. Among the 3,909 strains in the *E. coli* Keio library screened, 16 mutants with less susceptibility to *A. tumefaciens* C58 T6SS-dependent killing were identified, and four of them were validated by complementation test. Among the four, the clpP encoding ClpP protease, which is universal and highly conserved in both prokaryotes and eukaryotic organelles, was selected for further characterizations. We demonstrated that ClpP is responsible for enhancing susceptibility to the T6SS killing. Because ClpP protease depends on other adapter proteins such as ClpA and ClpX for substrate recognition, further mutant studies followed by complementation tests were carried out to reveal that ClpP-associated AAA+ ATPase ClpA, but not ClpX, is involved in enhancing susceptibility to *A. tumefaciens* T6SS killing. Moreover, functional and biochemical studies of various ClpP amino acid substitution variants provided evidence that ClpA–ClpP interaction is critical in enhancing susceptibility to the T6SS killing. This study highlights the importance of recipient factors in determining the outcome of the T6SS killing and shows the universal ClpP protease as a novel recipient factor hijacked by the T6SS of *A. tumefaciens*.

doi:10.6342/NTU202000295

Keywords: Type VI secretion system (T6SS), antibacterial activity, recipient cells, ClpP, ClpA, *Agrobacterium tumefaciens*, *Escherichia coli*

3.2 Introduction

Bacteria have evolved broad strategies in secreting antibiotics or protein toxins to antagonize other bacteria and gain fitness to fight for limited nutrients and space. Among them, the Gram-negative bacteria use a variety of protein secretion systems such as type I secretion system (T1SS) (García-Bayona, et al. 2019, García-Bayona, et al. 2017), type IV secretion system (T4SS) (Bayer-Santos, et al. 2019, Souza, et al. 2015), contact-dependent inhibition (CDI; belongs to type V secretion system) (Aoki, et al. 2010, Aoki, et al. 2005), and type VI secretion system (T6SS) (Basler, et al. 2013, LeRoux, et al. 2012) as antibacterial weapons. Bacteria that produce and deliver protein toxins, the effectors, through secretion systems to kill other bacteria are attacker cells, and the attacked cells are the recipient cells (Costa, et al. 2015, Filloux and Sagfors 2015). Attacker cells also produce cognate immunity proteins to neutralize effectors to prevent self-intoxication (Alteri and Mobley 2016, Lien and Lai 2017). A recipient cell is intoxicated if it does not have cognate immunity protein to neutralize the toxicity of its effector.

In the CDI system, non-immunity proteins in the recipient cell also participate in the bacterial competition outcome (Aoki, et al. 2008, Aoki, et al. 2010, Diner, et al. 2012, Jones, et al. 2017, Willett, et al. 2015). For example, the CDI effector CdiA-CT^{EC93} utilizes recipient's outer membrane protein BamA and the inner membrane protein AcrB to enter the recipient cell (Aoki, et al. 2008). BamA belongs to the BAM complex

doi:10.6342/NTU202000295

that functions in outer membrane β-barrel proteins (OMPs) biogenesis. AcrB is an inner membrane protein that belongs to the multidrug efflux pump TolC complex. Another example is the necessity of the recipient *O*-acetylserine sulfhydrylase A (CysK) to the CDI effector CdiA-CT^{EC536} (Diner, et al. 2012). In the recipient cell, CdiA-CT^{EC536} binds to CysK to increase its thermostability and its tRNase activity (Johnson, et al. 2016). Interestingly, this CysK.CdiA-CT^{EC536} complex mimics the CysK.CysE complex, which is typically formed during *de novo* cysteine biogenesis, with a higher binding affinity (Johnson, et al. 2016, Jones, et al. 2017). Other examples are the recipient elongation factor Tu (EF-Tu) in activating the toxicity of CdiA-CT^{EC869} and CdiA-CT^{NC101} (Jones, et al. 2017, Michalska, et al. 2017), and the involvement of recipient PtsG in CdiA-CT^{3006} and CdiA-CT^{NC101} entry (Willett, et al. 2015). To summarize, a variety of the non-immunity proteins in the recipient cells affect the CDI antagonizing outcome. As the bacterial secretion systems that serve as an antibacterial weapon share some universal characters, the above phenomenon raised a question of whether non-immunity proteins of the recipient cells also affect the bacterial antagonizing outcome in other secretion systems.

Recently, examples about the involvement of the recipient non-immunity proteins in T6SS competition outcome emerged. The first description is the involvement of the EF-Tu protein of the recipient cell for Tse6 effector-mediated killing by *Pseudomonas aeruginosa* (Whitney, et al. 2015). Although recipient's EF-Tu was initially proposed to grant access of Tse6 into the recipient cytoplasm (Whitney, et al. 2015), a further study demonstrated that Tse6 could penetrate the double bilayer of the EF-Tu-free liposome and exert its toxicity inside it (Quentin, et al. 2018). The role of the recipient EF-Tu involved in an interbacterial competition of Tse6 remains elusive. A T6SS study in

doi:10.6342/NTU202000295

Serratia marcescens demonstrated that the recipient protein DsbA plays a role in activating *S. marcescens* T6SS effectors Ssp2 and Ssp4, but not Rhs2 (Mariano, et al. 2018). The *S. marcescens* T6SS kills its Ssp2-sensitive siblings only when the recipient cells harbor *dsbA* homologs ($dsbA1^+$ $dsbA2^+$). The same results were also observed using Ssp4-sensitive recipient cells, but not Rhs2-sensitive strain as a recipient cell. The above findings highlight the necessity of a recipient factor to facilitate the T6SS attack. However, a systematic screening of the recipient factors that can either promote or reduce the susceptibility of the T6SS attack is still lacking.

This study aimed to explore the recipient genetic factors that affect the T6SS killing outcome using the well-characterized T6SS-possessing plant pathogen *Agrobacterium tumefaciens,* a causative agent of crown gall disease in many different plants. The *A. tumefaciens* strain C58 harbors three effector proteins: type VI DNase effector 1 (Tde1), Tde2, and putative type VI amidase effector (Tae). The Tde proteins are the main contributor to *A. tumefaciens* T6SS-dependent interbacterial competition and their DNase activity relies on the conserved HxxD motif (Ma, et al. 2014). Using the T6SS-lacking *Escherichia coli* K12 strain as a model recipient cell, we report here a high-throughput, population level, interbacterial competition screening platform for identifying the recipient genetic factors that contribute to *A. tumefaciens* C58 T6SS's killing outcome. Among the 3,909 *E. coli* Keio mutants screened, we confirmed that at least six of them play a role in enhancing susceptibility to *A. tumefaciens* T6SS attack by an interbacterial competition assay and by complementation *in trans*. One of the confirmed genes, *caseinolytic protease P* (*clpP*), was highlighted in this study owingzzz to its prominent phenotype. A functional ClpP complex consists of a tetradodecameric ClpP and its associated AAA^+ ATPase substrate-recognizing partner ClpA or ClpX

doi:10.6342/NTU202000295

(Olivares, et al. 2015). Further mutant studies showed that *clpA,* but not *clpX,* is involved in the outcome of *A. tumefaciens* T6SS killing. Our data also suggest that the ClpAP complex formation mediates the outcome of T6SS killing. This work not only provides a new screening platform for elucidating factors that are involved in the interbacterial competition but also strengthens the importance of recipient genetic factors in the outcome of the T6SS antibacterial activity.

3.3 Materials and Methods

Bacterial strains, plasmids, and growth conditions

The complete information about the strains and plasmids used in this study is described in Table 3-1. The *E. coli* Keio mutants (Baba, et al. 2006) and the BW25113 wild type were obtained from the Keio collection from NBRP (NIG, Japan) and used as the recipient cells unless otherwise indicated. *A. tumefaciens* strains C58, 1D132, 1D1108, and A6 wild type, as well as their corresponding *tssL* mutants (Δ*tssL*) were used as the attacker cells. *A. tumefaciens* was grown at 25 ^{o}C in 523 medium, and *E. coli* was grown in lysogeny broth (LB) medium at 37 ^{o}C unless indicated. The plasmids were maintained in 20 μg/mL kanamycin (Km), 100 μg/mL spectinomycin (Sp), 20 μg/mL gentamycin for *E. coli*.

Plasmid construction

All plasmids (Table 3-1) were confirmed by sequencing unless otherwise indicated. The complete list of primers used in this study is in Table 3-2. Plasmid pNptII was created by ligating the *Xho*I/*Bam*HI-digested *nptII* PCR product into the same restriction sites of pRL662. The plasmid was transformed into DH10B, and the resulting

doi:10.6342/NTU202000295

strain was designated as EML5395. The pRL-*rpsL*, pRL-*galK*, pRL-*nupG*, and pRL-*rpsL*^{Str} were created by ligating the *Xho*I/*Xba*I-digested PCR product into the same restriction sites of pRL662. The plasmid was transformed into DH10B, and the resulting strain was designated as EML5389, EML5390, EML5391, and EML5392. Plasmids pClpP-HA and pClpA-HA were created by ligating *Sac*I/*Pst*I-digested PCR products (*clpP* and *clpA* from BW25113 wild type without the stop codon, respectively) into pTrc200HA. The pClpP$_{S111A}$-HA was created by amplifying fragments using pTRC99C-F plus ClpP-S111A-rv and pTRC99C-R plus ClpP-S111A-fw as primers. The two fragments were then merged and amplified by PCR-Splicing by Overlapping Extension (SOEing) (Heckman and Pease 2007). The resulting full-length *clpP*-containing fragment was digested by *Sac*I/*Pst*I then ligated into pTrc200HA. All other pClpP-HA plasmids with a mutated form of ClpP were created similarly. The plasmid constructs ClpX (ClpX-ΔN-ter), wild-type ClpP-tev-His and green fluorescent protein (GFP)-ssrA were a kind gift from Dr. Robert T. Sauer (MIT, Cambridge, USA). Site-directed mutagenesis was performed to generate the ClpP variants. All plasmids of pClpP-tev-His with a mutated *clpP* gene was constructed similar to that of pClpP$_{S111A}$-HA mentioned above with the differences below: Primer T7 was used instead of pTRC99C-F, and primer T7T was used instead of pTRC99C-R, and the restriction sites used were *Xba*I/*Xho*I.

Interbacterial competition assay

The optical densities of the cultured *A. tumefaciens* and *E. coli* were measured and adjusted to OD_{600} equals to 3.0 in 0.9% NaCl (w/v). The recipient *E. coli* cells were then further diluted to OD_{600} equals to 0.3 or 0.1, depending on the need of the assay. Afterward, the attacker and the recipient cultures were mixed in equal volume to make

doi:10.6342/NTU202000295

the attacker: recipient ratio 10:1 or 30:1, respectively. Ten microliters of the mixed bacterial culture were then spotted onto *Agrobacterium* Kill-triggering medium (AK medium, 3 g K_2HPO_4, 1 g NaH_2PO_4, 1 g NH_4Cl, 0.15 g KCl, 9.76 g MES, pH5.5) solidified by 2% (w/v) agar, and then air-dried to enable contact-dependent competition. The competition plates were cultured at 25°C for 16 h. After the competition, bacteria were recovered using a loop and resuspended into 500 μL of 0.9% NaCl. The recovered bacterial suspension was then serially diluted and plated onto LB supplemented with spectinomycin to select recipient *E. coli* cells. After overnight culture at 37°C, the recovered colony formation unit (cfu) were counted and recorded. The T6SS-dependent susceptibility index (SI) was defined as the logarithm of the recovered *E. coli* cfu co-cultured with Δ*tssL* subtracted by that co-cultured with wild type *A. tumefaciens*.

The high-throughput interbacterial competition platform

Pipetting steps of the screening platform were performed by the pipetting robot EzMate401 (Arise Biotech, Taiwan) unless otherwise specified. Fifty microliters of the cultured attacker *A. tumefaciens* strain C58 or its *tssL* mutant was pelleted using 8,000 × g for 10 min at 15 °C. After the medium was removed, the pellet was washed twice using 0.9% NaCl (w/v) and then adjusted to OD_{600} equals to 3.0. The OD_{600}-adjusted attacker cells were then dispensed as 300 μL into each well of a 2.2 mL-Deepwell microplate (Basic Life, Taiwan). Each well was then added with 10 μL of the cultured recipient *E. coli* mutants and mixed well to make the attacker: recipient at 30:1 (v/v). After being mixed, the bacterial mixture was then added onto the competition plate. The competition plate was made by 25 mL of the AK medium with 2%(w/v) agarose solidified in a 96-well lid. The competition plate was then cultured at 25°C for 16 h before recovery. The recovery was performed by stamping a 96-well plate replicator to

doi:10.6342/NTU202000295

the competition spots followed by suspending the bacterial cells to a 96-well plate containing 200 μL of 0.9% NaCl in each well. After being mixed, 10 μL of the recovered bacterial suspension was spotted onto LB agar supplemented with kanamycin made in a 96-well lid, cultured at 37 ^{o}C overnight, and then was observed. In the first screening, only *A. tumefaciens* C58 wild type was used as the attacker. In the second screening, both wild type and Δ*tssL* were used as the attackers. For the groups co-cultured with *A. tumefaciens* C58 wild type, the recovery suspension was either undiluted or diluted to 5 and 25 times before spotted onto LB agar with kanamycin plate. For the groups co-cultured with *A. tumefaciens* C58 Δ*tssL*, the recovery suspensions were either undiluted or diluted to 10 and 100 times before spotted onto LB agar with kanamycin. At each stage, the *E. coli* mutants that formed multiple colonies were identified as the candidates. The second screening was performed by Chia Lee.

Protein production and purification

E. coli BL21(DE3) was used as a host to produce all proteins of interests. Cells were cultured in LB medium supplemented with appropriate antibiotics in 1-L flask. When OD_{600} reached 0.6, the bacterial culture was cooled to 16 °C, and IPTG was added (final concentration of 0.5 mM) for the overexpression of the protein. The cells were further allowed to grow for 16 h, followed by centrifugation to pellet them and then resuspended in lysis buffer (50 mM of Tris, pH 8.0, 300 mM of NaCl, 1% Triton X-100, 10 mM of beta-mercaptoethanol, 1 mM of DTT, and 10% Glycerol). The cells were lysed by sonication at 4 $^{\circ}$C (amplitude 10 for 5 sec, followed by 15-sec breaks; total sonication time was 6 min) (Pro Scientific, USA). The lysates were centrifuged at 20,000 rpm for 30 min at 4 ^{o}C. The supernatants were collected and loaded onto Ni-NTA column (GE Healthcare, USA) equilibrated with wash buffer (50 mM of Tris, pH

doi:10.6342/NTU202000295

8.0, and 300 mM of NaCl) and eluted by 6 mL of wash buffer containing 250 mM of imidazole. The eluted fractions of the protein were further subjected to size-exclusion chromatography (SEC) by Superdex 200,16/60 column (GE Life Science, USA) in buffer containing 50 mM of Tris pH 7.5, 100 mM of KCl, 25 mM of $MgCl_2$, 1 mM DTT, and 10% glycerol. The protein purity was confirmed on 12% sodium dodecyl sulfate–polyacrylamide gel electrophoresis (SDS-PAGE). The samples were flash-frozen and stored in -80 °C until further use.

Protein degradation assay

Green fluorescent protein (GFP) fluorescence based-degradation assays were carried out in Protein Degradation (PD) buffer (25 mM of HEPES, pH 7.5, 100 mM of KCl, 25 mM of $MgCl_2$, 1 mM of DTT, and 10% glycerol) containing 3 μM GFP-ssrA as substrate and ATP regeneration system (16 mM of creatine phosphatase and 0.32 mg/mL of creatine kinase) as described previously (Sriramoju, et al. 2018). In brief, 0.1 μM of $ClpX_6$ and 0.3 μM of $ClpP_{14}$ or its variants were mixed at 30 °C and allowed to stand for 2 min. The protein degradation reaction was started by addition of ATP to a final concentration of 5 mM. The changes in the fluorescence were measured at 511 nm with an excitation wavelength at 467 nm in a 96-well format using Infinite M1000 PRO plate reader (TECAN, Switzerland).

Plasmid degradation assay

E. coli BW25113 strains harboring empty vector pJN105 or its derivative expressing Tde1 were harvested and adjusted to OD_{600} of 0.2 in LB medium containing 1 mM IPTG for ClpP:HA induction for 4 h. After ClpP:HA induction, 0.2% L-arabinose was added to the medium for a further 1h to produce Tde1 toxins. Equal cell mass was

doi:10.6342/NTU202000295

collected in each group, and plasmid DNA was extracted by an equal volume of the elution buffer (10 mM Tris-HCl, pH 8.5). An equal volume of the eluted plasmid was loaded and separated by DNA gel before analysis. The plasmid levels were quantified by Fiji (version 2.0.0-rc-69/1.52p) (Schindelin, et al. 2012). The plasmid digestion rate (%) is determined by the ratio of the plasmid with and without induction.

SDS-PAGE and Western Blot analysis

To detect the ClpP:HA and its derivative levels, the Δ*clpP*:kan *E. coli* strains harboring ClpP:HA expressing plasmids were grown as the same procedure indicated in the *Interbacterial Competition Assay*. To detect the protein levels of the Tde1 catalytic mutant (Tde1M, Tde1H190AD193A) in *E. coli* strains, overnight cultures were washed and adjusted to OD_{600} of 0.3 in AK medium and then cultured for another 6 h before protein extraction. To detect the Tde1 levels, the *E. coli* strains were grown as the same procedure indicated in the *Plasmid degradation assay*, and samples were collected after arabinose induction. Cells were adjusted to OD_{600} of 5.0, collected at 5000 × g for 5 min, and directly resuspended in 1 × SDS sample buffer. The samples were incubated at 96 ^{o}C for 10 min and then analyzed by SDS-PAGE. Protein samples separated by SDS-PAGE were transferred to an Immobilon-P membrane (Merck Millipore, USA). The monoclonal anti-HA was used at a dilution of 1:10,000 (Yao-Hong Biotech Inc., Taiwan), the anti-Tde1 was used at a dilution of 1:4,000 (Yao-Hong Biotech Inc., Taiwan), and the goat-anti-rabbit conjugated to horseradish peroxidase secondary antibody was used at a dilution of 1:10,000 (GeneTex, Taiwan). The Western Lightning ECL Pro (PerkinElmer Life Sciences, USA) was used for color development and visualized by BioSpectrum 600 Imaging System (UVP, USA).

doi:10.6342/NTU202000295

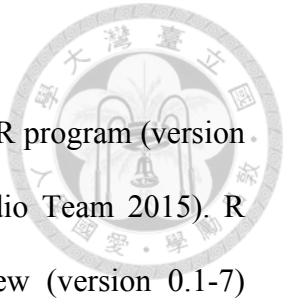

Statistical analysis and figure production

Statistical analyses and figure production were performed using the R program (version 3.5.1) (R Core Team 2018) and RStudio (version 1.1.456) (RStudio Team 2015). R packages plyr (version 1.8.4) (Wickham 2011) and multcompView (version 0.1-7) (Graves, et al. 2015) were used for statistical analyses. Figures were produced using the R packages ggplot2 (version 3.0.0) (Wickham 2016), Hmisc (version 4.1-1) (Harrell, et al. 2018), and ggpubr (version 0.2) (Kassambara 2018). Student's t-test, one-way analysis of variance (one-way ANOVA), and Tukey's honestly significant difference test (Tukey HSD test), in which significant difference threshold set as 0.05, were used in all case.

3.4 Results

The *A. tumefaciens* T6SS killing outcome differs between different *E. coli* strains

Using an optimized competition condition ("*Agrobacterium* Kill-triggering", AK medium agar that contains basic minerals at pH 5.5), we noticed that when co-cultured with wild type *A. tumefaciens* C58, the recovered colony-forming unit (cfu) of *E. coli* BW25113 was always lower than that of DH10B (Figure 3-1A). Meanwhile, the recovered cfu of both *E. coli* strains was the same when co-cultured with Δ*tssL A. tumefaciens* C58 (referred to Δ*tssL*), a T6SS secretion-deficient mutant (Figure 3-1A). For more intuitive readout, we introduced T6SS-dependent susceptibility index (SI), which reflects the strength of the T6SS killing. The SI was defined as the logarithm of the recovered *E. coli* cfu co-cultured with Δ*tssL* subtracted by that co-cultured with wild type. The mean SI between *A. tumefaciens* and BW25113 was significantly higher than that of between *A. tumefaciens* and DH10B with a *P*-value of 0.02 ($T \leq t$, two-tail,

doi:10.6342/NTU202000295

Figure 3-1B). This result suggests that some genetic factors of BW25113 may enhance the *A. tumefaciens* C58 killing outcome in a T6SS-dependent manner.

We tested whether the genes that are functional in BW25113 but not in DH10B could be the cause of the higher SI in BW25113. The *galK* and *nupG* genes are functional in BW25113 but are pseudogenes in DH10B. The *rpsL* has a mutation in DH10B ($rpsL^{Str}$), which renders the strain resistant to streptomycin, but not in BW25113. The *rpsL*, *galK*, or *nupG* genes from BW25113 was cloned into pRL662 and expressed by constitutive *lacZ* promoter in DH10B as a recipient for a T6SS interbacterial competition assay (Figure 3-1C). The DH10B expressing the $rpsL^{Str}$ (overexpressing $rpsL^{Str}$) was also included. The DH10B harboring empty vector (vec) served as a negative control. A group without attacker was also included to monitor whether the decrease in cfu after the competition solely comes from co-culture with *A. tumefaciens* attacker. The SIs were not significantly different between DH10B and any of the complemented groups, and each had an SI mean of about 2 (Figure 3-1C). The above approach was not able to identify the genetic factors that contributed to the enhanced resistance in DH10B, which may imply that precise control of transgene expression or multiple complementation would be required. Therefore, we developed a high-throughput screening method to identify the individual genes that contribute to the enhanced susceptibility of BW25113.

Establishment of a high-throughput interbacterial competition platform to identify recipient *E. coli* mutants with less susceptibility to *A. tumefaciens* C58 T6SS killing

We decided to screen the BW25113 single-gene mutant library (Keio collection from NBRP [NIG, Japan]: *E. coli*) for strains with less susceptibility to *A. tumefaciens* T6SS-mediated killing. An interbacterial competition assay starts from mixing the attacker

doi:10.6342/NTU202000295

and the recipient cells, followed by counting the recovered recipient *E. coli* on selective media (Figure 3-2A). This protocol only allowed screening of 10 mutants per day; which was not efficient enough for screening 3,909 strains of the Keio library.

Therefore, we developed a high-throughput interbacterial competition platform that enables 96 population-level, interbacterial competition simultaneously (Figure 3-2B). The recipient Keio *E. coli* strains were cultured in the 96-well, and the attacker *A. tumefaciens* was cultured in a flask. After the culture, the attacker was adjusted to OD_{600} equals to 3.0 and then dispensed to a 2.2 mL deep-well plate. The recipient cells were added into the attacker-containing plates in a volume ratio of 30 to 1. Ten microliters of the attacker-recipient mixtures were dropped on the competition surface made by agar solidified on a 96-well lid. A microplate replicator was used to stamp on the competition spots to recover the bacterial cells of each competition group. The recovered bacteria were suspended in the saline buffer (0.9% NaCl), mixed, and then spotted on the recipient-selection surface made by agar solidified on a microplate lid. The competition condition was set at the strength that enables *A. tumefaciens* to kill almost all wild-type BW25113 recipients so that only a few or no cells would survive. This setup made recognizing the resistant mutants simple — the ones with the multiple colonies are the candidates (Figure 3-2B).

All the 3,909 strains in the Keio were screened using *A. tumefaciens* C58 wild type as the attacker. In each screening, at least two wild type *E. coli* BW25113 replicates were incorporated and screened in parallel as parental controls (Appendix Figure 3). The Keio mutants that formed colonies in this stage were selected, and 196 strains showed enhanced resistant to *A. tumefaciens* C58 attack. The 196 strains were subjected to

doi:10.6342/NTU202000295

second screening using both wild type and Δ*tssL* as the attackers. At this stage, we incorporated a grading system: grade I mutants were at least 25 times less susceptible to C58 T6SS-dependent killing, whereas grade II mutants were at least ten times less susceptible. Six grade I mutants and 10 grade II mutants were identified.

Confirmation of the *E. coli* mutants with less susceptibility to *A. tumefaciens* C58 T6SS killing

The enhanced resistant of the six grade I mutants were further verified by an interbacterial competition assay and by complementation tests. For complementation, wild type genes from BW25113 were cloned into plasmid pTrc200HA plasmid and expressed by *trc* promoter. Five out of six showed lower susceptibility to *A. tumefaciens* T6SS attack than that of BW25113 wild type (Table 3-3, Appendix Figure 4). These are *clpP*, *gltA*, *ydhS*, *ydaE*, and *cbpA* mutants. The *yeaX* mutant, on the other hand, did not differ when compared with the wild type. The *cbpA* mutant showed a milder phenotype and could not be complemented *in trans* under the condition tested (Table 3-3, Appendix Figure 4). As *cbpA* is the first gene in its operon, the failure in complementation could be due to the requirement of other gene(s) in the operon. Nevertheless, the verification performed above showed that the high-throughput interbacterial competition platform was reliable in identifying the recipient genetic factors that participate in T6SS killing.

The ClpP protein plays a role in enhancing susceptibility to *A. tumefaciens* T6SS killing

Because known recipient cell factors affecting antibacterial activity are often conserved components, we selected Δ*clpP*:kan (labeled as Δ*clpP*) for further studies. ClpP is a

doi:10.6342/NTU202000295

highly conserved, house-keeping AAA^+ serine protease exists in both prokaryotes, plastids, and mitochondria (Alexopoulos, et al. 2012, Bhandari, et al. 2018, Mahmoud and Chien 2018). We performed quantitative interbacterial competition assay using *A. tumefaciens* as the attacker and either the BW25113 wild type, Δ*clpP,* or complemented strain $clpP^+$ as the recipient cells (Figure 3-3A). The initial cfu of the *E. coli* at 0 h was about 10^6 in all groups (one-way ANOVA with $P = 0.88$), indicating that any *E. coli* cfu difference at 16 h was not due to initial bacteria titer difference. The cfu among different recipient *E. coli* strains was not significantly different at 16 h when using *A. tumefaciens* Δ*tssL* (one-way ANOVA with $P = 0.67$), indicating that co-culture with T6SS-deficient strain will not cause recipient titer to differ. On the other hand, the recovered cfu of Δ*clpP* was about 10^4, whereas it was about 5×10^2 in BW25113 wild type and in $clpP^+$ after 16-h competition using wild-type *A. tumefaciens* (Figure 3-3A). The mean SI of the BW25113 wild type to *A. tumefaciens* C58 is significantly higher than that of Δ*clpP* (one-way ANOVA with $P = 0.02$, Figure 3-3B). The less susceptible phenotype of the Δ*clpP* can be fully complemented *in trans* ($clpP^+$) ($P = 0.96$ compared with BW25113 wild type). These results confirmed that *clpP* contributes to enhancing susceptibility to T6SS antibacterial activity of *A. tumefaciens* C58.

Effects of ClpP catalytic variants in enhancing *A. tumefaciens* T6SS antibacterial activity and protease activity

A functional ClpP complex consists of a tetradodecameric ClpP ($ClpP_{14}$) and its associated AAA^+ ATPase substrate-recognizing partner ClpA or ClpX, both in a hexameric form (Olivares, et al. 2015). The protease catalytic triad of the *E. coli* ClpP is composed of S111, H136, and D185 (counted from the Met1) (Maurizi, et al. 1990, Wang, et al. 1997). We tested whether the ClpP protease is essential in enhancing *E.*

doi:10.6342/NTU202000295

coli susceptibility to *A. tumefaciens* C58 T6SS attack. *E. coli* Δ*clpP* complemented with pTrc200HA expressing either wild-type or catalytic variants ClpP S111A, H136A, and D185A was used as a recipient strain. All ClpP variants contain a C-terminal HA tag. Two of the catalytic variants, $S111A^{+}$ and $H136A^{+}$, failed to complement, whereas surprisingly, the third catalytic variant $D185A^{+}$, can fully complement the phenotype (Figure 3-4A). The difference of ClpP catalytic variants to complement Δ*clpP* was not due to their protein-expression level as determined by Western blot (Figure 3-4B). The protein migration of the $ClpP_{S111A}$ and $ClpP_{H136A}$ was slower than that of the $ClpP_{wt}$ and $ClpP_{D185A}$ owing to their inability to remove the N-terminal propeptide (1-14 amino acids) as in $ClpP_{wt}$ and $ClpP_{D185A}$ (Bewley, et al. 2006, Maurizi, et al. 1990).

As $ClpP_{D185A}$ was able to complement the phenotype, we further investigated the ClpP protease activity of the above ClpP variants by a widely adopted ClpP protein degradation assay using GFP-ssrA as the model substrate (Sriramoju, et al. 2018, Weber-Ban, et al. 1999). Loss of GFP fluorescence is used as a reporter to monitor substrate degradation by ClpXP as a function of time (Sriramoju, et al. 2018, Weber-Ban, et al. 1999). The results showed that over time, wild-type ClpP effectively degraded GFP-ssrA with a half-life of about 30 min (Figure 3-5A). Meanwhile, less than a 10% decrease of the GFP-ssrA signal was observed in GFP-ssrA only and wild type without ATP groups, both served as negative controls. The decreasing rates of the GFP-ssrA fluorescence of $ClpP_{S111A}$, $ClpP_{H136A}$, and $ClpP_{D185A}$ were significantly slower than that of $ClpP_{WT}$ and showed no significant difference among the three variants at the end of the test (Figure 3-5A and 3-5B). Although $ClpP_{D185A}$ showed no statistically difference in GFP-ssrA degradation compared with $ClpP_{S111A}$ and $ClpP_{H136A}$

doi:10.6342/NTU202000295

at the final time point, it showed significantly lower GFP-ssrA signal to that of the negative control groups (Figure 3-5B).

The ClpP-associated AAA$^+$ ATPase ClpA but not ClpX is involved in enhancing susceptibility to *A. tumefaciens* T6SS activity

ClpP is a protein protease depending on other adapter proteins such as ClpA and ClpX for substrate recognition (Gottesman, et al. 1998, Maurizi 1991). Therefore, we next determined whether the resistant phenotype of Δ*clpP* is mediated by ClpA or ClpX through the interbacterial competition assay of the deletion mutants Δ*clpA*:kan (hereafter referred to as Δ*clpA*) and Δ*clpX*:kan (hereafter referred to as Δ*clpX*) as recipients. Susceptibility index demonstrates that Δ*clpA* was less susceptible to *A. tumefaciens* T6SS killing than that of BW25113 wild-type (P = 0.02) whereas Δ*clpX* was similar to BW25113 wild type (P = 1.00) (Figure 3-6A). The decreased *A. tumefaciens* T6SS killing phenotype of Δ*clpA* was fully complemented *in trans* (Figure 3-6B). No difference could be detected among the growth of the BW25113 wild-type, Δ*clpA*, Δ*clpP*, and their respective complemented strains when co-cultured with Δ*tssL* (P = 0.58) (Figure 3-6C). Therefore, the killing outcome is caused by *Agrobacterium* T6SS-mediated interbacterial competition rather than the growth rate of the different recipient strains under the competition condition. This suggested that ClpA could be the adapter that interacts with ClpP leading to the enhanced susceptibility to T6SS attack in BW25113 wild type. In this case, the interaction between ClpA and ClpP should be required for enhancing *A. tumefaciens* T6SS killing. The interaction between ClpA and ClpP is well studied, and it has been demonstrated that the R26A and D32A variants of ClpP lose their ability to bind to ClpA by 50 and 100%, respectively (Bewley, et al. 2006). Therefore, we complemented $ClpP_{R26A}$ and $ClpP_{D32A}$ in Δ*clpP* to determine

doi:10.6342/NTU202000295

whether the two variants could restore the susceptibility. The R26A^{+} was able to complement (P = 0.96, compared to ClpP^{+}) while D32A^{+} failed to complement and showed no statistical difference in SI than that of Δ*clpP* ($P < 10^{-4}$) (Figure 3-7). These results suggest that the phenotype observed in Δ*clpP* and in Δ*clpA* could be associated with ClpA-ClpP interaction. Because the retained N-terminal propeptide does not prevent ClpP-ClpA binding (Maurizi, et al. 1990), the inability of unprocessed $ClpP_{S111A}$ and $ClpP_{H136A}$ in enhanced susceptibility is independent of ClpP-ClpA complex formation.

The recipient's *clpP*-dependent enhanced *A. tumefaciens* T6SS antibacterial activity may results from reduced Tde1 toxicity

We next tested whether the recipient's *clpA*- and *clpP*-dependent enhanced *A. tumefaciens* C58 T6SS killing outcome applies to other strains. The susceptibility of the Δ*clpP* and Δ*clpA* to the T6SS attack using *A. tumefaciens* strains 1D132, 1D1108, and A6 was observed. Strains C58 and 1D132 harbor Tde1/2 homologs and belong to *A. tumefaciens* genomospecies G8, while 1D1108 and A6 lack Tde1/2 homologs and belong to genomospecies G1 (Wu, et al. 2019b). The Δ*clpP* also had reduced SI compared to that of the wild type when using strain 1D132 as an attacker, but not using strains 1D1108 and A6 (Figure 3-8A, 3-8B, and 3-8C). The Δ*clpA*, on the other hand, was not less susceptible to *A. tumefaciens* T6SS killing when 1D132, 1D1108, and A6 were used as attackers (Figure 3-8D, 3-8E, and 3-8F). The results demonstrated that *A. tumefaciens* strain 1D132, which belongs to the same genomospecies and harbors Tde1/2, also enhances its T6SS killing outcome in a *clpP*-dependent manner.

doi:10.6342/NTU202000295

As C58 and 1D132 both harbor Tde1/2 homologs and the main contributors to *A. tumefaciens* C58 T6SS antibacterial activity are the Tde DNase effectors (Ma, et al. 2014), we next tested whether the *clpP*-dependent enhanced T6SS killing outcome correlates with Tde1/2 DNase activity. The Tde1 DNase activity was demonstrated by the plasmid digestion assay in *E. coli* cells and by an in vitro nuclease activity assay, as described in Ma et al. (Ma, et al. 2014). The plasmid digestion rate of *E. coli* BW25113 wild type was higher than that of Δ*clpP* but was similar to that of $clpP^+$ (Figure 3-9). Meanwhile, the Tde1 protein level in Δ*clpP* was lower than that of BW25113 wild type and $clpP^+$ (Figure 3-9A). The results imply that the less susceptibility to *A. tumefaciens* T6SS killing in Δ*clpP* could result from lower Tde1 level and hence lower plasmid degradation. The lower Tde1 level in Δ*clpP* could result either from lower Tde1 production in the arabinose-inducible system or from a higher Tde1 degradation rate. To test the first possibility, we ectopically expressed the Tde1 catalytic mutant (Tde1M, H190AD193A) (Ma, et al. 2014) using the leaky *trc* promoter under the non-inducing condition. The result showed that the Tde1M protein level was lower in Δ*clpP* than that of wild type and Δ*clpX*; the latter two had a similar Tde1M level (Figure 3-10). This result indicates that the lower Tde1 level in Δ*clpP* was not due to the inducible system and is more likely the inert property of the Δ*clpP*. Surprisingly, the Tde1M level of the Δ*clpA* was significantly higher than that of the wild type (Figure 3-10). In summary, the evidence shows that *clpP* may participate in enhancing Tde1 toxicity presumably by stabilizing the Tde1 proteins and that the role of *clpA* in enhancing recipient susceptibility to *A. tumefaciens* T6SS attack may not be entirely the same with that of the *clpP*.

doi:10.6342/NTU202000295

3.5 Discussion

This study provides evidence that the genetic factors of the recipient cells play an important role in affecting the outcome of the T6SS antibacterial activity. The high throughput interbacterial competition platform developed in this study proved to be an effective method in identifying recipient factors that affect the outcome of *A. tumefaciens* T6SS antibacterial activity. Further exploration led to the confirmation of at least six genes (*clpP*, *clpA, gltA*, *ydhS*, *ydaE*, *cbpA*) encoding known or putative cytoplasmic proteins (Keseler, et al. 2016), whereas CbpA resides both in the cytoplasm and in the nucleoid (Orfanoudaki and Economou 2014). None of these gene products were localized to the inner membrane, periplasm, outer membrane, or extracellular milieu. This result implies that the process affecting the outcome of *A. tumefaciens* T6SS killing to *E. coli* occurs in the cytoplasm, presumably after the injection of the T6SS puncturing apparatus. Previous studies have mainly focused on how attacker T6SS is regulated and sensed (Alteri and Mobley 2016, Filloux and Sagfors 2015, Hood, et al. 2017). This study provides a new insight that recipient cell genes can also affect the T6SS killing outcome and that it could take place after the injection of the T6SS apparatus into the recipient cytoplasm.

Among the six confirmed recipient factors that participate in enhancing *A. tumefaciens* T6SS killing, the *clpP* and *clpA* products form the ClpAP complex, while the *curved DNA-binding protein A*, *cbpA*, is indirectly connected to ClpAP. The failure of the complementation test in the Δ*cbpA* could result from the polar effect as the *cbpA* operon contains two genes: *cbpA* and the downstream *cbpA* modulator *cbpM* (Chae, et al. 2004). The CbpA is a non-specific DNA binding protein and a co-chaperone of the DnaK that helps proteins remodeling and refolding in *E. coli* (Chae, et al. 2004, Ueguchi, et al.

doi:10.6342/NTU202000295

1994). The CbpM functions as a specific inhibitor to the CbpA that hinders both its co-chaperone and DNA binding activities (Chae, et al. 2004). Intriguingly, CbpM is a substrate for the ClpAP protease (Chenoweth and Wickner 2008). Further study is needed to elucidate whether *E. coli* recipient's CbpM, CbpA, ClpA, and ClpP participate in the same pathway to enhance *A. tumefaciens* T6SS killing. On the other hand, it is less obvious how *gltA*, *ydhS*, and *ydaE* connect to the former genes. The *gltA* is monocistronic that produces the citrate synthase, which catalyzes the first step of the citric acid cycle (Keseler, et al. 2016). The *ydhS* is a monocistronic gene composed of 1,605 base pairs with an unknown function (Keseler, et al. 2016). The *ydaE* is a short gene that consists of 171 base pairs that lie downstream of the *kilR*, which is the *kil* gene of the lambdoid prophage Rac (Conter, et al. 1996). The *kilR-ydaE* was proposed to functionally reminiscent of the toxin-antitoxin (TA) system (Masuda, et al. 2016), but their biological evidence remains elusive. YdaE binds to one zinc ion by four of its cysteine residue (Blindauer, et al. 2002). How these recipient genes participate in enhancing *A. tumefaciens* T6SS killing could be a promising future direction in elucidating their molecular mechanisms.

Our data showed that ClpA but not ClpX, together with ClpP, contributes to the susceptibility of the recipient *E. coli* to *A. tumefaciens* T6SS killing. The *clpX* transcripts level drops and fades 15 min after the onset of carbon starvation (Li, et al. 2000), which is the condition used for our interbacterial competition. Thus, ClpX is probably not available to form the ClpXP complex during *Agrobacterium* T6SS attacks. The Δ*clpA* was indeed identified in the first screening but was accidentally misplaced and did not enter the second screening process. Therefore, Δ*clpA* did not appear in our final candidate list until we obtained the correct strain for confirmation. The results that

doi:10.6342/NTU202000295

the three catalytic variants $ClpP_{S111A}$, $ClpP_{H136A}$, and $ClpP_{D185A}$ did not significantly differ in their ability to degrade GFP-ssrA substrate suggested that the protease activity may not be the leading cause in enhancing *A. tumefaciens* T6SS attack. On the other hand, unlike $ClpP_{S111A}$ and $ClpP_{H136A}$, which do not exhibit significant protease activity as compared to with of the negative controls, $ClpP_{D185A}$ may possess weak protease activity, as the GFP-ssrA fluorescence level is significantly lower than that of the negative controls at the final time point. Thus, the involvement of the ClpP protease activity cannot be completely ruled out as the weak protease activity of $ClpP_{D185A}$ may be sufficient to exhibit its function in enhancing *A. tumefaciens* T6SS attack. Of note, the ClpP protease activity monitored by the *in vitro* protease activity assay using either ClpX or ClpA as a protein unfoldase showed a highly similar pattern among 24 ClpP variants (Bewley, et al. 2006). As this GFP-ssrA degradation assay is an *in vitro* system and that it is difficult to monitor the ClpP protease activity of the recipient under competition condition, the role of ClpP protease remains elusive.

Our data also suggest that ClpAP complex is required in enhancing recipient susceptibility during *A. tumefaciens* T6SS killing on the bases of the results that ClpP variant that loses its ability to form a complex with ClpA did not complement the phenotype whereas those with ClpA binding ability do. This implies that the ClpA-ClpP complex, rather than ClpP alone, is the cause of the enhanced susceptibility to T6SS attack. As ClpP allosterically activates the polypeptide translocation activity of ClpA (Miller, et al. 2013), the necessity of the ClpAP complex may depend on the unfoldase activity of ClpA. The detailed mechanism on how recipient ClpAP is involved in T6SS susceptibility enhancement awaits further investigations. One promising future direction

doi:10.6342/NTU202000295

would be identifying the potential ClpA substrates and their effects on increasing susceptibility of T6SS attack.

Hijacking a highly conserved and essential molecule of the recipient cell to improve attacker fitness is not uncommon. The examples are CdiA-CT^{EC93} hijacking essential proteins BamA and AcrB, CdiA-CT^{EC536} hijacking the recipient CysK, and Ssp2 and Ssp4 hijacking recipient DsbA (Aoki, et al. 2008, Diner, et al. 2012, Mariano, et al. 2018). The ClpP protease, on the other hand, is highly conserved in both prokaryotes and eukaryotic organelles like plastid and mitochondria (Culp and Wright 2016, Moreno, et al. 2017). The ClpP protease cooperates with different AAA$^+$ ATPases in different organisms. It works with ClpA and ClpX in Gram-negative bacteria; with ClpC, and ClpE in Gram-positive bacteria; with ClpC1, ClpC2, and ClpD in the chloroplast; and with ClpX in human mitochondria. In all these cases, the ClpP protease seems to play a central role in protein homeostasis. Dysfunction of the system can lead to severe developmental defects, a reduction in the pathogenicity, or lethality (Bhandari, et al. 2018, Cole, et al. 2015, Nishimura and van Wijk 2015). The current result suggests that the ClpP protease system could be another target hijacked by the T6SS attacker to improve its competitive advantage. The results that the Δ*clpP* had lower Tde1 level, plasmid degradation, as well as susceptibility to *A. tumefaciens* T6SS attack suggest that Tde1 effector might hijack the ClpP. The *A. tumefaciens* strains lacking the Tde1/2 homologs did not show *clpP*-dependent enhanced T6SS killing outcome moonlight this viewpoint. The result that ClpP could be required for Tde1 to exert full toxicity is consistent with the known recipient factors that contribute to improving attacker fitness to a specific effector. Further studies to demonstrate ClpP-Tde1 interaction as well as how ClpP alters the toxicity of Tde1 are required.

doi:10.6342/NTU202000295

To our knowledge, the involvement of the ClpAP complex in enhancing the recipient's susceptibility to *A. tumefaciens* T6SS activity has not been described in the contact-dependent competitor elimination systems in Gram-negative bacteria like T1SS, T4SS, CDI, and T6SS. It would be of interest to uncover how and what *A. tumefaciens* factors hijacks this universal and highly conserved ClpP and its associated AAA^+ ATPase substrate recognizing partner. The current finding provides additional evidence to support that T6SS can manipulate the essential and highly conserved molecules of recipient cells to achieve better inhibiting of the performance (Russell, et al. 2014). Elucidating the underlying molecular mechanisms of ClpAP and other recipient factors would be the next direction to understand further how genetic factors can affect the recipient susceptibility to the T6SS attacks.

doi:10.6342/NTU202000295

Table 3-1. Bacterial strains and plasmids used in chapter 3.

Strain/Plasmid	Relevant characteristics	Source/reference
A. tumefaciens		
C58	wild type virulence strain containing pTiC58 and pAtC58; EML530	Eugene Nester
C58:Δ*atu4333*	*atu4333* (*tssL*) in-frame deletion mutant of C58 background; EML1073	(Ma, et al. 2012)
1D132	wild type virulence strain to pear; EML305	Lab collection
1D132:Δ*tssL*	*tssL* in-frame deletion mutant of 1D132 background; EML4720	(Wu, et al. 2019b)
1D1108	wild type virulence strain to Euonymus; EML302	Lab collection
1D1108:Δ*tssL*	*tssL* in-frame deletion mutant of 1D1108 background; EML4631	(Wu, et al. 2019b)
A6	wild type virulence strain containing pTiA6; EML464	Lab collection
A6:Δ*tssL*	*tssL* in-frame deletion mutant of A6 background; EML4627	(Wu, et al. 2019b)
E. coli		
DH10B	Host for DNA cloning	Invitrogen
BW25113	wild type strain of the Keio Collection. *rrnB* DE*lacZ*4787 *HsdR*514 DE(*araBAD*)567 DE(*rhaBAD*)568 *rph*-1.	(Baba, et al. 2006)
Keio collection	Systematic single-gene knock-out mutants of *E. coli* BW25113	(Baba, et al. 2006)
JW0427	BW25113 *clpP*:*kan*	(Baba, et al. 2006)
JW0866	BW25113 *clpA*:*kan*	(Baba, et al. 2006)
JW0428	BW25113 *clpX*:*kan*	(Baba, et al. 2006)
EML5395	DH10B harboring pNptII	This study
EML5393	BW25113 wild type harboring pNptII	This study
BL21(DE3)	Host for protein expression	(Studier and Moffatt 1986)
Plasmids		
pTrc200HA	Sp^R, pTrc200 harboring C-terminal influenza hemagglutinin (HA) epitope, P*trc*, $lacI^q$, pVS1 origin	Laboratory collection
pRL662	Gm^R, a non-transferable broad-host range vector derived from pBBR1MCS2	(Vergunst, et al. 2000)
pET22b(+)	Ap^R, *E. coli* overexpression vector harboring C-terminal 6xHis epitope	Novagen
pJN105	Gm^R, Arabinose induced promoter in pBBR1MCS5 background	(Newman and Fuqua 1999)
pRL-*rpsL*	Gm^R, pRL662 expressing BW25113 *rpsL* gene	This study
pRL-*galk*	Gm^R, pRL662 expressing BW25113 *galK* gene	This study
pRL-*nupG*	Gm^R, pRL662 expressing BW25113 *nupG* gene	This study

doi:10.6342/NTU202000295

pRL-*rpsL*^{Str}	Gm^R, pRL662 expressing DH10B *rpsL*^{Str} gene	This study
pNptII	Km^R, Gm^R, pRL662 expressing *nptII* gene	This study
pClpP-HA	Sp^R, pTrc200HA expressing ClpP-HA fusion protein	This study
pClpA-HA	Sp^R, pTrc200HA expressing ClpA-HA fusion protein	This study
pClpP$_{S111A}$-HA	Sp^R, pTrc200HA expressing ClpP-HA fusion protein with S111A substitution	This study
pClpP$_{H136A}$-HA	Sp^R, pTrc200HA expressing ClpP-HA fusion protein with H136A substitution	This study
pClpP$_{D185A}$-HA	Sp^R, pTrc200HA expressing ClpP-HA fusion protein with D185A substitution	This study
pClpP$_{R26A}$-HA	Sp^R, pTrc200HA expressing ClpP-HA fusion protein with R26A substitution	This study
pClpP$_{D32A}$-HA	Sp^R, pTrc200HA expressing ClpP-HA fusion protein with D32A substitution	This study
pClpX-ΔN-ter	plasmid used for purifying ClpX- ΔN	Robert T. Sauer
pGFP-ssrA	plasmid used for purifying GFP-ssrA	Robert T. Sauer
pClpP-tev-His	Ap^R, pET22b(+) expressing ClpP-tev-His, in which ClpP protein is fused with a TEV protease cleavage site and a His-tag in its C-terminal	Robert T. Sauer
pClpP$_{S111A}$-tev-His	Ap^R, pET22b(+) expressing ClpP-tev-His with ClpP S111A substitution	This study
pClpP$_{H136A}$-tev-His	Ap^R, pET22b(+) expressing ClpP-tev-His with ClpP H136A substitution	This study
pClpP$_{D185A}$-tev-His	Ap^R, pET22b(+) expressing ClpP-tev-His with ClpP D185A substitution	This study
pJN4350	Gm^R, pJN105 expressing Tde1 (Atu4350)	(Ma, et al. 2014)
pTde1M:HA	Sp^R, pTrc200HA expressing Tde1M-HA fusion protein. Tde1M: Tde1H190AD193A	Lab collection

doi:10.6342/NTU202000295

Table 3-2. Primers used in chapter 3.

Primer	Sequence (5'-3')[a]	Plasmids
T7	TAATACGACTCACTATAGGG	pET22b(+)
T7T	GCTAGTTATTGCTCAGCGG	
pTRC99C-F	TTGCGCCGACATCATAAC	pTrc200HA
pTRC99C-R	CTGCGTTCTGATTTAATCTG	
rpsL-fw	AAAAACTCGAGGCAAAAGCTAAAACCAGGA	1. pRL-*rpsL*
rpsL-rv	AAAAATCTAGACTTACTTAACGGAGAACCA	2. pRL-rpsL^{Str}
galK-fw	AAAAACTCGAGCAGTCAGCGATATCCATT	pRL-galk
galK-rv	AAAAATCTAGAGCAAAGTTAACAGTCGGT	
nupG-fw	AAAAACTCGAGTCAAACACTCATCCGCAT	pRL-nupG
nupG-rv	AAAAATCTAGACCCGTTTTTCTTTGCGTAA	
NptII-fw-XhoI	AAAAACTCGAGAGACTGGGCGGTTTTATGGA	pNptII
NptII-rv-HindIII	AAAAAAAGCTTCTCTAGCGAACCCCAGAGTC	
ClpP-SacI-fw	AAAAAGAGCTCATGTCATACAGCGGCGAACG AGATAAC	pClpP-HA
ClpP-PstI-rv	AAAAACTGCAGATTACGATGGGTCAGAATCG AATCGAC	
ClpA-SacI-fw	AAAAAGAGCTCATGCTCAATCAAGAACTGGA ACTCAGTTT	pClpA-HA
ClpA-PstI-rv	AAAAACTGCAGATGCGCTGCTTCCGCCTTGTG CTTT	
ClpP-S111A-fw	TGTATGGGCCAGGCGGCC**GCG**ATGGGCGCTTT CTTGCTG	1. pClpP$_{S111A}$-HA
ClpP-S111A-rv	CAGCAAGAAAGCGCCCAT**CGC**GGCCGCCTGG CCCATACA	2. pClpP$_{S111A}$-tev-His
ClpP-H136A-fw	AATTCGCGCGTGATGATT**GCC**CAACCGTTGGG CGGCTAC	1. pClpP$_{H136A}$-HA
ClpP-H136A-rv	GTAGCCGCCCAACGGTTG**GGC**AATCATCACGC GCGAATT	2. pClpP$_{H136A}$-tev-His
ClpP-D185A-fw	GAACGTGATACCGAGCGC**GCT**CGCTTCCTTTC CGCCCCT	1. pClpP$_{D185A}$-HA
ClpP-D185A-rv	AGGGGCGGAAAGGAAGCG**AGC**GCGCTCGGTA TCACGTTC	2. pClpP$_{D185A}$-tev-His
ClpP-R26A-fw	GTCATTGAACAGACCTCA**GCC**GGTGAGCGCTC TTTTGAT	pClpP$_{R26A}$-HA
ClpP-R26A-rv	ATCAAAAGAGCGCTCACC**GGC**TGAGGTCTGTT CAATGAC	
ClpP-D32A-fw	CGCGGTGAGCGCTCTTTT**GCT**ATCTATTCTCGT CTACTT	pClpP$_{D32A}$-HA
ClpP-D32A-rv	AAGTAGACGAGAATAGAT**AGC**AAAAGAGCGC TCACCGCG	

a: Restriction enzyme sites are underlined, and mutated sequences are in bold type.

doi:10.6342/NTU202000295

Table 3-3. *E. coli* strains that showed reduced susceptibility to *A. tumefaciens* T6SS attack.

No.	Resource (JW ID)	disrupted gene	Gene products affected by Kanamycin cassette insertion[a]	reduced susceptibility[b]	trans complementation[c]
1	JS0427	*clpP*	ClpAXP, ClpXP, ClpAP	O	O
2	JW0710	*gltA*	citrate synthase	O	O
3	JW1658	*ydhS*	FAD/NAD(P) binding domain-containing protein YdhS	O	O
4	JW1346	*ydaE*	Rac prophage; zinc-binding protein	O	Δ
5	JW0985	*cbpA*	curved DNA-binding protein	O	X
6	JW1792	*yeaX*	carnitine monooxygenase	X	n.d.

[a] Gene products information was obtained from the EcoCyc database (Keseler, et al. 2016)
[b] Mutant strains with reduced susceptible index (SI) and showed significant difference under $P < 0.05$ was labelled as O, with no significant difference to that of wild type was labelled in X.
[c] Plasmid-born gene that can fully complement the disrupted gene is labelled in O, partially complemented is labelled in Δ, and cannot be complemented labelled in X.
n.d.: not determined.

doi:10.6342/NTU202000295

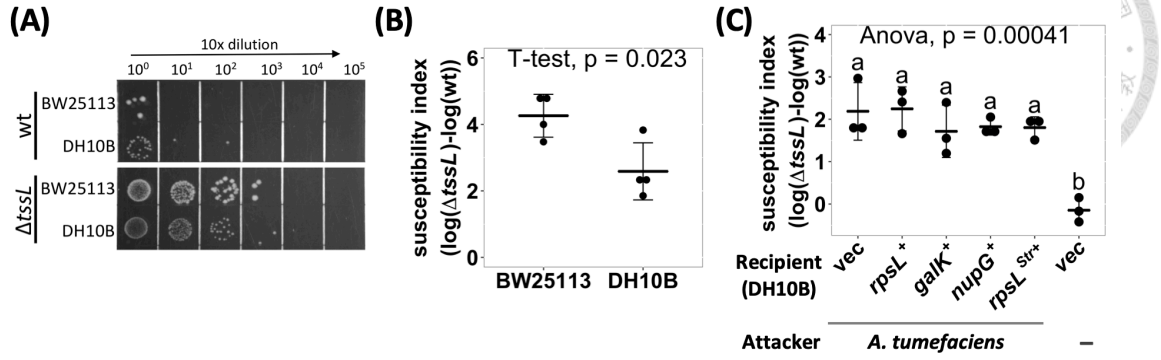

Figure 3-1. *A. tumefaciens* T6SS-dependent antibacterial activity against *E. coli* strains.

(A, B) *A. tumefaciens* T6SS antibacterial activity against *E. coli* strains DH10B and BW25113. *A. tumefaciens* was co-cultured at a ratio of 30:1 with *E. coli* DH10B or BW25113, both *E. coli* strains harboring vector pRL662, on *Agrobacterium* Kill (AK) agar medium for 16 h. The bacterial mixtures were serially diluted and spotted (A) or quantified by counting cfu (B) on gentamicin-containing lysogeny broth (LB) agar plates to selectively recover *E. coli*. **(C)** E. coli DH10B was complemented by either vector only (vec) or derivative expressing *rpsL*, *galK*, *nupG*, or $rpsL^{Str}$ in trans before being subjected to *A. tumefaciens* T6SS-dependent antibacterial activity assay as described in (B). Susceptibility index (SI) was defined as the subtraction difference of the recovery log(cfu) of that attacked by Δ*tssL* to that attacked by wild-type *A. tumefaciens* C58. Data are mean ± SD of three independent experiments calculated by *t*-test with $P < 0.05$ for statistical significance (B) or single-factor analysis of variance (ANOVA) and Tukey honestly significant difference (HSD), in which two groups with significant differences are indicated with different letters (a and b) (C).

doi:10.6342/NTU202000295

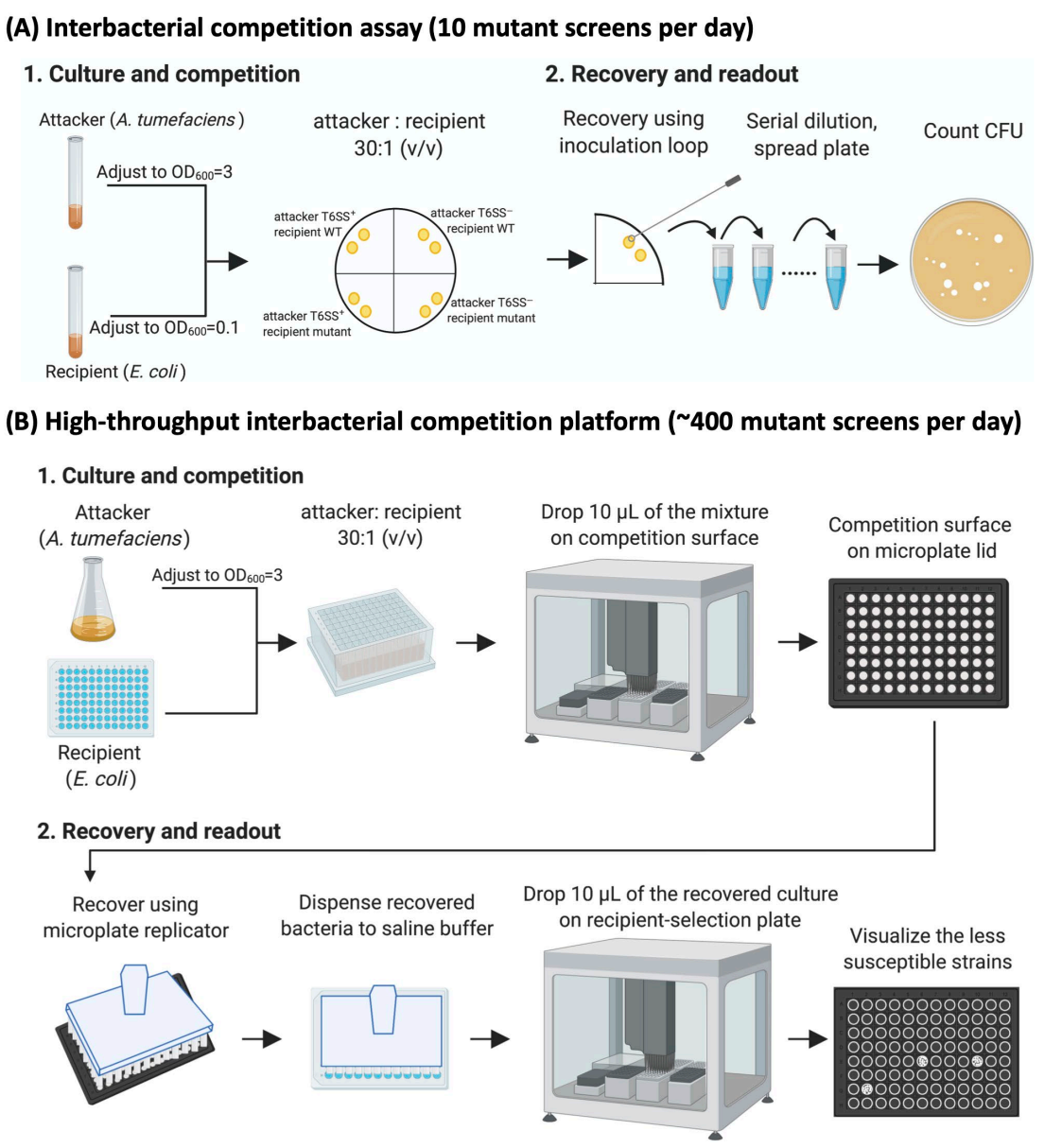

Figure 3-2. The high-throughput interbacterial competition platform.

(A) Interbacterial competition assay. Cultured attacker *A. tumefaciens* and recipient *E. coli* were mixed and then spotted on the AK agar medium to allow interbacterial competition for 16 h at 25oC followed by recovery of mixed cultures, serial diluted, and then spread onto LB plate supplemented with appropriate antibiotics to select for recipient cells. **(B)** High-throughput interbacterial competition screening platform. Recipient cells were grown and mixed with attacker *A. tumefaciens* in a 96-well plate.

doi:10.6342/NTU202000295

The bacterial mixture was dropped onto the AK agar medium competition surface using an automated pipetting system. The competition surface was made on a microplate lid. Recovery was performed using microplate replicator. The candidates are the strains that show multiple colonies grown after recovery as opposed to wild type controls and most strains with no or few colonies. This high-throughput *A. tumefaciens* T6SS killing platform enables ~400 mutant screens per day. This figure was created with BioRender (https://biorender.com/).

doi:10.6342/NTU202000295

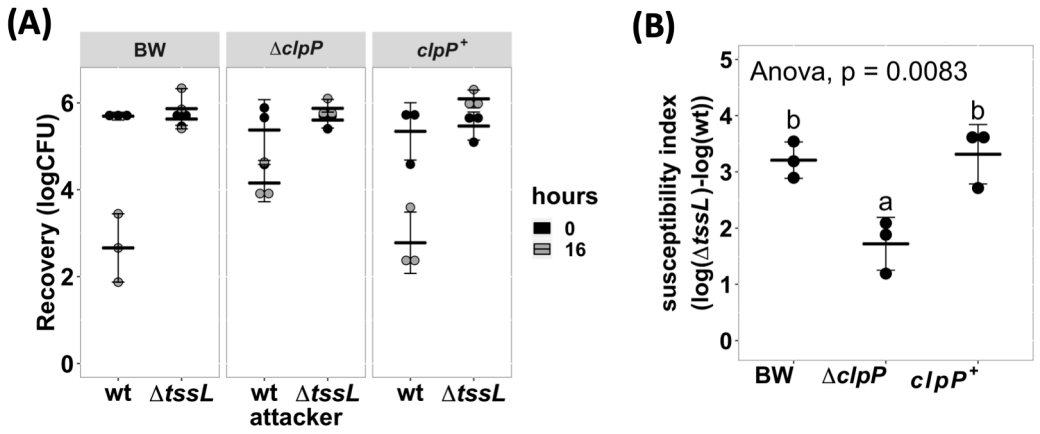

Figure 3-3. *A. tumefaciens* susceptibility to T6SS-dependent antibacterial activity was reduced in *E. coli* Δ*clpP*:*kan* and can be fully complemented *in trans*.

(A) Recovery of surviving *E. coli* cells at 0 h and 16 h after being co-cultured with either *A. tumefaciens* wild type C58 (wt) or Δ*tssL* at a ratio of 30:1. (B) The susceptibility index (SI) of *E. coli* BW25113 wild type (BW), Δ*clpP*, and Δ*clpP* complemented with *clpP* expressed on plasmid (*clpP*$^{+}$) was calculated from the recovery rate shown in (A). Statistical analysis involved single-factor analysis of variance (ANOVA) and Tukey honestly significant difference (HSD). Data are mean ± SD of three independent experiments, and two groups with significant differences are indicated with different letters (a and b) ($P < 0.05$ for statistical significance).

doi:10.6342/NTU202000295

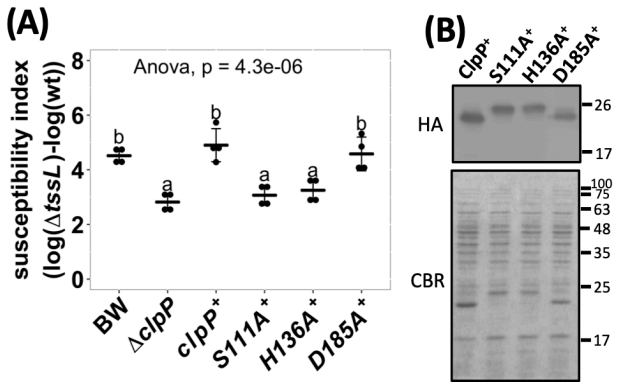

Figure 3-4. Effects of ClpP protease catalytic variants in enhancing *A. tumefaciens* T6SS antibacterial activity.

(A) The susceptibility index calculated from *A. tumefaciens* interbacterial activity assay against *Escherichia coli*. The *A. tumefaciens* C58 wild-type or Δ*tssL* were co-cultured at a ratio of 10:1 with *E. coli* BW25113 wild type (BW), Δ*clpP*, and Δ*clpP* complemented with *clpP* and its variants expressed on plasmid. The complemented *clpP* strains were either wild type ($clpP^+$) or catalytic variants $ClpP_{S111A}$ ($S111A^+$), $ClpP_{H136A}$ ($H136A^+$), and $ClpP_{D185A}$ ($D185A^+$), with C-terminus HA-tag. The susceptibility index (SI) of each *E. coli* was calculated from the logarithm recovery rate of the Δ*tssL* co-cultured group minus that of the wild-type co-cultured group. Data are mean ± SD of four biological replicates from two independent experiments. Statistical analysis involved single-factor analysis of variance (ANOVA) and Tukey honestly significant difference (HSD) with $P < 0.05$ for statistical significance. Two groups with significant differences are indicated with different letters (a and b). **(B)** The ClpP protein levels of the Δ*clpP* complemented strains used in (A). The ClpP-expressing *E. coli* strains were cultured at the same condition used in interbacterial competition assay. Instead of co-culture with *A. tumefaciens*, protein samples were collected, normalized, and subjected to Western blot analysis. Representative result of three independent experiments is shown.

doi:10.6342/NTU202000295

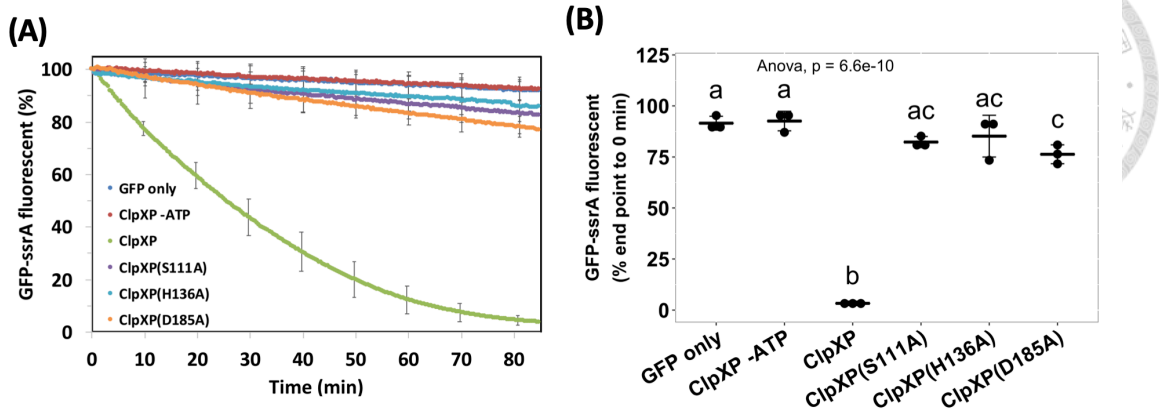

Figure 3-5. Protease activity assay of the ClpP and its catalytic variants.

The wild-type ClpP and its catalytic variants were each pre-assembled with ClpX followed by providing its substrate, the ssrA-tagged green fluorescent protein (GFP). The GFP fluorescent signals were monitored **(A)** over time, and **(B)** statistical analysis was measured at the end of the assay. Statistical analysis involved single-factor analysis of variance (ANOVA) and Tukey honestly significant difference (HSD) with $P < 0.05$ for statistical significance. Two groups with significant differences are indicated with different letters (a and b). Data are mean ± SD of three biological replicates from one representative result of at least two independent experiments.

doi:10.6342/NTU202000295

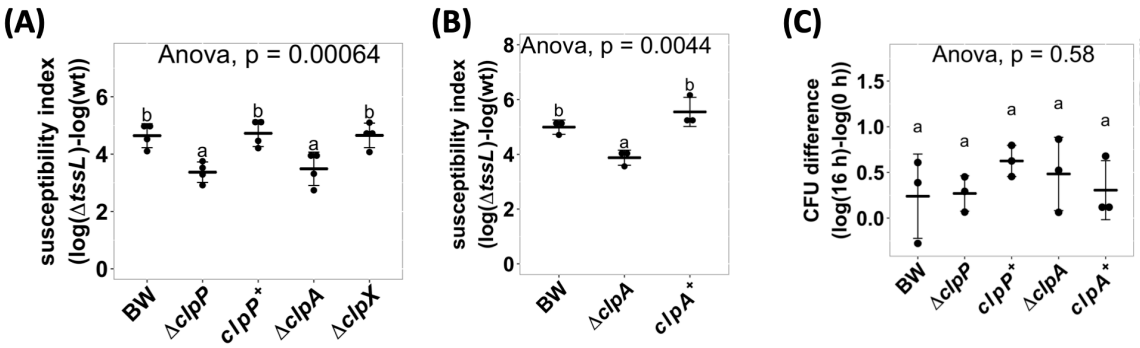

Figure 3-6. ClpP associated AAA+ ATPase ClpA but not ClpX is involved in enhancing *A. tumefaciens* T6SS antibacterial activity.

(A) *A. tumefaciens* T6SS antibacterial activity against *Escherichia coli* Δ*clpP* and its complement strain, Δ*clpA* and Δ*clpX*. The *A. tumefaciens* and the *E. coli* were co-cultured at a ratio of 10:1 on Agrobacterium Kill (AK) agar medium for 16 h. Afterward, the recovery of *E. coli* strains was quantified, and the susceptibility index was calculated by subtracting the difference of the recovered log(cfu) of that attacked by 1tssL to that by wild-type *A. tumefaciens* C58. **(B)** *A. tumefaciens* T6SS antibacterial activity assay and the susceptibility index were performed as described in (A) using *E. coli* wild type (BW), Δ*clpA*, and Δ*clpA* complemented with *clpA* expressed on plasmid ($clpA^+$). **(C)** Growth of *E. coli* when co-culturing with the Δ*tssL A. tumefaciens*. Data in (A–C) are mean ± SD of at least three independent experiments. Statistical analysis involved single-factor analysis of variance (ANOVA) and Tukey honestly significant difference (HSD) with $P < 0.05$ for statistical significance. Two groups with significant differences are indicated with different letters (a and b).

doi:10.6342/NTU202000295

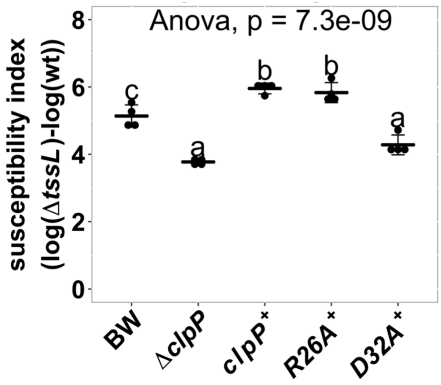

Figure 3-7. Effects of ClpP variants impaired with ClpA-binding ability in enhancing *A. tumefaciens* T6SS antibacterial activity.

Interbacterial competition assay between *A. tumefaciens* and *E. coli* wild type, Δ*clpP*, and Δ*clpP* complement strains expressing wild-type ClpP (*clpP*$^{+}$), ClpAP complex formation mutants $ClpP_{R26A}$ ($R26A^{+}$), and $ClpP_{D32A}$ ($D32A^{+}$). The ClpAP complex forming ability is half than that of wild-type ClpP in $ClpP_{R26A}$ and is completely lost in $ClpP_{D32A}$ (Bewley et al., 2006). The T6SS killing data are mean ± SD of four biological replicates from two independent experiments. Statistical analysis involved single-factor analysis of variance (ANOVA) and Tukey honestly significant difference (HSD) with $P < 0.05$ for statistical significance. Two groups with significant differences are indicated with different letters (a and b).

doi:10.6342/NTU202000295

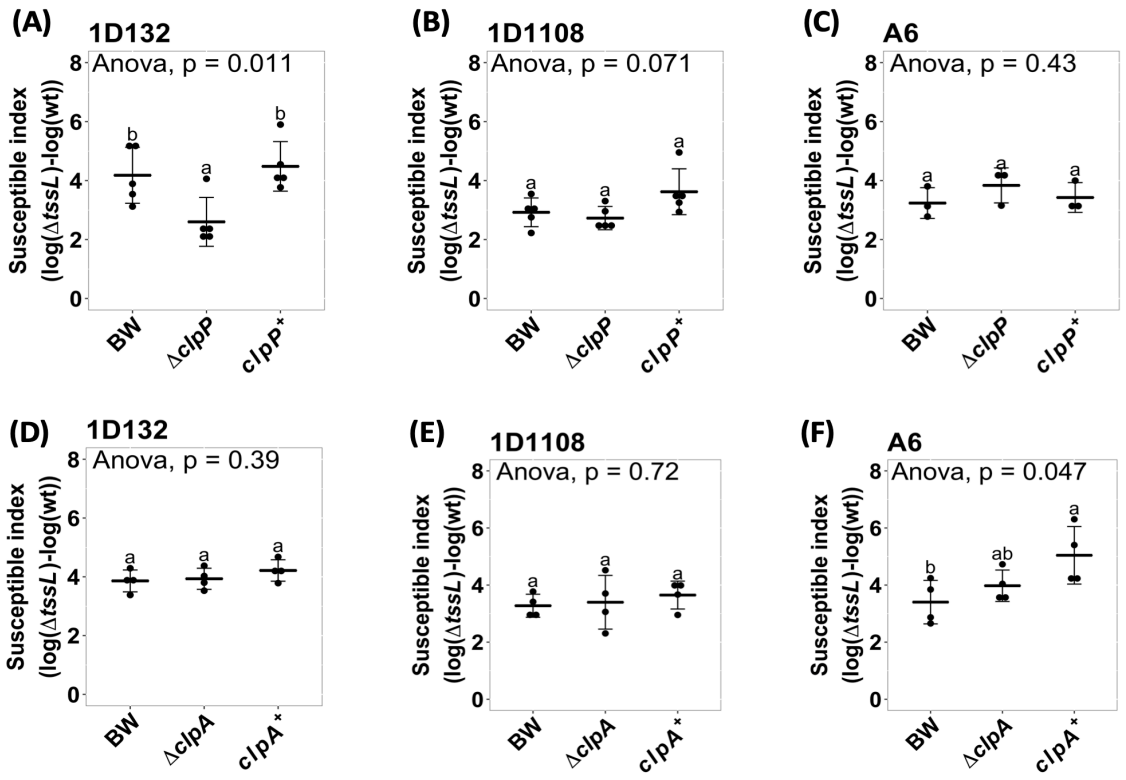

Figure 3-8 Interbacterial competition between *A. tumefaciens* and *E. coli* Δ*clpP*:kan or Δ*clpA*:kan strain.

(A)-(C) The susceptible index (SI) of *E. coli* BW25113 wild type (BW), Δ*clpP*, and $clpP^+$ obtained when using *A. tumefaciens* strain (A) 1D132, (B) 1D1108, and (C) A6 as an attacker. **(D)-(F)** The susceptible index (SI) of BW, Δ*clpA*, and $clpA^+$ obtained when using *A. tumefaciens* strain (D) 1D132, (E) 1D1108, and (F) A6 as an attacker. Interbacterial competition assay was performed as that described in Figure 3-4. Statistical analysis involved single factor analysis of variance (ANOVA) and TukeyHSD. Data are mean ± SD of three independent experiments and two groups with significant differences are indicated with different letters (a and b) ($P < 0.05$ for statistical significance).

doi:10.6342/NTU202000295

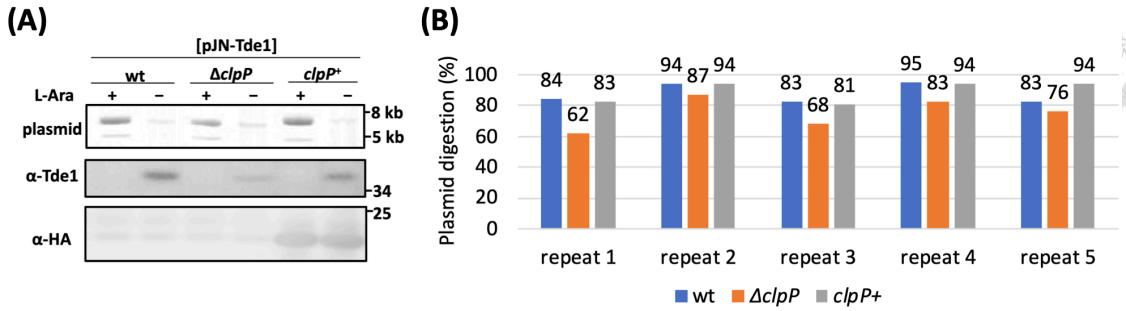

Figure 3-9. Plasmid degradation by Tde1 in *E. coli* BW25113.

(A) A representative result of the Tde1-dependent plasmid degradation. The *E. coli* BW25113 strains harboring plasmid expressing Tde1 were sub-cultured in AK liquid medium and induced with (+) or without (-) L-arabinose for 2h. After the induction, a same cell mass was collected from each group for plasmid and cellular protein extraction. An equal volume of the plasmid was analyzed on 1% agarose gel, and the cellular protein was detected using antibodies against the Tde1 and HA as described in (Ma, et al. 2014). wt: BW25113 wildtype, Δ*clpP*: Δ*clpP*:kan, $clpP^{+}$: Δ*clpP* harboring pClpP-HA. The plasmid levels were quantified by Fiji (version 2.0.0-rc-69/1.52p) (Schindelin, et al. 2012). The plasmid digestion (%) is the percentage of the plasmid signal with and without induction. **(B)** The quantification results of the Tde1-dependent plasmid degradation as described in (A).

doi:10.6342/NTU202000295

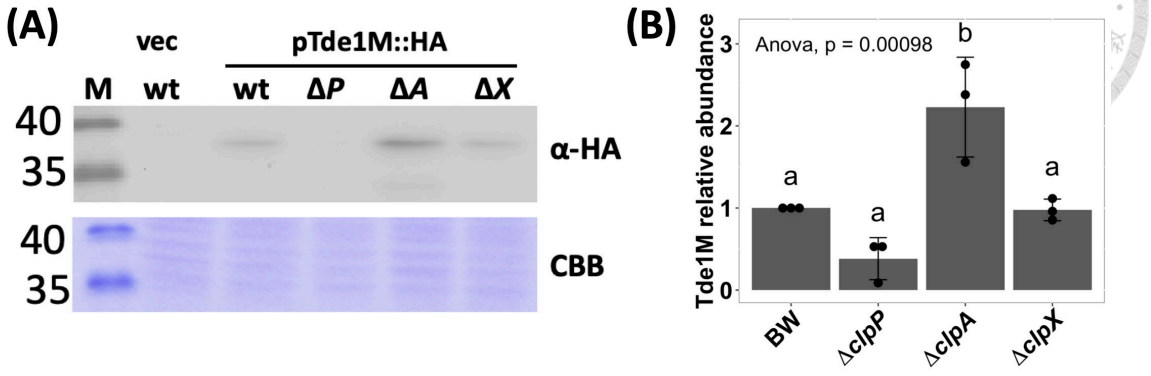

Figure 3-10. ***A. tumefaciens*** **effector Tde1 protein level in the recipient cells.**

(A) Western blot and **(B)** its quantitative analysis of total proteins isolated from *E. coli* BW25113 harboring the vector (vec) or Tde1 catalytic mutant (H190AD193A) (Ma, et al. 2014) with C-terminal HA tag (Tde1M::HA) expressing plasmid. Bacteria were grown in AK liquid culture, and their proteins were detected with anti-HA antibody. The Coomassie Brilliant Blue (CBB) staining served as a loading control. The protein levels were quantified by Fiji (version 2.0.0-rc-69/1.52p) (Schindelin, et al. 2012). The molecular weight standards are labeled on the left. Data are mean ± SD of three independent experiments and two groups with significant differences are indicated with different letters (a and b) ($P < 0.05$ for statistical significance).

doi:10.6342/NTU202000295

Chapter 4. Concluding remarks and discussion

The biological functions of the bacterial T6SS have been intensively studied in the past ten years, which have led to the discovery of its roles in microbe-host interaction and interbacterial competition (Bernal, et al. 2018, Cianfanelli, et al. 2015, Hachani, et al. 2016). Albeit present in more than a quarter of the sequenced Gram-negative bacteria including many plant-associated bacteria (Abby, et al. 2016, Coulthurst 2013), the biological roles of the T6SS are much less understood than that of the animal-associated bacteria (Bernal, et al. 2018, Hood, et al. 2017, Russell, et al. 2014, Ryu 2015). At the time when I began my Ph.D. study, the biological functions of T6SS in plant-associated bacteria were largely unknown. In symbiotic bacteria, the only clue was the implication that T6SS of the *R. leguminosarum* RBL5787 may participate in legume-rhizobium host range determination (Bladergroen, et al. 2003), but direct evidence was lacking. In phytopathogen, it had been shown that T6SS is weakly related to pathogenicity in both *A. tumefaciens* and *P. syringae* pv. tomato DC3000 (Haapalainen, et al. 2012, Wu, et al. 2008). The antibacterial activity of T6SS, which was newly discovered by then, was only shown in *P. syringae* pv. tomato DC3000 and the killing is much weaker (less than half a log) than that demonstrated in animal pathogens (more than two logs) (Basler, et al. 2013, Haapalainen, et al. 2012, Hood, et al. 2010). Therefore, the biological functions and mode of actions of T6SS in phytopathogens await further studied. This prompted me to explore the functions and underlying mechanisms of the T6SS in plant-associated bacteria, especially those involved in mutualistic and parasitic interactions.

Since legume–rhizobium symbiosis is a classic example of mutualism, I chose *A. caulinodans*-*S. rostrata* symbiotic system as a research model to elucidate the biological functions of T6SS. We found that T6SS did not affect the phenotypes, growth, and the

doi:10.6342/NTU202000295

free-living nitrogen-fixing ability of *A. caulinodans* (Figure 2-3 and Appendix Figure 2). We also observed that the *A. caulinodans* T6SS mutant showed no defect in forming root and stem nodules, nor did the nodules had abnormal phenotypes (Figures 2-5 and 2-6). The symbiotic competitiveness, on the other hand, was affected by the T6SS of *A. caulinodans* (Figures 2-7 and 2-8). The antibacterial activity of T6SS, which had been demonstrated in many pathogens, was not observed in *A. caulinodans* under various conditions tested (Figure 2-4). We conclude that the T6SS of *A. caulinodans* participates specifically in symbiotic competitiveness. The involvement of T6SS in symbiotic competitiveness was also demonstrated recently in legume-symbiotic *P. phymatum* (de Campos, et al. 2017). More recently, the involvement of T6SS in legume-rhizobium symbiosis is also shown in *R. etli* Mim1 (Salinero-Lanzarote, et al. 2019). In the case of *R. etli* Mim1, the deletion of T6SS had a substantial defect in symbiosis effectiveness, and their effect in symbiosis competitiveness was not reported. Taken together, these data provide direct evidence that rhizobial T6SS is involved in legume-rhizobium symbiosis efficacy or competitiveness.

Based on our current results, further studies in elucidating how T6SS contributes to symbiotic competitiveness in *A. caulinodans* would be of particular interest. The first step would be to dissect the timing when T6SS is active during the infection process by monitoring Hcp's secretion. This question could be done by staining the ultrathin sections of the stem nodules at different dpi with immunogold-labeled anti-Hcp and observed by transmission electron microscopy. As the T6SS mutants had no defect in symbiosis effectiveness, a nodule induced by a T6SS mutant would serve as a negative control. Another important direction is characterizing the *A. caulinodans* T6SS effector(s) that involved in enhancing the symbiotic competitiveness by performing

doi:10.6342/NTU202000295

symbiotic competitiveness assay using putative effector-deletion strains. A future study could also focus on evidence that T6SS provides *A. caulinodans* with better symbiotic competitiveness under natural conditions, as demonstrated by *P. phymatum* (de Campos, et al. 2017). Theoretically, this could be tested by measuring the nodule occupancy under mixed inoculation conditions using different *S. rostrata* effective symbionts. Consider the high specificity of the *A. caulinodans*-*S. rostrata* system, such design requires isolating strains other than ORS571 that can form effective nodules with *S. rostrata* in nature.

T6SS is the third bacterial secretion system known to participate in legume-rhizobium symbiosis, together with T3SS and T4SS (de Campos, et al. 2017, Hubber, et al. 2004, Okazaki, et al. 2013, Salinero-Lanzarote, et al. 2019). In all cases, the secretion systems take part in the host-range determination or symbiotic competitiveness. Interestingly, all the T3SS, T4SS, and T6SS are able to form a tube/filament-like structure that may penetrate the host membrane (Cherrak, et al. 2019, Galán, et al. 2014, Grohmann, et al. 2018). The presence of secretion systems can have either a positive or negative effect on legume symbiosis, depending on the combination of the rhizobium-legume pair (Nelson and Sadowsky 2015, Okazaki, et al. 2013, Okazaki, et al. 2009, Teulet, et al. 2019). The presence of T3SS hinders *Bradyrhizobium elkanii* USDA61 to form nodules with *Vigna radiata* cv. KPS1 but enables USDA61 to form nodules with *Glycine max* cv. Clark *rj1* (rj_irj_i) (Okazaki, et al. 2009). On the other hand, T4SS benefits *Sinorhizobium meliloti* HK46c with better symbiotic competitiveness in *M. truncatula*−*S. meliloti* HK46c wild type ($t4ss^+$) occupied 61-65% of the infected nodules while its T4SS mutant counterparts only occupied 33-35% when co-infected to *M. truncatula* genotypes A17 or R108 (Nelson, et al. 2017). Under the *S. meliloti* HK46c wild type plus HK46cΔ*t4ss*

doi:10.6342/NTU202000295

mixed inoculation experiment, less than 5% of the nodules were occupied by both strains. This study showed that the mean nodule occupancy of the *A. caulinodans* wild type (*t6ss*$^{+}$) was about 60-65% while the *t6ss*$^{-}$ was about 40-45% in ORS571(pGusA) plus Δ*imp*(pLacZ) group. The results that T4SS and T6SS enhance *rhizobium* with a better but not dominant symbiotic competitiveness suggest that secretion systems could play an assisting role during nodule organogenesis or maturation.

The identification of protein substrates from the T3SS and T4SS that participate in legume-rhizobium symbiosis has just begun. The T3SS effector ErnA enables *B. elkanii* USDA61 to form symbiotic relationship with *Aeschynomene indica* (Teulet, et al. 2019). The presence of T4SS and its substrates Type IV effector protein A (TfeA) in *Sinorhizobium* HK46c increased the nodule number in *M. truncatula* A17 and *M. truncatula* R108 (Nelson, et al. 2017). It is expected more effectors from T3SS, T4SS, and T6SS that participate in legume-rhizobium symbiosis will be characterized in the near future. Considering the involvement of T3SS, T4SS, and T6SS in host-range determination, I would argue that studies on the molecular mechanisms of how these secretion systems affect legume symbiosis would shed light on expanding the host range of the rhizobia. I would further suggest that the knowledge gained from such studies would contribute to sustainable agriculture.

T6SS involved in interbacterial competition is also investigated in the second part of my Ph.D. (chapter III). By the time I started this part of the research, the antibacterial activity of T6SS in *A. tumefaciens* and the effectors involved were published (Ma, et al. 2014). The evidence suggested that the *A. tumefaciens* killing outcome is recipient cell-dependent, which was also demonstrated or implied in many animal-associated bacteria

doi:10.6342/NTU202000295

(Basler, et al. 2013, Chatzidaki-Livanis, et al. 2016, Ma, et al. 2014, Sana, et al. 2016, Unterweger, et al. 2014). Intriguingly, no T6SS antibacterial activity could be detected even if the recipient cells lack the cognate immunity proteins in some cases (Basler, et al. 2013, Chatzidaki-Livanis, et al. 2016, Sana, et al. 2016, Unterweger, et al. 2014). This inconsistency of T6SS killing outcome to the effector-immunity pairs suggests that the recipient's genetic factors other than immunity protein participate in determining the T6SS antibacterial activity. On the other hand, while the 'tit-for-tat' model could explain the recipient-cell dependency (Basler, et al. 2013), it failed to explain the different killing outcomes using two T6SS-lacking strains (Fig. 3-1). Thus, I decided to systematically explore the recipient factors involved in T6SS killing using *A. tumefaciens* as a model attacker and T6SS-lacking *E. coli* as a model recipient to avoid the 'tit-for-tat' interference. We confirmed that at least *clpP*, *gltA*, *ydhS*, *ydaE*, *cbpA*, and *clpA* participate in enhancing susceptibility to *A. tumefaciens* T6SS attack (Table 3-3, Fig. 3-3, Fig. 3-6), and further elucidated that the ClpAP complex formation enhances the outcome of *A. tumefaciens* T6SS killing (Fig. 3-7). For the first time, this study provides a systematic effort to identify the non-immunity genes that play a role in T6SS susceptibility in the recipient cells.

Together with this study, recent scientific advances confirmed that the involvement of non-immunity recipient genes in T6SS killing outcomes. In this study, we show that recipient *clpP*, *gltA*, *ydhS*, *ydaE*, *cbpA*, and *clpA* take part in *enhancing A. tumefaciens* T6SS-mediated antibacterial activity. In *P. aeruginosa*, it is proposed that recipient Elongation factor-Tu (EF-Tu) participate in T6SS killing based on the observation that interaction with EF-Tu is required for T6SS effector Tse6 toxicity (Quentin, et al. 2018, Whitney, et al. 2015). In *S. marcescens*, the T6SS effectors Ssp2 and Ssp4 require

doi:10.6342/NTU202000295

DsbA in the recipient cell to appear their toxicity (Mariano, et al. 2018). The *P. aeruginosa* and the *S. marcescens* are the animal-associated bacteria. Thus, the non-immunity recipient factors involved in T6SS killing is a general phenomenon, and the results gained in this study could shed light on the T6SS research community.

Many of the non-immunity recipient factors involved for T6SS killing identified to date are cytoplasmic proteins, suggesting that the recipient factors work after T6SS firing. One of the possibilities would be that recipient factors act for effector activation, which works in the CDI system (Diner, et al. 2012, Johnson, et al. 2016, Jones, et al. 2017). Thus, whether the recipient factors identified in this study are involved in effector activation would be an exciting direction to carry on. As Tde1 and Tde2 are the only known cytosolic T6SS effectors in *A. tumefaciens* C58, and that both of them participate in the antibacterial competition, elucidating whether these recipient factors engage in Tde1/2 activation would be of particular interest. Current data point out that the recipient *clpP* could be engaged in Tde1 toxicity through regulating its protein level (Figure 3-9 and 3-10).

Overall, my findings expand our understanding of the T6SS in several aspects that are not confined to plant-associated bacteria. First, it provides direct evidence that rhizobial T6SS is involved in plant-microbe interactions, particularly in symbiotic competitiveness, which has not been determined in phytopathogen and animal-associated bacteria to the best of my knowledge. Second, it expands our understanding of the previous undervalued yet universal phenomena that the recipient cell types affect the outcome of a T6SS killing and provides molecular clues to the mechanism underlies. Third, the high-throughput interbacterial competition platform developed in

doi:10.6342/NTU202000295

this study is applicable to screen for novel genetic factors (both in the attacker and recipient cells) involved in an interbacterial competition of any secretion systems (CDI, T6SS, T1SS, and T4SS). My work on the *A. caulinodans* and the *A. tumefaciens* T6SS that focused on both the attacker and the recipient cell point of view contributes to the fields of bacterial secretion and microbial interactions.

doi:10.6342/NTU202000295

Appendices

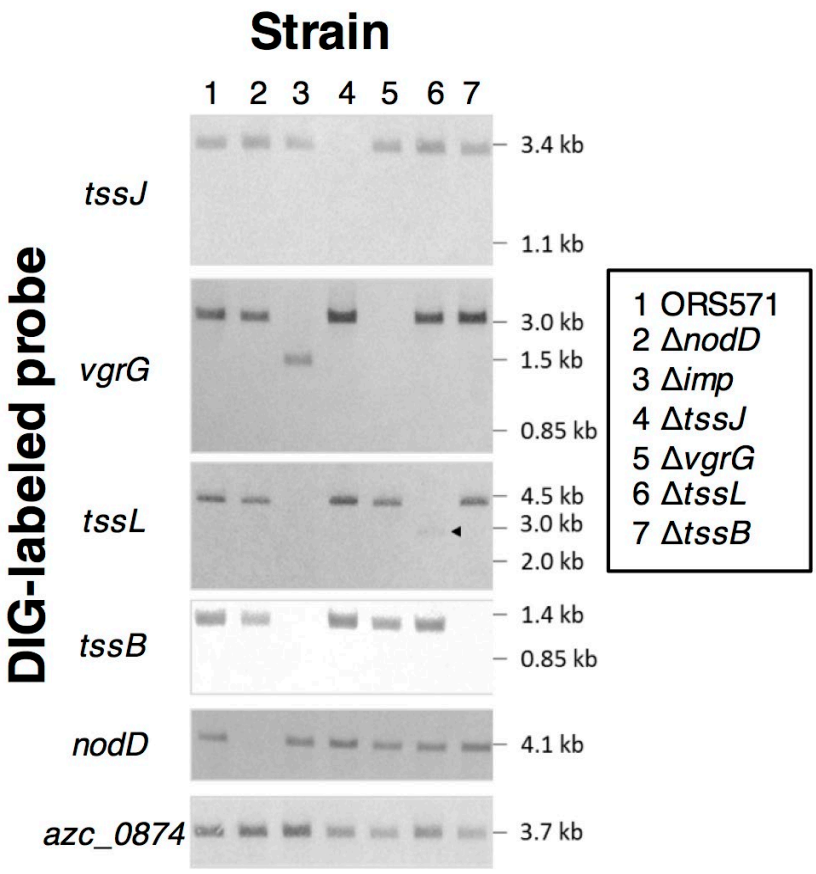

Appendix Figure 1. Genotype confirmed by Southern blot analysis.

Strain abbreviations are explained on the right. Genomic DNA isolated from each *A. caulinodans* strain was digested with *Xho*I and *Hin*dIII. The Southern blot was analyzed by using DIG-labled PCR probes specific for each of the *tssJ*, *vgrG*, *tssL*, *tssB, nodD,* and *azc_0874* genes. Genotypes for T6SS- and symbiosis-related genes were confirmed on the basis of the signal loss in the respective mutant. Probe-G, which was amplified by primer Azc_0874-P3 and Azc_0874-P4, was a positive control for the ORS571 genome. Black triangle highlights bands with weak signal. This data was generated by Hsin-Mei Huang.

doi:10.6342/NTU202000295

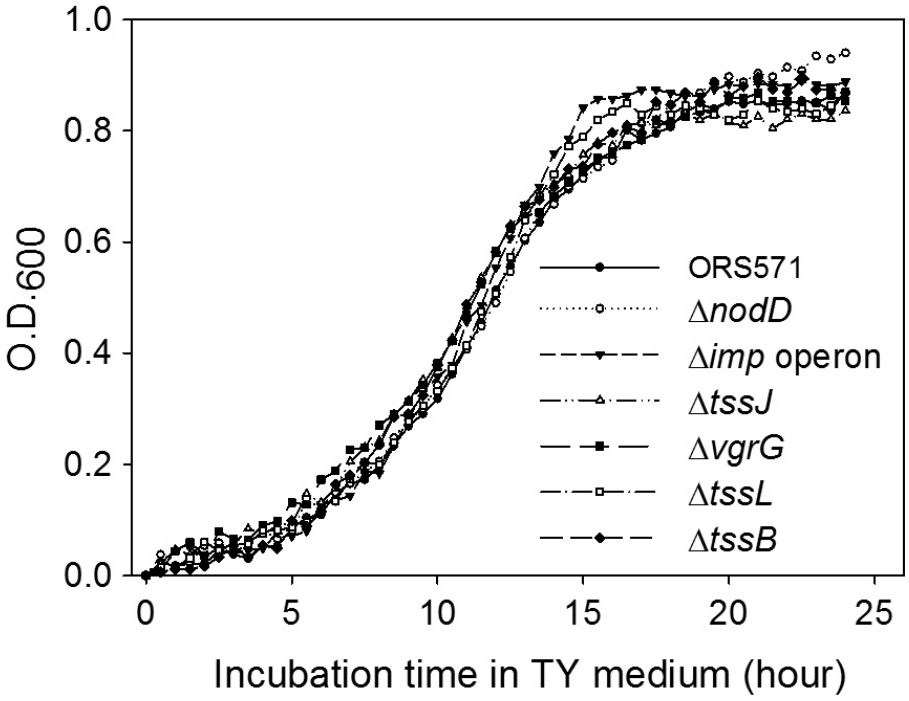

Appendix Figure 2. Growth curves of the *A. caulinodans* T6SS mutants.

Bacteria cells were growth in rich medium TY under 37℃, 200 rpm, and the OD_{600} was measured every 30 minutes. Three biological replicates were performed and the average OD_{600} are shown here. One-way ANOVA with $p<0.05$ and Holm-Sidak method were used for statistical analysis. No significant were found at any different time points measured. This data was generated by Hsin-Mei Huang.

doi:10.6342/NTU202000295

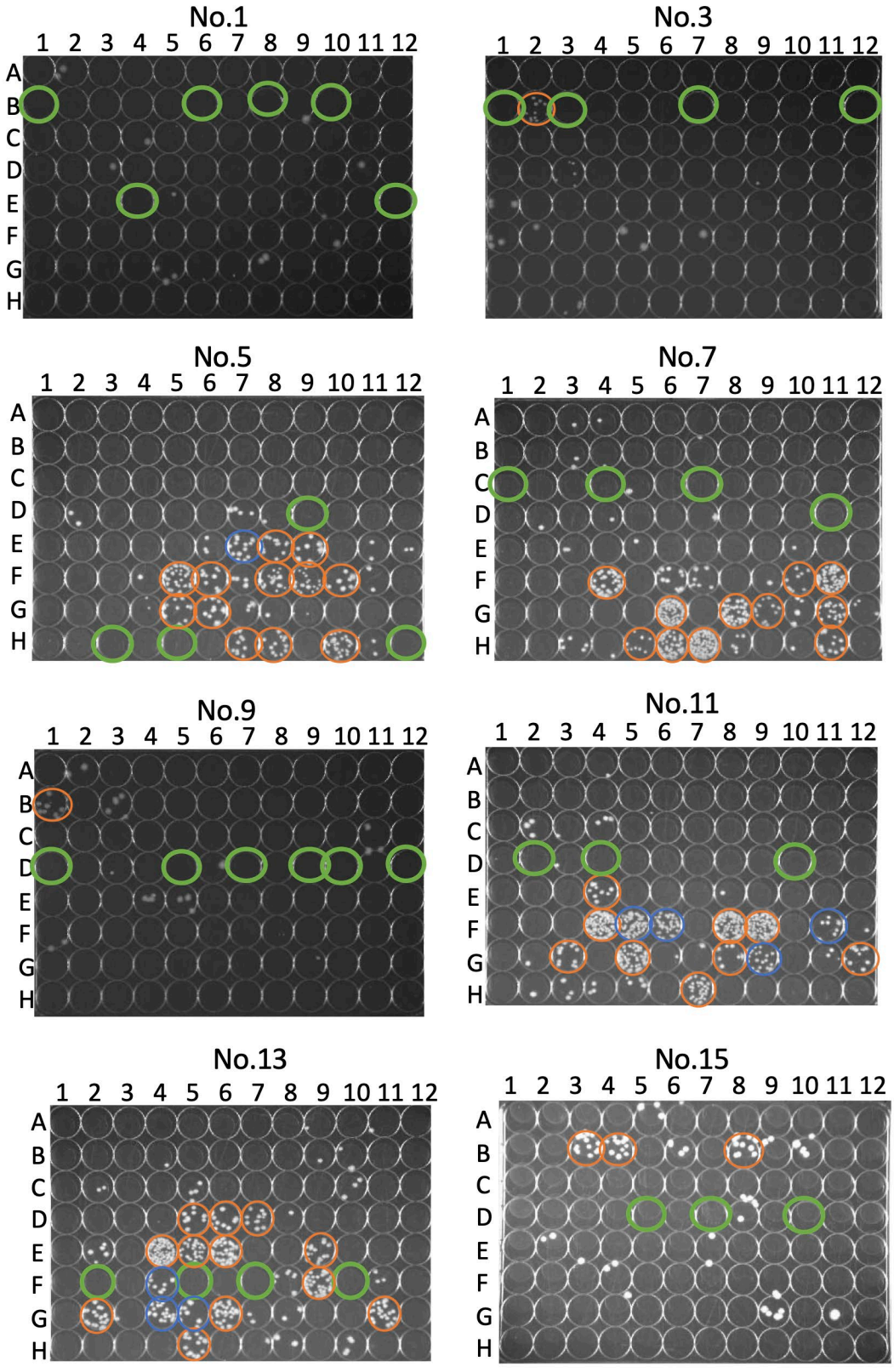

doi:10.6342/NTU202000295

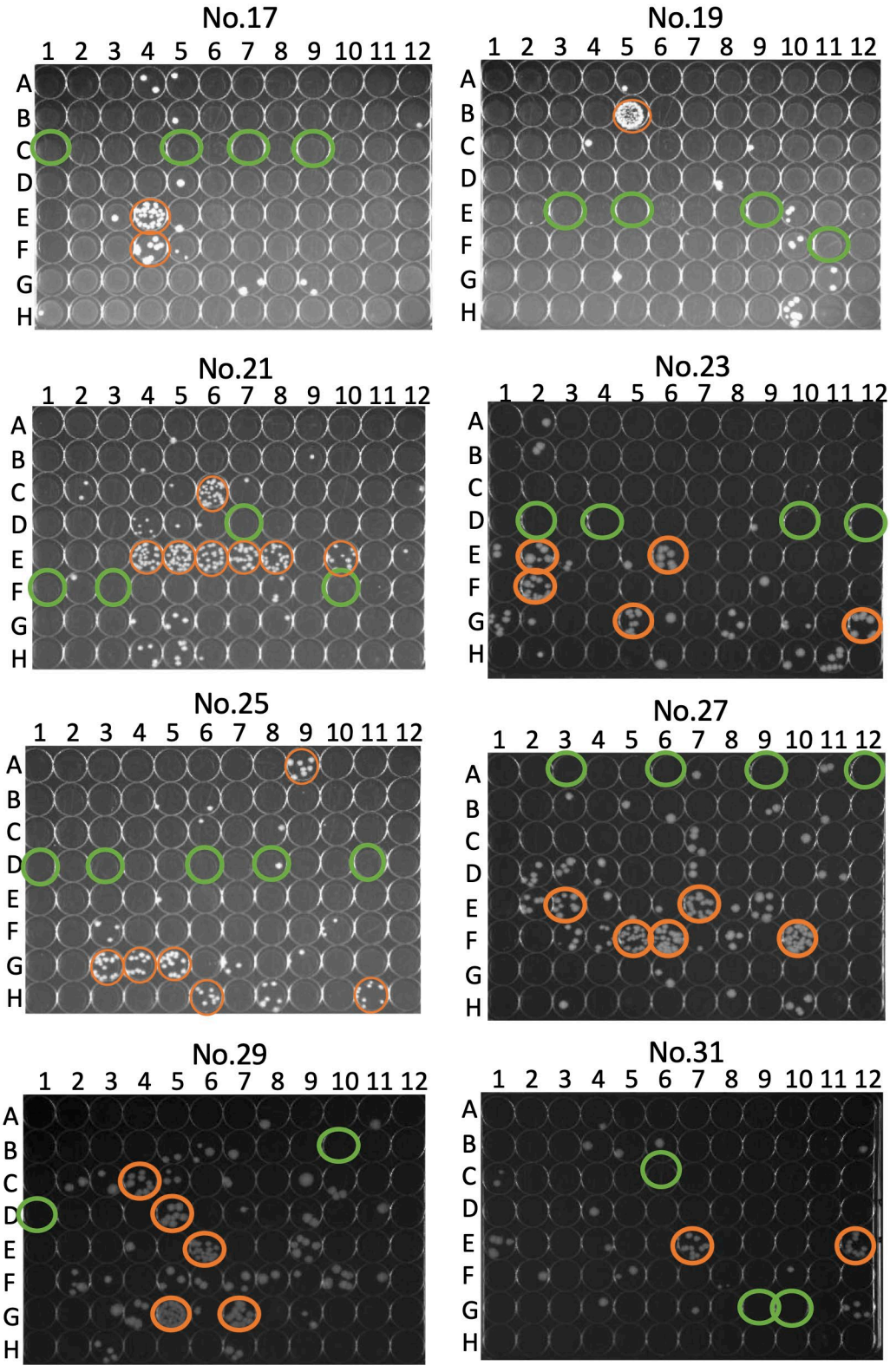

doi:10.6342/NTU202000295

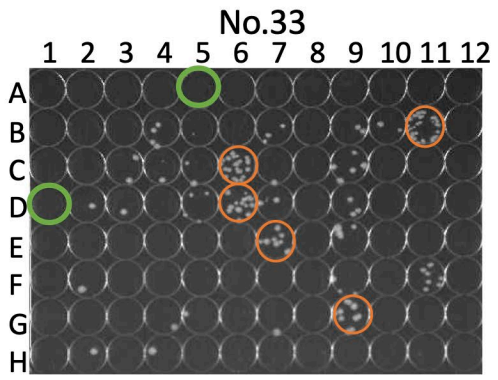

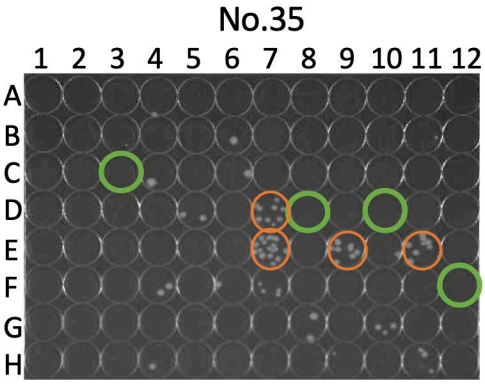

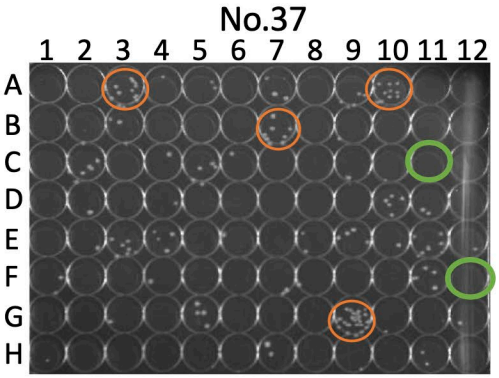

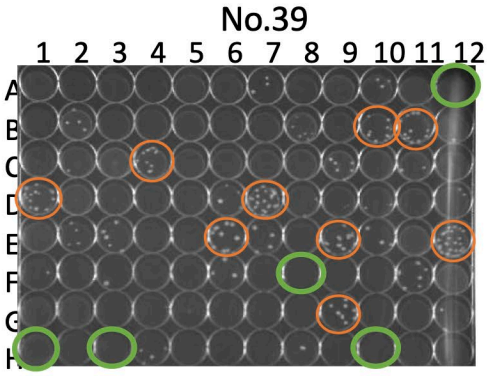

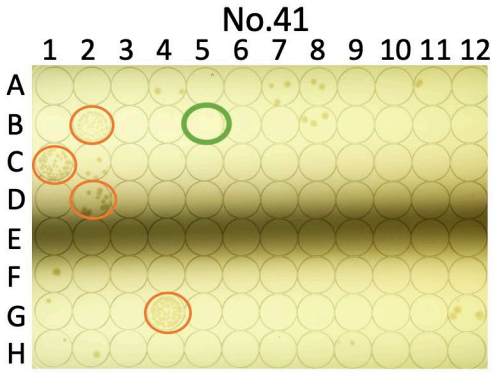

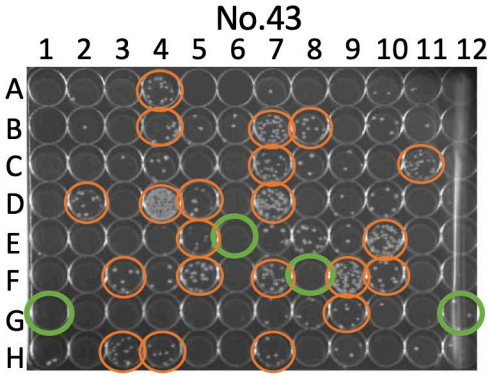

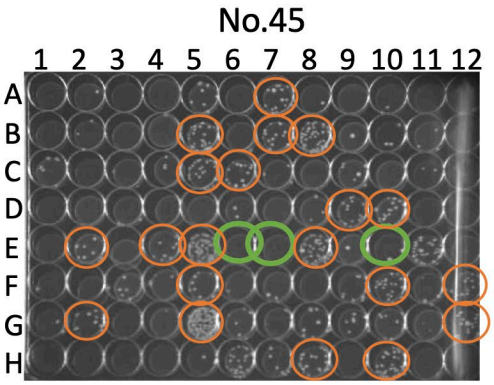

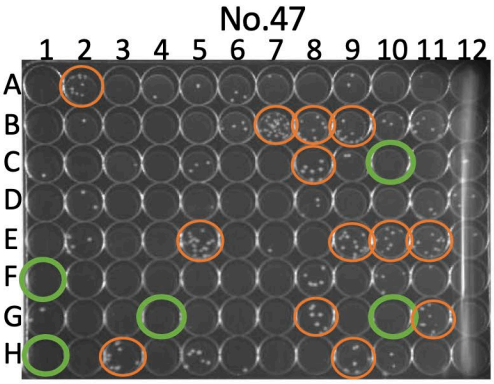

doi:10.6342/NTU202000295

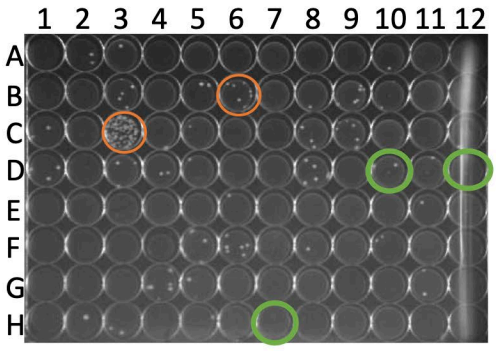

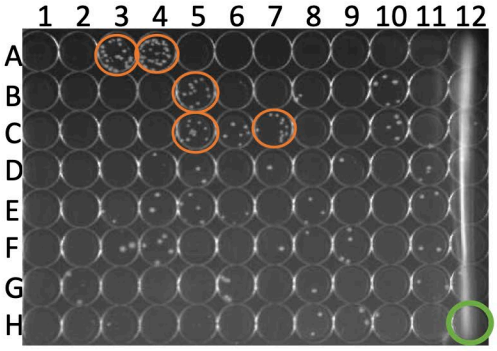

No.53

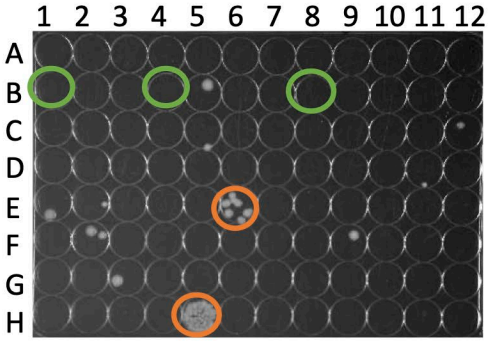

No.55

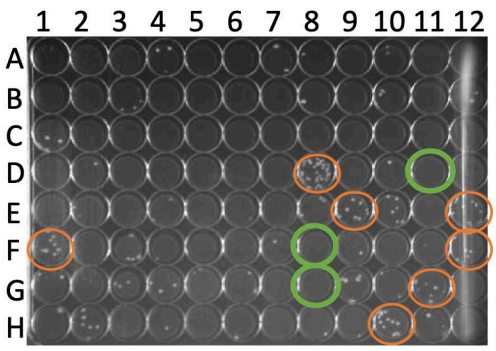

No.57

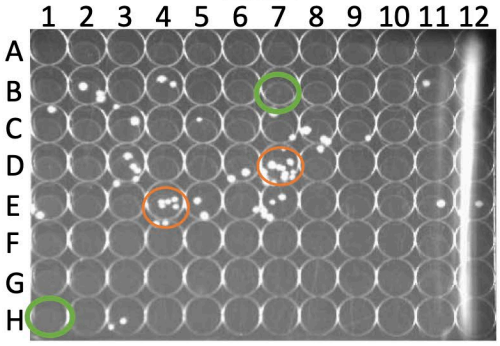

No.59

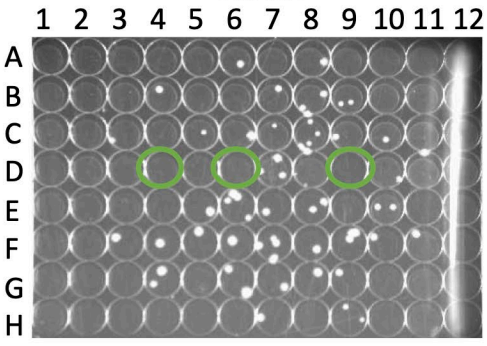

No.61

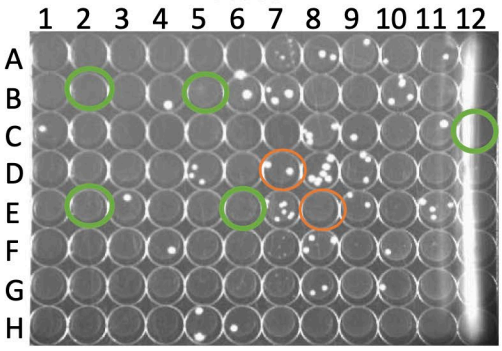

No.63

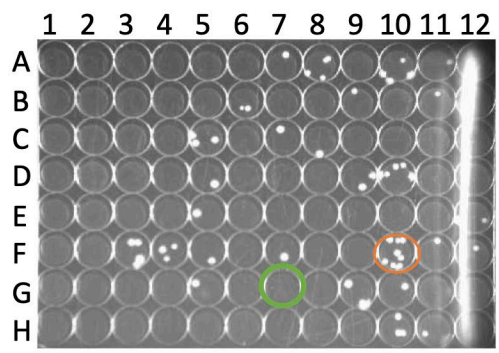

doi:10.6342/NTU202000295

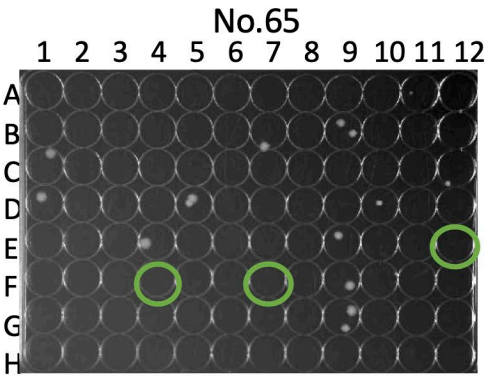

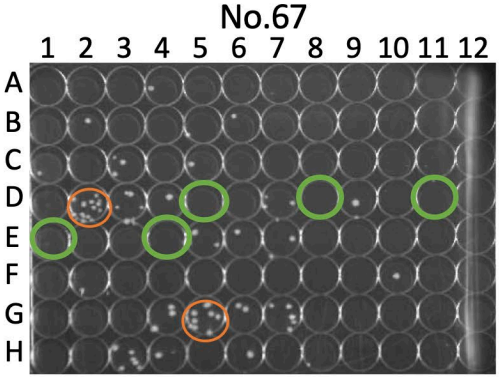

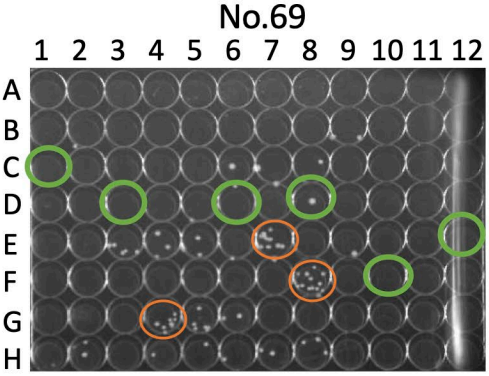

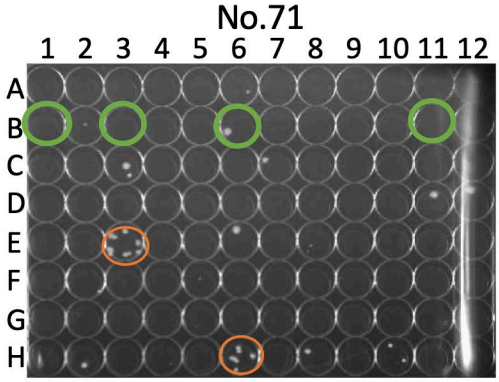

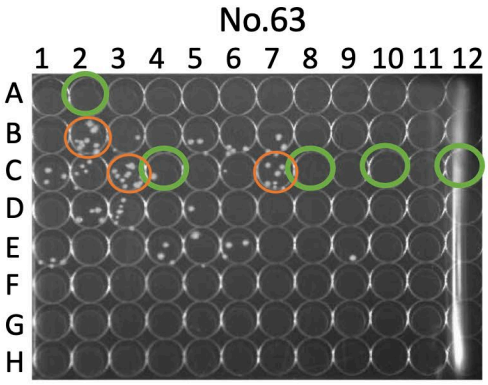

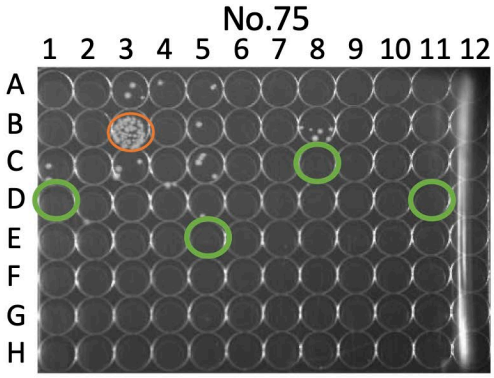

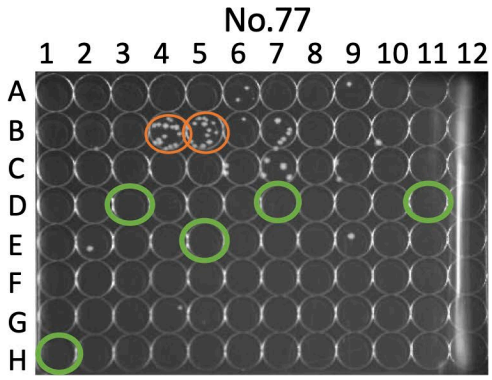

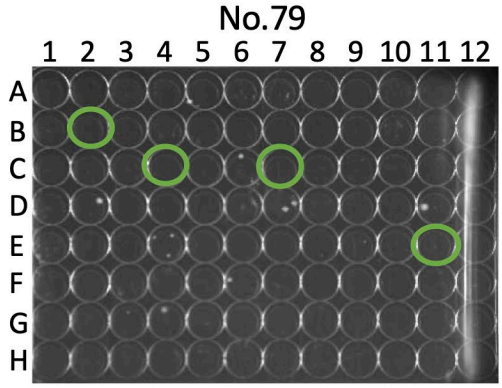

doi:10.6342/NTU202000295

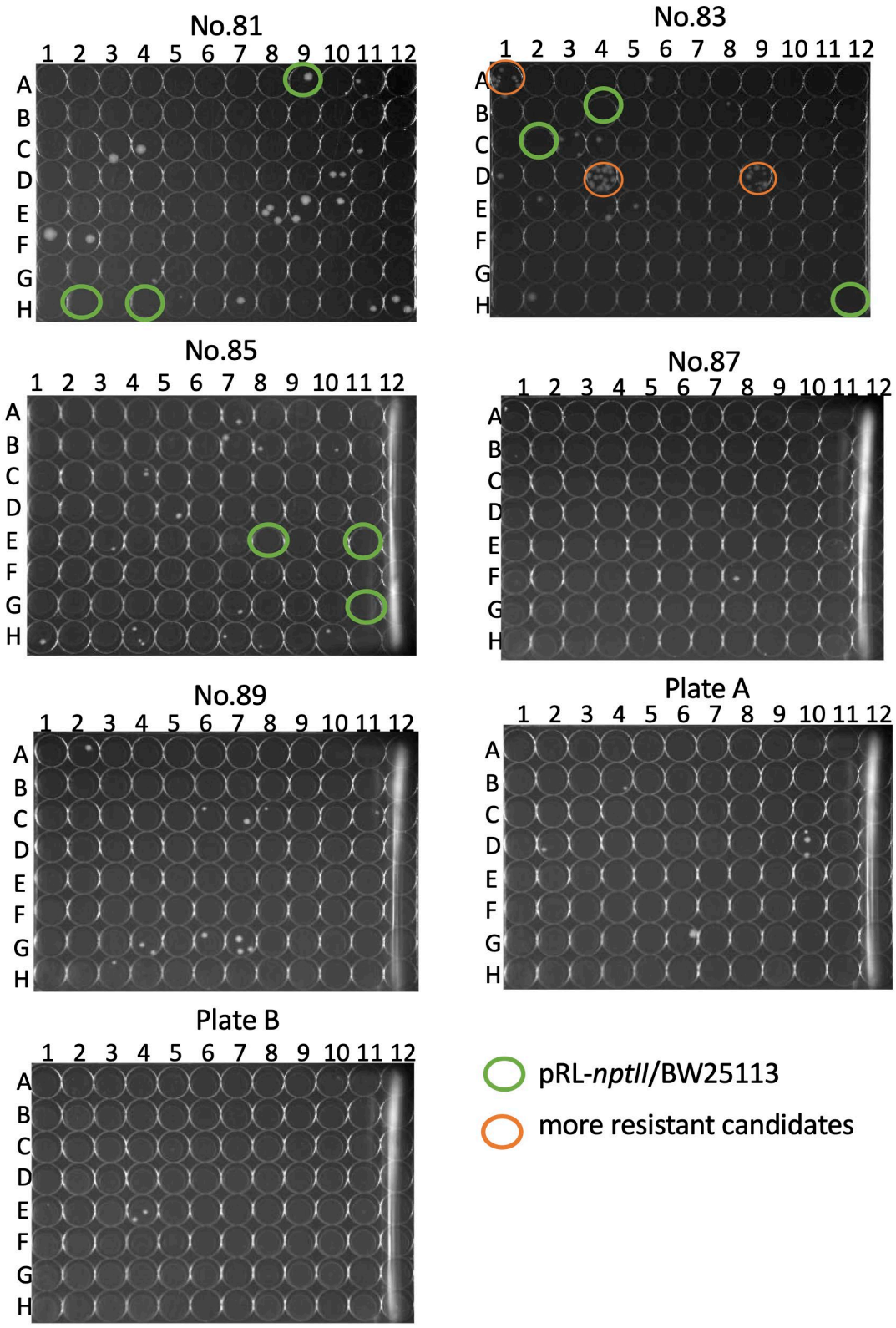

doi:10.6342/NTU202000295

Appendix Figure 3. Interbacterial competition of *A. tumefaciens* and the *E. coli* Keio strains.

Overnight culture of *A. tumefaciens* was adjusted to OD_{600}= 3.0 then mix with *E. coli* Keio strains with the ratio of 30:1 (v/v) and spotted onto AK medium to allow competition. The cells were recovered using microplate replicator then spotted onto LB with kanamycin to select for recipient *E. coli* cells. After overnight culture, photos were taken and the Keio strains showing > 7 colonies were marked as less-susceptible candidates. The green circle marks the place of the BW25113 harboring pRL-*nptII* that served as a negative control, and the orange circle marks the place of the candidates. This figure showed the results from the first screening, and the second screening was performed similarly by Chia Lee with little modification during the recovery stage (see Materials and Methods in the chapter III for details).

doi:10.6342/NTU202000295

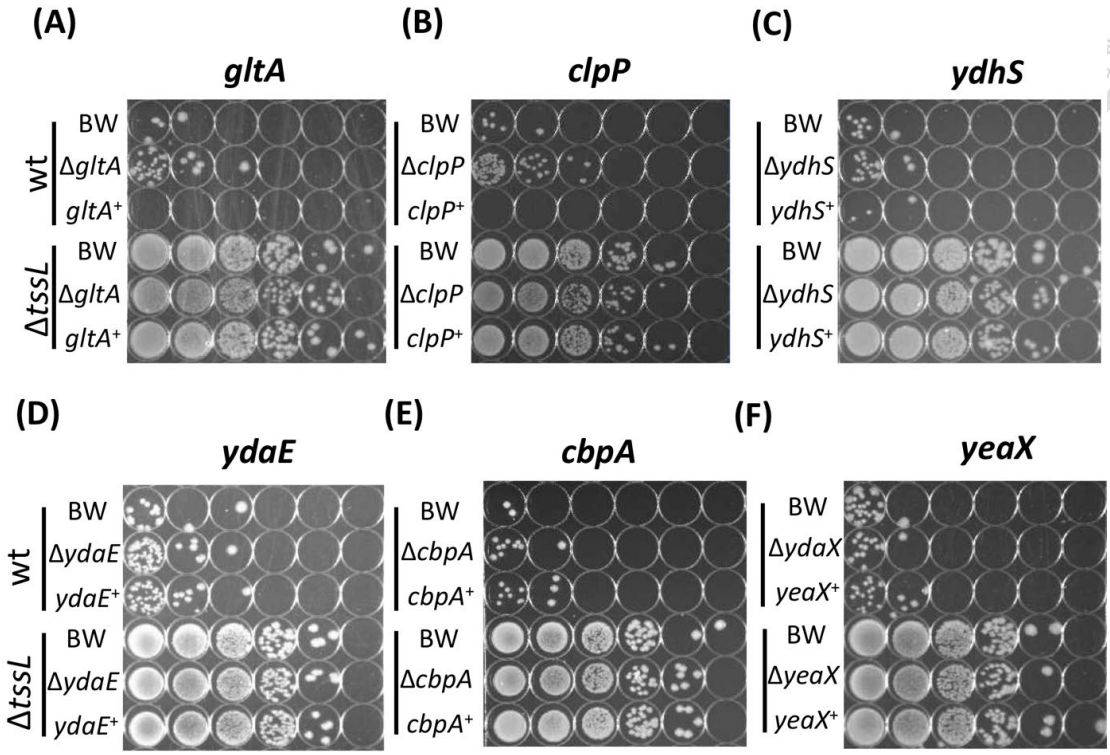

Appendix Figure 4. Interbacterial competition assay between *A. tumefaciens* C58 and the *E. coli* candidates that were less susceptible to T6SS killing.

The *A. tumefaciens* C58 wild-type or Δ*tssL* were co-cultured at a ratio of 30:1 with *E. coli* BW25113 wild type (BW), the Keio mutant strains, and complemented strains expressing the mutated genes *in trans*. The Keio strain used was **(A)** Δ*gltA*, **(B)** Δ*clpP*, **(C)** Δ*ydhS*, **(D)** Δ*ydaE*, **(E)** Δ*cbpA*, and **(F)** Δ*yeaX*. Data shown are its representative results; at least two independent experiments were performed in each group.

doi:10.6342/NTU202000295

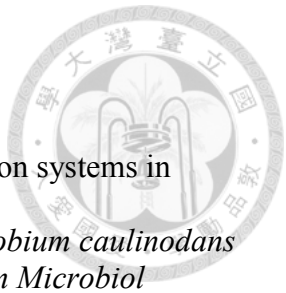

References

Abby SS, Cury J, Guglielmini J *et al.* Identification of protein secretion systems in bacterial genomes. *Sci Rep* 2016;**6**: 23080.

Adebayo A, Watanabe I, Ladha JK. Epiphytic occurrence of *Azorhizobium caulinodans* and other rhizobia on host and nonhost legumes. *Appl Environ Microbiol* 1989;**55**: 2407-9.

Akiyoshi DE, Morris RO, Hinz R *et al.* Cytokinin/auxin balance in crown gall tumors is regulated by specific loci in the T-DNA. *Proc Natl Acad Sci USA* 1983;**80**: 407-11.

Alcoforado Diniz J, Liu Y-C, Coulthurst SJ. Molecular weaponry: diverse effectors delivered by the type VI secretion system. *Cell Microbiol* 2015;**17**: 1742-51.

Alexopoulos JA, Guarné A, Ortega J. ClpP: A structurally dynamic protease regulated by AAA+ proteins. *J Struct Biol* 2012;**179**: 202-10.

Alteri CJ, Mobley HLT. The versatile type VI secretion system. *Microbiol Spectr* 2016;**4**.

Aoki ASK, C. MJ, Kyle J *et al.* Contact-dependent growth inhibition requires the essential outer membrane protein BamA (YaeT) as the receptor and the inner membrane transport protein AcrB. *Mol Microbiol* 2008;**70**: 323-40.

Aoki SK, Diner EJ, de Roodenbeke CtK *et al.* A widespread family of polymorphic contact-dependent toxin delivery systems in bacteria. *Nature* 2010;**468**: 439.

Aoki SK, Pamma R, Hernday AD *et al.* Contact-dependent inhibition of growth in *Escherichia coli*. *Science* 2005;**309**: 1245-8.

Ates LS, Houben ENG, Bitter W. Type VII secretion: a highly versatile secretion system. *Microbiol Spectr* 2016;**4**.

Baba T, Ara T, Hasegawa M *et al.* Construction of *Escherichia coli* K-12 in-frame, single-gene knockout mutants: the Keio collection. *Mol Syst Biol* 2006;**2**: 2006.0008.

Barret M, Egan F, O'Gara F. Distribution and diversity of bacterial secretion systems across metagenomic datasets. *Environ Microbiol Rep* 2013;**5**: 117-26.

Barry GF, Rogers SG, Fraley RT *et al.* Identification of a cloned cytokinin biosynthetic gene. *Proc Natl Acad Sci USA* 1984;**81**: 4776-80.

Basler M. Type VI secretion system: secretion by a contractile nanomachine. *Philos Trans R Soc Lond, B, Biol Sci* 2015;**370**.

Basler M, Ho BT, Mekalanos JJ. Tit-for-tat: type VI secretion system counterattack during bacterial cell-cell interactions. *Cell* 2013;**152**: 884-94.

Basler M, Pilhofer M, Henderson GP *et al.* Type VI secretion requires a dynamic contractile phage tail-like structure. *Nature* 2012;**483**: 182-6.

Bayer-Santos E, Cenens W, Matsuyama BY *et al.* The opportunistic pathogen *Stenotrophomonas maltophilia* utilizes a type IV secretion system for interbacterial killing. *PLoS Path* 2019;**15**: e1007651-e.

Bergersen FJ, Turner GL, Bogusz D *et al.* Effects of O_2 concentrations and various haemoglobins on respiration and nitrogenase activity of bacteroids from stem and root nodules of *Sesbania rostrata* and of the same bacteria from continuous cultures. *J Gen Microbiol* 1986;**132**: 3325-36.

Bernal P, Allsopp LP, Filloux A *et al.* The *Pseudomonas putida* T6SS is a plant warden against phytopathogens. *ISME J* 2017;**11**: 972–87.

Bernal P, Llamas MA, Filloux A. Type VI secretion systems in plant-associated bacteria. *Environ Microbiol* 2018;**20**: 1-15.

doi:10.6342/NTU202000295

Bertani G. Studies on lysogenesis I.: The mode of phage liberation by lysogenic *Escherichia coli*. *J Bacteriol* 1951;**62**: 293-300.
Bewley MC, Graziano V, Griffin K *et al.* The asymmetry in the mature amino-terminus of ClpP facilitates a local symmetry match in ClpAP and ClpXP complexes. *J Struct Biol* 2006;**153**: 113-28.
Bhandari V, Wong KS, Zhou JL *et al.* The role of ClpP protease in bacterial pathogenesis and human diseases. *ACS Chem Biol* 2018;**13**: 1413-25.
Bingle LEH, Bailey CM, Pallen MJ. Type VI secretion: a beginner's guide. *Curr Opin Microbiol* 2008;**11**: 3-8.
Bladergroen MR, Badelt K, Spaink HP. Infection-blocking genes of a symbiotic *Rhizobium leguminosarum* strain that are involved in temperature-dependent protein secretion. *Mol Plant-Microbe Interact* 2003;**16**: 53-64.
Blindauer CA, Harrison MD, Robinson AK *et al.* Multiple bacteria encode metallothioneins and SmtA-like zinc fingers. *Mol Microbiol* 2002;**45**: 1421-32.
Bondage DD, Lin J-S, Ma L-S *et al.* VgrG C terminus confers the type VI effector transport specificity and is required for binding with PAAR and adaptor–effector complex. *Proc Natl Acad Sci USA* 2016;**113**: E3931-E40.
Bönemann G, Pietrosiuk A, Diemand A *et al.* Remodelling of VipA/VipB tubules by ClpV-mediated threading is crucial for type VI protein secretion. *EMBO J* 2009;**28**: 315-25.
Bottai D, Gröschel MI, Brosch R. Type VII secretion systems in Gram-positive bacteria. In: Bagnoli F, Rappuoli R (eds.) *Protein and sugar export and assembly in Gram-positive bacteria*, DOI 10.1007/82_2015_5015. Cham: Springer International Publishing, 2017, 235-65.
Boyer F, Fichant G, Berthod J *et al.* Dissecting the bacterial type VI secretion system by a genome wide *in silico* analysis: what can be learned from available microbial genomic resources? *BMC Genom* 2009;**10**: 104.
Brackmann M, Nazarov S, Wang J *et al.* Using force to punch holes: mechanics of contractile nanomachines. *Trends Cell Biol* 2017;**27**: 623-32.
Bromfield ESP, Jones DG. The competitive ability and symbiotic effectiveness of doubly labelled antibiotic resistant mutants of *Rhizobium trifolii*. *Ann Appl Biol* 1979;**91**: 211-9.
Brunet YR, Zoued A, Boyer F *et al.* The Type VI Secretion TssEFGK-VgrG Phage-Like Baseplate Is Recruited to the TssJLM Membrane Complex via Multiple Contacts and Serves As Assembly Platform for Tail Tube/Sheath Polymerization. *PLOS Genetics* 2015;**11**: e1005545.
Buchmann I, Marner FJ, Schröder G *et al.* Tumour genes in plants: T-DNA encoded cytokinin biosynthesis. *EMBO J* 1985;**4**: 853-9.
Capoen W, Oldroyd G, Goormachtig S *et al. Sesbania rostrata*: a case study of natural variation in legume nodulation. *New Phytol* 2010;**186**: 340-5.
Chae C, Sharma S, Hoskins JR *et al.* CbpA, a DnaJ homolog, is a DnaK co-chaperone, and its activity is modulated by CbpM. *J Biol Chem* 2004;**279**: 33147-53.
Chang Y-W, Rettberg LA, Ortega DR *et al. In vivo* structures of an intact type VI secretion system revealed by electron cryotomography. *EMBO Rep* 2017;**18**: 1090-9.
Charles TC, Nester EW. A chromosomally encoded two-component sensory transduction system is required for virulence of *Agrobacterium tumefaciens*. *J Bacteriol* 1993;**175**: 6614-25.
Charpentier M, Oldroyd G. How close are we to nitrogen-fixing cereals? *Curr Opin Plant Biol* 2010;**13**: 556-64.

doi:10.6342/NTU202000295

Chatzidaki-Livanis M, Geva-Zatorsky N, Comstock LE. *Bacteroides fragilis* type VI secretion systems use novel effector and immunity proteins to antagonize human gut *Bacteroidales* species. *Proc Natl Acad Sci USA* 2016;**113**: 3627-32.
Chen L, Chen Y, Wood DW *et al.* A new type IV secretion system promotes conjugal transfer in *Agrobacterium tumefaciens*. *J Bacteriol* 2002;**184**: 4838-45.
Chenoweth MR, Wickner S. Complex regulation of the DnaJ homolog CbpA by the global Regulators σS and Lrp, by the specific inhibitor CbpM, and by the proteolytic degradation of CbpM. *J Bacteriol* 2008;**190**: 5153-61.
Cherrak Y, Flaugnatti N, Durand E *et al.* Structure and activity of the type VI secretion system. *Microbiol Spectr* 2019;**7**.
Chien H-L, Huang W-Z, Tsai M-Y *et al.* Overexpression of the chromosome partitioning Gene *parA* in *Azorhizobium caulinodans* ORS571 alters the bacteroid morphotype in *Sesbania rostrata* stem nodules. *Front Microbial* 2019;**10**.
Chilton M-D, Drummond MH, Merlo DJ *et al.* Stable incorporation of plasmid DNA into higher plant cells: the molecular basis of crown gall tumorigenesis. *Cell* 1977;**11**: 263-71.
Chilton MD, Saiki RK, Yadav N *et al.* T-DNA from *Agrobacterium* Ti plasmid is in the nuclear DNA fraction of crown gall tumor cells. *Proc Natl Acad Sci USA* 1980;**77**: 4060-4.
Christie PJ. The rich tapestry of bacterial protein translocation systems. *Protein J* 2019;**38**: 389-408.
Cianfanelli FR, Monlezun L, Coulthurst SJ. Aim, load, fire: the type VI secretion system, a bacterial nanoweapon. *Trends Microbiol* 2015;**24**: 51-62.
Cocking EC. Xylem colonization of tomato by *Azorhizobium caulinodans* ORS571. *Acta Biol Hung* 2001;**52**: 189-94.
Cocking EC. OBPC Symposium: Maize 2004 & beyond - intracellular colonization of cereals and other crop plants by nitrogen-fixing bacteria for reduced inputs of synthetic nitrogen fertilizers. *In Vitro Cell Dev Biol, Plant* 2005;**41**: 369-73.
Cocking EC, Stone PJ, Davey MR. Symbiosome-like intracellular colonization of cereals and other crop plants by nitrogen-fixing bacteria for reduced inputs of synthetic nitrogen fertilizers. *Sci China Ser C-Life Sci* 2005;**48**: 888-96.
Cole A, Wang Z, Coyaud E *et al.* Inhibition of the mitochondrial protease ClpP as a therapeutic strategy for human acute myeloid leukemia. *Cancer Cell* 2015;**27**: 864-76.
Conter A, Bouché JP, Dassain M. Identification of a new inhibitor of essential division gene *ftsZ* as the *kil* gene of defective prophage Rac. *J Bacteriol* 1996;**178**: 5100-4.
Costa TRD, Felisberto-Rodrigues C, Meir A *et al.* Secretion systems in Gram-negative bacteria: structural and mechanistic insights. *Nat Rev Micro* 2015;**13**: 343-59.
Coulthurst SJ. The type VI secretion system – a widespread and versatile cell targeting system. *Res Microbiol* 2013;**164**: 640-54.
Culp E, Wright GD. Bacterial proteases, untapped antimicrobial drug targets. *J Antibiot* 2016;**70**: 366.
Cummings SP, Gyaneshwar P, Vinuesa P *et al.* Nodulation of *Sesbania* species by *Rhizobium* (*Agrobacterium*) strain IRBG74 and other rhizobia. *Environ Microbiol* 2009;**11**: 2510-25.
de Bruijn FJ. *The model legume Medicago truncatula, 2 Volume Set*: Wiley, 2020.

doi:10.6342/NTU202000295

de Campos SB, Lardi M, Gandolfi A *et al.* Mutations in two *Paraburkholderia phymatum* type VI secretion systems cause reduced fitness in interbacterial competition. *Front Microbial* 2017;**8**.
De Geyter J, Smets D, Karamanou S *et al.* Inner membrane translocases and insertases. In: Kuhn A (ed.) *Bacterial Cell Walls and Membranes*, DOI 10.1007/978-3-030-18768-2_11. Cham: Springer International Publishing, 2019, 337-66.
Decoin V, Barbey C, Bergeau D *et al.* A type VI secretion system is involved in *Pseudomonas fluorescens* bacterial competition. *PLoS ONE* 2014;**9**: e89411.
Deng W, Marshall NC, Rowland JL *et al.* Assembly, structure, function and regulation of type III secretion systems. *Nat Rev Microbiol* 2017;**15**: 323-37.
Diner EJ, Beck CM, Webb JS *et al.* Identification of a target cell permissive factor required for contact-dependent growth inhibition (CDI). *Genes Dev* 2012;**26**: 515-25.
Dombrecht B, Vanderleyden J, Michiels J. Stable RK2-derived cloning vectors for the analysis of gene expression and gene function in Gram-negative bacteria. *Mol Plant-Microbe Interact* 2001;**14**: 426-30.
Doyle JJ. Phylogenetic perspectives on the origins of nodulation. *Mol Plant-Microbe Interact* 2011;**24**: 1289-95.
Dreyfus B, Diem HG, Freire J *et al.* Nitrogen fixation in tropical agriculture and forestry. Oxford: Oxford University, 1987.
Dreyfus B, Garcia JL, Gillis M. Characterization of *Azorhizobium caulinodans* gen. nov., sp. nov., a stem-nodulating nitrogen-fixing bacterium isolated from *Sesbania rostrata*. *Int J Syst Bacteriol* 1988;**38**: 89-98.
Dreyfus BL, Dommergues YR. Nitrogen-fixing nodules induced by *Rhizobium* on the stem of the tropical legume *Sesbania rostrata*. *FEMS Microbiol Lett* 1981a;**10**: 313-7.
Dreyfus BL, Dommergues YR. *Stem nodules on the tropical legume Sesbania rostrata. In Current perspectives in nitrogen fixation*. In Current perspectives in nitrogen fixation: proceedings of the Fourth International Symposium on Nitrogen Fixation held in Canberra, Australia, 1 to 5 December 1980: Elsevier/North-Holland Biomedical Press, 1981b.
Dreyfus BL, Elmerich C, Dommergues YR. Free-living *Rhizobium* strain able to grow on N_2 as the sole nitrogen source. *Appl Environ Microbiol* 1983;**45**: 711-3.
Duodu S, Brophy C, Connolly J *et al.* Competitiveness of a native *Rhizobium leguminosarum* biovar *trifolii* strain for nodule occupancy is manifested during infection. *Plant Soil* 2008;**318**: 117.
Elmerich C, Dreyfus BL, Reysset G *et al.* Genetic-analysis of nitrogen-fixation in a tropical fast-growing *Rhizobium*. *EMBO J* 1982;**1**: 499-503.
Felisberto-Rodrigues C, Durand E, Aschtgen M-S *et al.* Towards a structural comprehension of bacterial type VI secretion systems: characterization of the TssJ-TssM complex of an *Escherichia coli* pathovar. *PLoS Path* 2011;**7**: e1002386.
Fernández-López M, Goormachtig S, Gao M *et al.* Ethylene-mediated phenotypic plasticity in root nodule development on *Sesbania rostrata*. *Proc Natl Acad Sci USA* 1998;**95**: 12724-8.
Filloux A, Hachani A, Bleves S. The bacterial type VI secretion machine: yet another player for protein transport across membranes. *Microbiology* 2008;**154**: 1570-83.
Filloux A, Sagfors A. 3 - News and views on protein secretion systems. In: Alouf J, Ladant D, Popoff MR (eds.) *The Comprehensive Sourcebook of Bacterial*

doi:10.6342/NTU202000295

Protein Toxins (Fourth Edition), DOI https://doi.org/10.1016/B978-0-12-800188-2.00003-3. Boston: Academic Press, 2015, 77-108.
Franceschini A, Szklarczyk D, Frankild S *et al.* STRING v9.1: protein-protein interaction networks, with increased coverage and integration. *Nucleic Acids Res* 2013;**41**: D808-D15.
Galán JE, Lara-Tejero M, Marlovits TC *et al.* Bacterial type III secretion systems: specialized nanomachines for protein delivery into target cells. *Annu Rev Microbiol* 2014;**68**: 415-38.
Gallique M, Bouteiller M, Merieau A. The type VI secretion system: a dynamic system for bacterial communication? *Front Microbial* 2017a;**8**.
Gallique M, Decoin V, Barbey C *et al.* Contribution of the *Pseudomonas fluorescens* MFE01 type VI secretion system to biofilm formation. *PLOS ONE* 2017b;**12**: e0170770.
Gao R, Lynn DG. Environmental pH sensing: resolving the VirA/VirG two-component system inputs for *Agrobacterium* pathogenesis. *J Bacteriol* 2005;**187**: 2182-9.
García-Bayona L, Gozzi K, Laub MT. Mechanisms of resistance to the contact-dependent bacteriocin CdzC/D in *Caulobacter crescentus*. *J Bacteriol* 2019;**201**: e00538-18.
García-Bayona L, Guo MS, Laub MT. Contact-dependent killing by *Caulobacter crescentus* via cell surface-associated, glycine zipper proteins. *eLife* 2017;**6**: e24869.
Gebhardt C, Turner GL, Gibson AH *et al.* Nitrogen-fixing growth in continuous culture of a strain of *Rhizobium* sp. isolated from stem nodules on *Sesbania rostrata*. *J Gen Microbiol* 1984;**130**: 843-8.
Gelvin S. Traversing the cell: *Agrobacterium* T-DNA's journey to the host genome. *Front Plant Sci* 2012;**3**.
Gnanamanickam SS. *Plant-associated bacteria*, DOI https://doi.org/10.1007/978-1-4020-4538-7: Dordrecht : Springer, 2006.
Goethals K, Gao M, Tomekpe K *et al.* Common *nodABC* genes in *Nod* locus 1 of *Azorhizobium caulinodans*: Nucleotide sequence and plant-inducible expression. *Mol Gen Genet* 1989;**219**: 289-98.
Gohlke J, Deeken R. Plant responses to *Agrobacterium tumefaciens* and crown gall development. *Front Plant Sci* 2014;**5**.
Gopalaswamy G, Kannaiyan S, O'Callaghan K *et al.* The xylem of rice (*Oryza sativa*) is colonized by *Azorhizobium caulinodans*. *Proc R Soc B* 2000;**267**: 103-7.
Gottesman S, Roche E, Zhou Y *et al.* The ClpXP and ClpAP proteases degrade proteins with carboxy-terminal peptide tails added by the SsrA-tagging system. *Genes Dev* 1998;**12**: 1338-47.
Graves S, Piepho H-P, Selzer L *et al.* multcompView: visualizations of paired comparisons. *R package version 01-7*, 2015.
Green ER, Mecsas J. Bacterial secretion systems: an overview. *Microbiol Spectr* 2016;**4**.
Grohmann E, Christie PJ, Waksman G *et al.* Type IV secretion in Gram-negative and Gram-positive bacteria. *Mol Microbiol* 2018;**107**: 455-71.
Gu S, Shevchik VE, Shaw R *et al.* The role of intrinsic disorder and dynamics in the assembly and function of the type II secretion system. *Biochim Biophys Acta* 2017;**1865**: 1255-66.
Haag AF, Arnold MFF, Myka KK *et al.* Molecular insights into bacteroid development during *Rhizobium*–legume symbiosis. *FEMS Microbiol Rev* 2013;**37**: 364-83.

doi:10.6342/NTU202000295

Haapalainen M, Mosorin H, Dorati F *et al.* Hcp2, a secreted protein of the phytopathogen *Pseudomonas syringae* pv. tomato DC3000, is required for competitive fitness against bacteria and yeasts. *J Bacteriol* 2012;**194**: 4810-22.
Hachani A, Wood TE, Filloux A. Type VI secretion and anti-host effectors. *Curr Opin Microbiol* 2016;**29**: 81-93.
Harrell FE, Jr,, Dupont C, others m. Hmisc: Harrell miscellaneous, 2018.
Heckman KL, Pease LR. Gene splicing and mutagenesis by PCR-driven overlap extension. *Nat Protocols* 2007;**2**: 924-32.
Hood RD, Peterson SB, Mougous JD. From striking out to striking gold: discovering that type VI secretion targets bacteria. *Cell Host & Microbe* 2017;**21**: 286-9.
Hood RD, Singh P, Hsu F *et al.* A type VI secretion system of *Pseudomonas aeruginosa* targets a toxin to bacteria. *Cell host & microbe* 2010;**7**: 25-37.
Hooykaas PJJ, van Brussel AAN, den Dulk-Ras H *et al.* Sym plasmid of *Rhizobium trifolii* expressed in different rhizobial species and *Agrobacterium tumefaciens*. *Nature* 1981;**291**: 351-3.
Hubber A, Vergunst AC, Sullivan JT *et al.* Symbiotic phenotypes and translocated effector proteins of the *Mesorhizobium loti* strain R7A VirB/D4 type IV secretion system. *Mol Microbiol* 2004;**54**: 561-74.
Hwang H-H, Yu M, Lai E-M. *Agrobacterium*-mediated plant transformation: biology and applications. *The Arabidopsis Book* 2017;**2017**.
Inzé D, Follin A, Van Lijsebettens M *et al.* Genetic analysis of the individual T-DNA genes of *Agrobacterium tumefaciens*; further evidence that two genes are involved in indole-3-acetic acid synthesis. *Mol Gen Genet* 1984;**194**: 265-74.
Jensen E, Peoples M, Boddey R *et al.* Legumes for mitigation of climate change and the provision of feedstock for biofuels and biorefineries. A review. *Agron Sustain Dev* 2012;**32**: 329-64.
Ji ZJ, Yan H, Cui QG *et al.* Competition between rhizobia under different environmental conditions affects the nodulation of a legume. *Syst Appl Microbiol* 2017;**40**: 114-9.
Johnson PM, Beck CM, Morse RP *et al.* Unraveling the essential role of CysK in CDI toxin activation. *Proc Natl Acad Sci USA* 2016;**113**: 9792-7.
Jones AM, Garza-Sánchez F, So J *et al.* Activation of contact-dependent antibacterial tRNase toxins by translation elongation factors. *Proc Natl Acad Sci USA* 2017;**114**: E1951-E7.
Kado CI. *Plant bacteriology*. St. Paul, Minn.: American Phytopathological Society, 2010.
Kado CI. Historical account on gaining insights on the mechanism of crown gall tumorigenesis induced by *Agrobacterium tumefaciens*. *Front Microbial* 2014;**5**: 340.
Kado CI, Heskett MG. Selective media for isolation of *Agrobacterium*, *Corynebacterium*, *Erwinia*, *Pseudomonas*, and *Xanthomonas*. *Phytopathology* 1970;**60**: 969-76.
Kanehisa M, Goto S. KEGG: Kyoto Encyclopedia of Genes and Genomes. *Nucleic Acids Res* 2000;**28**: 27-30.
Kanonenberg K, Spitz O, Erenburg IN *et al.* Type I secretion system—it takes three and a substrate. *FEMS Microbiol Lett* 2018;**365**.
Kassambara A. ggpubr: 'ggplot2' Based Publication Ready Plots, 2018.
Kelley LA, Mezulis S, Yates CM *et al.* The Phyre2 web portal for protein modeling, prediction and analysis. *Nat Protocols* 2015;**10**: 845-58.

doi:10.6342/NTU202000295

Kereszt A, Mergaert P, Kondorosi E. Bacteroid development in legume nodules: evolution of mutual benefit or of sacrificial victims? *Mol Plant-Microbe Interact* 2011;**24**: 1300-9.
Keseler IM, Mackie A, Santos-Zavaleta A *et al.* The EcoCyc database: reflecting new knowledge about *Escherichia coli* K-12. *Nucleic Acids Res* 2016;**45**: D543-D50.
Kitts CL, Ludwig RA. *Azorhizobium caulinodans* respires with at least four terminal oxidases. *J Bacteriol* 1994;**176**: 886-95.
Lai E-M, Kado CI. Processed VirB2 is the major subunit of the promiscuous pilus of *Agrobacterium tumefaciens*. *J Bacteriol* 1998;**180**: 2711-7.
Lai E-M, Kado CI. The T-pilus of *Agrobacterium tumefaciens*. *Trends Microbiol* 2000;**8**: 361-9.
Lasica AM, Ksiazek M, Madej M *et al.* The type IX secretion system (T9SS): highlights and recent insights into its structure and function. *Front Cell Infect Microbiol* 2017;**7**.
Lee KB, De Backer P, Aono T *et al.* The genome of the versatile nitrogen fixer *Azorhizobium caulinodans* ORS571. *BMC Genom* 2008;**9**: 271.
Leiman PG, Basler M, Ramagopal UA *et al.* Type VI secretion apparatus and phage tail-associated protein complexes share a common evolutionary origin. *Proc Natl Acad Sci USA* 2009;**106**: 4154-9.
LeRoux M, De Leon JA, Kuwada NJ *et al.* Quantitative single-cell characterization of bacterial interactions reveals type VI secretion is a double-edged sword. *Proc Natl Acad Sci USA* 2012;**109**: 19804-9.
Lesic B, Starkey M, He J *et al.* Quorum sensing differentially regulates *Pseudomonas aeruginosa* type VI secretion locus I and homologous loci II and III, which are required for pathogenesis. *Microbiology* 2009;**155**: 2845-55.
Li C, Tao YP, Simon LD. Expression of different-size transcripts from the *clpP-clpX* operon of *Escherichia coli* during carbon deprivation. *J Bacteriol* 2000;**182**: 6630-7.
Li YG, Hu B, Christie PJ. Biological and structural diversity of type IV secretion systems. *Microbiol Spectr* 2019;**7**.
Liang X, Kamal F, Pei T-T *et al.* An onboard checking mechanism ensures effector delivery of the type VI secretion system in *Vibrio cholerae*. *Proc Natl Acad Sci USA* 2019;**116**: 23292-8.
Lien Y-W, Lai E-M. Type VI secretion effectors: methodologies and biology. *Front Cell Infect Microbiol* 2017;**7**.
Lin B-C, Kado CI. Studies on *Agrobacterium tumefaciens*. VII. Avirulence induced by temperature and ethidium bromide. *Can J Microbiol* 1977;**23**: 1554-61.
Lin J, Zhang W, Cheng J *et al.* A *Pseudomonas* T6SS effector recruits PQS-containing outer membrane vesicles for iron acquisition. *Nat Commun* 2017;**8**: 14888.
Lin J-S, Ma L-S, Lai E-M. Systematic dissection of the *Agrobacterium* type VI secretion system reveals machinery and secreted components for subcomplex formation. *PLoS ONE* 2013;**8**: e67647.
Lin J-S, Pissaridou P, Wu H-H *et al.* TagF-mediated repression of bacterial type VI secretion systems involves a direct interaction with the cytoplasmic protein Fha. *J Biol Chem* 2018, DOI 10.1074/jbc.RA117.001618.
Lin J-S, Wu H-H, Hsu P-H *et al.* Fha interaction with phosphothreonine of TssL cctivates type VI secretion in *Agrobacterium tumefaciens*. *PLoS Pathog* 2014;**10**: e1003991.

doi:10.6342/NTU202000295

Liu C-T, Lee K-B, Wang Y-S *et al.* Involvement of the *Azorhizobial* chromosome partition gene (*parA*) in the onset of bacteroid differentiation during *Sesbania rostrata* stem nodule development. *Appl Environ Microbiol* 2011;**77**: 4371-82.
Liu W, Yang J, Sun Y *et al. Azorhizobium caulinodans* transmembrane chemoreceptor TlpA1 involved in host colonization and nodulation on roots and stems. *Front Microbial* 2017;**8**.
Lodwig EM, Hosie AHF, Bourdes A *et al.* Amino-acid cycling drives nitrogen fixation in the legume-*Rhizobium* symbiosis. *Nature* 2003;**422**: 722-6.
Long SR. *Rhizobium*-legume nodulation: Life together in the underground. *Cell* 1989;**56**: 203-14.
Lossi NS, Manoli E, Förster A *et al.* The HsiB1C1 (TssB-TssC) complex of the *Pseudomonas aeruginosa* type VI secretion system forms a bacteriophage tail sheathlike structure. *J Biol Chem* 2013;**288**: 7536-48.
Ma L-S, Hachani A, Lin J-S *et al. Agrobacterium tumefaciens* deploys a superfamily of type VI secretion DNase effectors as weapons for interbacterial competition *in planta*. *Cell Host & Microbe* 2014;**16**: 94-104.
Ma L-S, Lin J-S, Lai E-M. An Icmf family protein, ImpLM, is an integral inner membrane protein interacting with ImpKL, and its walker A motif is required for type VI secretion system-mediated Hcp secretion in *Agrobacterium tumefaciens*. *J Bacteriol* 2009;**191**: 4316-29.
Ma L-S, Narberhaus F, Lai E-M. IcmF family protein TssM exhibits ATPase activity and energizes type VI secretion. *J Biol Chem* 2012;**287**: 15610-21.
MacIntyre DL, Miyata ST, Kitaoka M *et al.* The *Vibrio cholerae* type VI secretion system displays antimicrobial properties. *Proc Natl Acad Sci USA* 2010;**107**: 19520-4.
Maffei B, Francetic O, Subtil A. Tracking proteins secreted by bacteria: what's in the toolbox? *Front Cell Infect Microbiol* 2017;**7**: 221-.
Mahmoud SA, Chien P. Regulated proteolysis in bacteria. *Annu Rev Biochem* 2018;**87**: 677-96.
Mansfield J, Genin S, Magori S *et al.* Top 10 plant pathogenic bacteria in molecular plant pathology. *Mol Plant Pathol* 2012;**13**: 614-29.
Marchler-Bauer A, Bo Y, Han L *et al.* CDD/SPARCLE: functional classification of proteins via subfamily domain architectures. *Nucleic Acids Res* 2017;**45**: D200-D3.
Mariano G, Monlezun L, Coulthurst SJ. Dual role for DsbA in attacking and targeted bacterial cells during type VI secretion system-mediated competition. *Cell Rep* 2018;**22**: 774-85.
Masuda H, Awano N, Inouye M. *ydfD* encodes a novel lytic protein in *Escherichia coli*. *FEMS Microbiol Lett* 2016;**363**: fnw039.
Mattinen L, Nissinen R, Riipi T *et al.* Host-extract induced changes in the secretome of the plant pathogenic bacterium *Pectobacterium atrosepticum*. *Proteomics* 2007;**7**: 3527-37.
Maurizi MR. ATP-promoted interaction between Clp A and Clp P in activation of Clp protease from *Escherichia coli*. *Biochem Soc Trans* 1991;**19**: 719-23.
Maurizi MR, Clark WP, Kim SH *et al.* Clp P represents a unique family of serine proteases. *J Biol Chem* 1990;**265**: 12546-52.
McBride MJ. *Bacteroidetes* gliding motility and the type IX secretion system. *Microbiol Spectr* 2019;**7**.
McCarthy RR, Yu M, Eilers K *et al.* Cyclic di-GMP inactivates T6SS and T4SS activity in *Agrobacterium tumefaciens*. *Mol Microbiol* 2019;**0**.

doi:10.6342/NTU202000295

Meuskens I, Saragliadis A, Leo JC *et al.* Type V secretion systems: an overview of passenger domain functions. *Front Microbial* 2019;**10**.
Michalska K, Gucinski GC, Garza-Sánchez F *et al.* Structure of a novel antibacterial toxin that exploits elongation factor Tu to cleave specific transfer RNAs. *Nucleic Acids Res* 2017;**45**: 10306-20.
Miller JM, Lin J, Li T *et al. E. coli* ClpA catalyzed polypeptide translocation Is allosterically controlled by the protease ClpP. *J Mol Biol* 2013;**425**: 2795-812.
Miyata ST, Bachmann V, Pukatzki S. Type VI secretion system regulation as a consequence of evolutionary pressure. *J Med Microbiol* 2013;**62**: 663-76.
Moreno JC, Tiller N, Diez M *et al.* Generation and characterization of a collection of knock-down lines for the chloroplast Clp protease complex in tobacco. *J Exp Bot* 2017;**68**: 2199-218.
Mougous JD, Cuff ME, Raunser S *et al.* A virulence locus of *Pseudomonas aeruginosa* encodes a protein secretion apparatus. *Science* 2006;**312**: 1526-30.
Mulley G, White JP, Karunakaran R *et al.* Mutation of GOGAT prevents pea bacteroid formation and N_2 fixation by globally downregulating transport of organic nitrogen sources. *Mol Microbiol* 2011;**80**: 149-67.
Murdoch SL, Trunk K, English G *et al.* The opportunistic pathogen *Serratia marcescens* utilizes type VI secretion to target bacterial competitors. *J Bacteriol* 2011;**193**: 6057-69.
Nelson MS, Chun CL, Sadowsky MJ. Type IV effector proteins involved in the *Medicago-Sinorhizobium* symbiosis. *Mol Plant-Microbe Interact* 2017;**30**: 28-34.
Nelson MS, Sadowsky MJ. Secretion systems and signal exchange between nitrogen-fixing rhizobia and legumes. *Front Plant Sci* 2015;**6**.
Newman JR, Fuqua C. Broad-host-range expression vectors that carry the L-arabinose-inducible *Escherichia coli araBAD* promoter and the *araC* regulator. *Gene* 1999;**227**: 197-203.
Nishimura K, van Wijk KJ. Organization, function and substrates of the essential Clp protease system in plastids. *Biochim Biophys Acta* 2015;**1847**: 915-30.
Novichkov PS, Kazakov AE, Ravcheev DA *et al.* RegPrecise 3.0 – A resource for genome-scale exploration of transcriptional regulation in bacteria. *BMC Genom* 2013;**14**: 745.
Okazaki S, Kaneko T, Sato S *et al.* Hijacking of leguminous nodulation signaling by the rhizobial type III secretion system. *Proc Natl Acad Sci USA* 2013;**110**: 17131-6.
Okazaki S, Zehner S, Hempel J *et al.* Genetic organization and functional analysis of the type III secretion system of *Bradyrhizobium elkanii*. *FEMS Microbiol Lett* 2009;**295**: 88-95.
Olivares AO, Baker TA, Sauer RT. Mechanistic insights into bacterial AAA+ proteases and protein-remodelling machines. *Nat Rev Microbiol* 2015;**14**: 33.
Orfanoudaki G, Economou A. Proteome-wide subcellular topologies of *E. coli* polypeptides database (STEPdb). *Mol Cell Proteomics* 2014;**13**: 3674-87.
Ownley BH, Trigiano RN. *Plant Pathology Concepts and Laboratory Exercises*: 3rd Edition. Boca Raton: CRC Press, 2016.
Pajuelo E, Stougaard J. *Lotus japonicus*'s a model system. In: Márquez AJ (ed.) *Lotus japonicus Handbook*, DOI 10.1007/1-4020-3735-x_1. Dordrecht: Springer Netherlands, 2005, 3-24.
Panagiotis F. Sarris, Emmanouil A. Trantas, Nicholas Skandalis *et al.* Phytobacterial type VI secretion system - gene distribution, phylogeny, structure and biological

doi:10.6342/NTU202000295

functions. In: Cumagun DCJ (ed.) *Plant Pathol*, DOI 10.5772/33235: InTech, 2012, 53-84.
Pazour GJ, Das A. Characterization of the VirG binding site of *Agrobacterium tumefaciens*. *Nucleic Acids Res* 1990;**18**: 6909-13.
Poole P, Allaway D. Carbon and nitrogen metabolism in *Rhizobium. Adv Microb Physiol* volume 43: Academic Press, 2000, 117-63.
Popp C, Ott T. Regulation of signal transduction and bacterial infection during root nodule symbiosis. *Curr Opin Plant Biol* 2011;**14**: 458-67.
Prell J, Bourdès A, Kumar S *et al.* Role of Symbiotic Auxotrophy in the *Rhizobium*-Legume Symbioses. *PLoS ONE* 2010;**5**: e13933.
Preston GM, Studholme DJ, Caldelari I. Profiling the secretomes of plant pathogenic *Proteobacteria*. *FEMS Microbiol Rev* 2005;**29**: 331-60.
Pukatzki S, Ma AT, Sturtevant D *et al.* Identification of a conserved bacterial protein secretion system in *Vibrio cholerae* using the *Dictyostelium* host model system. *Proc Natl Acad Sci USA* 2006;**103**: 1528-33.
Quentin D, Ahmad S, Shanthamoorthy P *et al.* Mechanism of loading and translocation of type VI secretion system effector Tse6. *Nat Microbiol* 2018;**3**: 1142-52.
R Core Team. R: A language and environment for statistical computing. Vienna, Austria: R Foundation for Statistical Computing, 2018.
Rapisarda C, Cherrak Y, Kooger R *et al. In situ* and high-resolution cryo-EM structure of a bacterial type VI secretion system membrane complex. *EMBO J* 2019;**38**: e100886.
Rayle DL, Cleland RE. The Acid Growth Theory of auxin-induced cell elongation is alive and well. *Plant Physiology* 1992;**99**: 1271-4.
Records AR, Gross DC. Sensor kinases RetS and LadS regulate *Pseudomonas syringae* type VI secretion and virulence factors. *J Bacteriol* 2010;**192**: 3584-96.
Reed KC, Mann DA. Rapid transfer of DNA from agarose gels to nylon membranes. *Nucleic Acids Res* 1985;**13**: 7207-21.
Rinaudo G, Dreyfus B, Dommergues Y. *Sesbania rostrata* green manure and the nitrogen content of rice crop and soil. *Soil Biol Biochem* 1983;**15**: 111-3.
Robb CS, Assmus M, Nano FE *et al.* Structure of the T6SS lipoprotein TssJ1 from *Pseudomonas aeruginosa*. *Acta Crystallogr Sect F: Struct Biol Cryst Commun* 2013;**69**: 607-10.
Roest HP, Mulders IHM, Spaink HP *et al.* A *Rhizobium leguminosarum* biovar *trifolii* locus not localized on the Sym plasmid hinders effective nodulation on plants of the pea cross-inoculation group. *Mol Plant-Microbe Interact* 1997;**10**: 938-41.
Ronson CW, Lyttleton P, Robertson JG. C4-dicarboxylate transport mutants of *Rhizobium trifolii* form ineffective nodules on *Trifolium repens*. *Proc Natl Acad Sci USA* 1981;**78**: 4284-8.
RStudio Team. RStudio: Integrated Development for R. Boston, MA RStudio, Inc., 2015.
Russell AB, Peterson SB, Mougous JD. Type VI secretion system effectors: poisons with a purpose. *Nat Rev Micro* 2014;**12**: 137-48.
Ryu C-M. Against friend and foe: Type 6 effectors in plant-associated bacteria. *J Microbiol* 2015;**53**: 201-8.
Ryu M-H, Zhang J, Toth T *et al.* Control of nitrogen fixation in bacteria that associate with cereals. *Nat Microbiol* 2019, DOI 10.1038/s41564-019-0631-2.
Salinero-Lanzarote A, Pacheco-Moreno A, Domingo-Serrano L *et al.* The type VI secretion system of *Rhizobium etli* Mim1 has a positive effect in symbiosis. *FEMS Microbiol Ecol* 2019;**95**.

doi:10.6342/NTU202000295

Sana TG, Flaugnatti N, Lugo KA *et al.* *Salmonella* Typhimurium utilizes a T6SS-mediated antibacterial weapon to establish in the host gut. *Proc Natl Acad Sci USA* 2016;**113**: E5044-E51.
Schäfer A, Tauch A, Jäger W *et al.* Small mobilizable multi-purpose cloning vectors derived from the *Escherichia coli* plasmids pK18 and pK19: selection of defined deletions in the chromosome of *Corynebacterium glutamicum*. *Gene* 1994;**145**: 69-73.
Schell MA, Ulrich RL, Ribot WJ *et al.* Type VI secretion is a major virulence determinant in *Burkholderia mallei*. *Mol Microbiol* 2007;**64**: 1466-85.
Schindelin J, Arganda-Carreras I, Frise E *et al.* Fiji: an open-source platform for biological-image analysis. *Nat Methods* 2012;**9**: 676-82.
Schneider JP, Nazarov S, Adaixo R *et al.* Diverse roles of TssA-like proteins in the assembly of bacterial type VI secretion systems. *EMBO J* 2019;**38**: e100825.
Schröder G, Waffenschmidt S, Weiler EW *et al.* The T-region of Ti plasmids codes for an enzyme synthesizing indole-3-acetic acid. *Eur J Biochem* 1984;**138**: 387-91.
Scott JD, Ludwig RA. *Azorhizobium caulinodans* electron-transferring flavoprotein N electrochemically couples pyruvate dehydrogenase complex activity to N_2 fixation. *Microbiology* 2004;**150**: 117-26.
Sgro GG, Oka GU, Souza DP *et al.* Bacteria-killing type IV secretion systems. *Front Microbial* 2019;**10**.
Shalom G, Shaw JG, Thomas MS. *In vivo* expression technology identifies a type VI secretion system locus in *Burkholderia pseudomallei* that is induced upon invasion of macrophages. *Microbiology* 2007;**153**: 2689-99.
Shneider MM, Buth SA, Ho BT *et al.* PAAR-repeat proteins sharpen and diversify the type VI secretion system spike. *Nature* 2013;**500**: 350-3.
Shyntum DY, Theron J, Venter SN *et al.* *Pantoea ananatis* utilizes a type VI secretion system for pathogenesis and bacterial competition. *Mol Plant-Microbe Interact* 2015;**28**: 420-31.
Si M, Zhao C, Burkinshaw B *et al.* Manganese scavenging and oxidative stress response mediated by type VI secretion system in *Burkholderia thailandensis*. *Proc Natl Acad Sci USA* 2017;**114**: E2233-E42.
Silverman Julie M, Agnello Danielle M, Zheng H *et al.* Haemolysin coregulated protein is an exported receptor and chaperone of type VI secretion substrates. *Mol Cell* 2013;**51**: 584-93.
Silverman JM, Brunet YR, Cascales E *et al.* Structure and regulation of the type VI secretion system. *Annu Rev Microbiol* 2012;**66**: 453-72.
Simon R, Priefer U, Puhler A. A broad host range mobilization system for *in vivo* genetic engineering: Transposon mutagenesis in Gram negative bacteria. *Nat Biotech* 1983;**1**: 784-91.
Smith EF, Townsend CO. A plant-tumor of bacterial origin. *Science* 1907;**25**: 671-3.
Souza DP, Oka GU, Alvarez-Martinez CE *et al.* Bacterial killing via a type IV secretion system. *Nat Commun* 2015;**6**: 6453.
Sriramoju MK, Chen Y, Lee Y-TC *et al.* Topologically knotted deubiquitinases exhibit unprecedented mechanostability to withstand the proteolysis by an AAA+ protease. *Sci Rep* 2018;**8**: 7076.
Stachel SE, Messens E, Van Montagu M *et al.* Identification of the signal molecules produced by wounded plant cells that activate T-DNA transfer in *Agrobacterium tumefaciens*. *Nature* 1985;**318**: 624-9.

doi:10.6342/NTU202000295

Stone PJ, O'Callaghan KJ, Davey MR *et al. Azorhizobium caulinodans* ORS571 colonizes the xylem of *Arabidopsis thaliana*. *Mol Plant-Microbe Interact* 2001;**14**: 93-7.
Studier FW, Moffatt BA. Use of bacteriophage T7 RNA polymerase to direct selective high-level expression of cloned genes. *J Mol Biol* 1986;**189**: 113-30.
Suzuki S, Aono T, Lee K-B *et al.* Rhizobial factors required for stem nodule maturation and maintenance in *Sesbania rostrata-Azorhizobium caulinodans* ORS571 symbiosis. *Appl Environ Microbiol* 2007;**73**: 6650-9.
Szklarczyk D, Gable AL, Lyon D *et al.* STRING v11: protein–protein association networks with increased coverage, supporting functional discovery in genome-wide experimental datasets. *Nucleic Acids Res* 2018;**47**: D607-D13.
Tamura K, Stecher G, Peterson D *et al.* MEGA6: Molecular Evolutionary Genetics Analysis Version 6.0. *Mol Biol Evol* 2013;**30**: 2725-9.
Teulet A, Busset N, Fardoux J *et al.* The rhizobial type III effector ErnA confers the ability to form nodules in legumes. *Proc Natl Acad Sci USA* 2019;**116**: 21758-68.
Tseng T-T, Tyler B, Setubal J. Protein secretion systems in bacterial-host associations, and their description in the Gene Ontology. *BMC Microbiol* 2009;**9**: S2.
Tsien HC, Dreyfus BL, Schmidt EL. Initial stages in the morphogenesis of nitrogen-fixing stem nodules of *Sesbania rostrata*. *J Bacteriol* 1983;**156**: 888-97.
Tsukada S, Aono T, Akiba N *et al.* Comparative genome-wide transcriptional profiling of *Azorhizobium caulinodans* ORS571 grown under free-living and symbiotic conditions. *Appl Environ Microbiol* 2009;**75**: 5037-46.
Ueguchi C, Kakeda M, Yamada H *et al.* An analogue of the DnaJ molecular chaperone in *Escherichia coli*. *Proc Natl Acad Sci USA* 1994;**91**: 1054-8.
Unterweger D, Kostiuk B, Ötjengerdes R *et al.* Chimeric adaptor proteins translocate diverse type VI secretion system effectors in *Vibrio cholerae*. *EMBO J* 2015;**34**: 2198-210.
Unterweger D, Kostiuk B, Pukatzki S. Adaptor proteins of type VI secretion system effectors. *Trends Microbiol* 2017;**25**: 8-10.
Unterweger D, Miyata ST, Bachmann V *et al.* The *Vibrio cholerae* type VI secretion system employs diverse effector modules for intraspecific competition. *Nat Commun* 2014;**5**.
Venkateshwaran M. Exploring the feasibility of transferring nitrogen fixation to cereal crops. In: Lugtenberg B (ed.) *Principles of Plant-Microbe Interactions: Microbes for Sustainable Agriculture*, DOI 10.1007/978-3-319-08575-3_42. Cham: Springer International Publishing, 2015, 403-10.
Vergunst AC, Schrammeijer B, den Dulk-Ras A *et al.* VirB/D4-dependent protein translocation from *Agrobacterium* into plant cells. *Science* 2000;**290**: 979-82.
Vergunst AC, van Lier MCM, den Dulk-Ras A *et al.* Positive charge is an important feature of the C-terminal transport signal of the VirB/D4-translocated proteins of *Agrobacterium*. *Proc Natl Acad Sci USA* 2005;**102**: 832-7.
Vladimirov IA, Matveeva TV, Lutova LA. Opine biosynthesis and catabolism genes of *Agrobacterium tumefaciens* and *Agrobacterium rhizogenes*. *Russ J Genet* 2015;**51**: 121-9.
von Bodman SB, McCutchan JE, Farrand SK. Characterization of conjugal transfer functions of *Agrobacterium tumefaciens* Ti plasmid pTiC58. *J Bacteriol* 1989;**171**: 5281-9.
Wang J, Brodmann M, Basler M. Assembly and subcellular localization of bacterial type VI secretion systems. *Annu Rev Microbiol* 2019;**73**: 621-38.

doi:10.6342/NTU202000295

Wang J, Hartling JA, Flanagan JM. The structure of ClpP at 2.3 Å resolution suggests a model for ATP-dependent proteolysis. *Cell* 1997;**91**: 447-56.
Weber-Ban EU, Reid BG, Miranker AD *et al.* Global unfolding of a substrate protein by the Hsp100 chaperone ClpA. *Nature* 1999;**401**: 90-3.
Wenren LM, Sullivan NL, Cardarelli L *et al.* Two independent pathways for self-recognition in *Proteus mirabilis* are linked by type VI-dependent export. *mBio* 2013;**4**.
Whitney JC, Chou S, Russell AB *et al.* Identification, structure, and function of a novel type VI secretion peptidoglycan glycoside hydrolase effector-immunity pair. *J Biol Chem* 2013;**288**: 26616-24.
Whitney John C, Quentin D, Sawai S *et al.* An interbacterial NAD(P)+ glycohydrolase toxin requires elongation factor Tu for delivery to target cells. *Cell* 2015;**163**: 607-19.
Wickham H. The split-apply-combine strategy for data analysis. *J Stat Softw* 2011;**40**: 29.
Wickham H. *ggplot2: elegant graphics for data analysis*: Springer-Verlag New York, 2016.
Wielbo J, Kuske J, Marek-Kozaczuk M *et al.* The competition between *Rhizobium leguminosarum* bv. viciae strains progresses until late stages of symbiosis. *Plant Soil* 2010;**337**: 125-35.
Willett JLE, Gucinski GC, Fatherree JP *et al.* Contact-dependent growth inhibition toxins exploit multiple independent cell-entry pathways. *Proc Natl Acad Sci USA* 2015;**112**: 11341-6.
Willmitzer L, De Beuckeleer M, Lemmers M *et al.* DNA from Ti plasmid present in nucleus and absent from plastids of crown gall plant cells. *Nature* 1980;**287**: 359-61.
Winans SC. Two-way chemical signaling in *Agrobacterium*-plant interactions. *Microbiol Rev* 1992;**56**: 12-31.
Wood DW, Setubal JC, Kaul R *et al.* The genome of the natural genetic engineer *Agrobacterium tumefaciens* C58. *Science* 2001;**294**: 2317-23.
Wu C-F, Lien Y-W, Bondage D *et al.* Effector loading onto the VgrG carrier activates type VI secretion system assembly. *EMBO Rep* 2019a;**n/a**: e47961.
Wu C-F, Lin J-S, Shaw G-C *et al.* Acid-induced type VI secretion system is regulated by ExoR-ChvG/ChvI signaling cascade in *Agrobacterium tumefaciens*. *PLoS Pathog* 2012;**8**: e1002938.
Wu C-F, Santos MNM, Cho S-T *et al.* Plant pathogenic *Agrobacterium tumefaciens* strains have diverse type VI effector-immunity pairs and vary in *in planta* competitiveness. *Mol Plant-Microbe Interact* 2019b;**32**: 961-71.
Wu H-Y, Chung P-C, Shih H-W *et al.* Secretome analysis uncovers an Hcp-family protein secreted via a type VI secretion system in *Agrobacterium tumefaciens*. *J Bacteriol* 2008;**190**: 2841-50.
Young JPW, Crossman LC, Johnston AW *et al.* The genome of *Rhizobium leguminosarum* has recognizable core and accessory components. *Genome Biol* 2006;**7**: 1-20.
Zamioudis C, Pieterse CMJ. Modulation of host immunity by beneficial microbes. *Mol Plant-Microbe Interact* 2012;**25**: 139-50.
Zhang L, Xu J, Xu J *et al.* TssB is essential for virulence and required for Type VI secretion system in *Ralstonia solanacearum*. *Microb Pathog* 2014;**74**: 1-7.
Zhang XY, Brunet YR, Logger L *et al.* Dissection of the TssB-TssC interface during type VI secretion sheath complex formation. *PLOS ONE* 2013;**8**: e81074.

doi:10.6342/NTU202000295

Zheng J, Leung KY. Dissection of a type VI secretion system in *Edwardsiella tarda*. *Mol Microbiol* 2007;**66**: 1192-206.
Zoued A, Brunet YR, Durand E *et al.* Architecture and assembly of the type VI secretion system. *Biochim Biophys Acta* 2014;**1843**: 1664-73.
Zoued A, Durand E, Brunet YR *et al.* Priming and polymerization of a bacterial contractile tail structure. *Nature* 2016;**531**: 59-63.
Zoued A, Durand E, Santin YG *et al.* TssA: The cap protein of the Type VI secretion system tail. *Bioessays* 2017;**39**: 1600262.

doi:10.6342/NTU202000295